

## Electronic Supplementary Information

### **Do 2-Coordinate Iodine(I) and Silver(I) Complexes Form Nucleophilic Iodonium Interactions (NIIs) in Solution?**

Scott Wilcox, Daniel Sethio, James Ward, Antonio Frontera, Roland Lindh, Kari Rissanen, and Máté Erdélyi

#### Table of Contents

<b>1. Synthesis</b>	<b>S2</b>
1.1. General Information	S2
1.2. Synthesis	S3
1.3. $^{19}\text{F}$ DOSY Data	S5
<b>2. NMR Spectra</b>	<b>S6</b>
2.1. Synthesised Compounds	S6
2.2. Mixtures of Complexes & Addition of Reagents	S28
<b>3. Computations</b>	<b>S72</b>
3.1. Computational Methods	S72
3.2. Computational Results	S73
3.3. Cartesian coordinates ( $\text{\AA}$ ) of optimized structures	S76
<b>4. References</b>	<b>S88</b>

*Original FID's of NMR spectra are available, free of charge at Zenodo at DOI: 10.5281/zenodo.6078936*

## 1. Synthesis

### 1.1 General Information

The solvents  $\text{CH}_2\text{Cl}_2$  and  $\text{CD}_2\text{Cl}_2$  were distilled over  $\text{CaH}_2$ , whilst *n*-hexane was distilled over Na, benzophenone and tetraglyme. These dry solvents were stored in a glovebox over 3 Å molecular sieves, with  $\text{CD}_2\text{Cl}_2$  being stored at -35 °C. All chemicals were purchased from commercial suppliers and were used without prior purification. For all syntheses and analyses, glassware was either dried at 150 °C or under high vacuum overnight prior to use. A glovebox was used for preparation of  $\text{Ag}^+$  and  $\text{I}^-$  complex samples, where  $\text{Ag}^+$  salts and  $\text{I}_2$  were stored prior to use. An Eppendorf Centrifuge 5702 was used to centrifuge samples.

NMR spectra were recorded on an Agilent MR400-DD2 spectrometer fitted with a OneNMR probe. Chemical shifts were reported on the  $\delta$  scale (ppm), with the residual solvent signal or with TMS as an internal reference;  $\text{CD}_2\text{Cl}_2$  ( $\delta_{\text{H}}$  5.32,  $\delta_{\text{C}}$  53.84), TMS ( $\delta_{\text{H}}$  0.00,  $\delta_{\text{C}}$  0.00). Nitromethane ( $\delta_{\text{N}}$  0.0) was used as an external standard for  $^{15}\text{N}$ . For  $^1\text{H}, ^{15}\text{N}$  HMBC spectra, a capillary containing 1-methyl pyridinium iodide (0.45 M) in  $\text{CD}_3\text{CN}$  was inserted into the sample to act as an external reference ( $\delta_{\text{H}}$  5.18,  $\delta_{\text{N}}$  -177.79). For most  $^1\text{H}, ^{15}\text{N}$  HMBC spectra, a spectral window of 10 ppm ( $^1\text{H}$ ) and 80 ppm ( $^{15}\text{N}$ ) were used, with 721 points in the direct dimension and 256 increments used in the indirect dimension, affording a resolution of 0.31 ppm/point in f1.  $^1\text{H}$  NMR resonances were assigned considering chemical shift ( $\delta$ ), multiplicity, coupling constants ( $J$  Hz) and the number of hydrogens, and multiplicities of these were denoted as s (singlet), d (doublet), t (triplet), q (quartet), hept (heptet) and m (multiplet). MestReNova 14.2.1 was used to process NMR spectra.

Diffusion coefficients for  $^1\text{H}$  nuclei were calculated according to an adjusted Stokes-Einstein equation,<sup>1</sup> which takes into account a correction factor for small, flat, linear molecules.

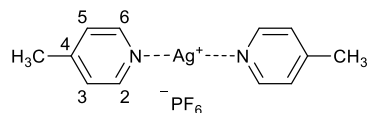
$$D = \frac{k_B T}{6 \pi \eta r_H} \rightarrow D = \frac{k_B T}{c f_s \pi \eta r_H} \quad \text{Eq. 1}$$

where  $D$  is the diffusion coefficient ( $\text{m}^2 \text{s}^{-1}$ ),  $k_B$  is Boltzmann's constant,  $T$  the temperature,  $c$  the c-factor for small molecules,  $f_s$  the form factor for non-spherical molecules,  $\eta$  the dynamic viscosity and  $r_H$  the hydrodynamic radius. The expected  $V_{\text{vdW}}$  from Eq. 1 for  $\text{Ag}^+$  and  $\text{I}^-$  complexes, (1) and (2), is  $\sim 200 \text{ \AA}^3$  (from an  $r_{\text{vdW}} \sim 3.6 \text{ \AA}$ ) - comparable to that of tolane, a monomeric species.

Diffusion NMR was also performed on  $^{19}\text{F}$  nuclei upon the counter-anion of the  $\text{Ag}^+$  and  $\text{I}^-$  4-methylpyridine complexes,  $\text{PF}_6^-$ . Diffusion coefficients were calculated using a standard Stokes-Einstein equation (*left, Eq. 1*), as the anion itself is spherical in shape. Values were corrected for the gyromagnetic ratio of  $^{19}\text{F}$ , relative to those of  $^1\text{H}$ , using  $\gamma^{19}\text{F}/\gamma^1\text{H} = 0.8858$ .<sup>2</sup> Results are shown in *Table S1*.

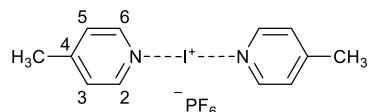
## 1.2 Synthesis

### [Bis(4-methylpyridine)silver(I)]hexafluorophosphate (**1**).<sup>3</sup>



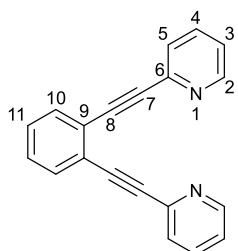
In a glovebox, AgPF<sub>6</sub> (0.100 g, 0.40 mmol) was dissolved in dry CH<sub>2</sub>Cl<sub>2</sub> (2 mL) with stirring in a dry vial. 4-Methylpyridine (0.077 mL, 0.79 mmol) was added and the mixture was stirred for 5 min before removal of stirrer bar. Dry *n*-Hexane (4 mL) was added to the mixture to precipitate the Ag<sup>+</sup> complex **1**. The vial was then centrifuged for 10 min at 4400 rpm, the supernatant was removed, and the precipitate was dried *in vacuo* overnight to yield **1** as a white powder (0.171 g, 0.39 mmol, 98 %). <sup>1</sup>H NMR (400 MHz, 25 °C, CD<sub>2</sub>Cl<sub>2</sub>) δ [ppm] = 8.47 (d, *J* = 5.4 Hz, 2H, H-2/6), 7.41 (d, *J* = 5.4 Hz, 2H, H3/5), 2.48 (s, 3H, -CH<sub>3</sub>). <sup>13</sup>C NMR (101 MHz, 25 °C, CD<sub>2</sub>Cl<sub>2</sub>) δ [ppm] = 152.9 (C4), 151.6 (C2/6), 127.1 (C3/5), 21.6 (-CH<sub>3</sub>). <sup>15</sup>N NMR (41 MHz, detected *via* <sup>1</sup>H-<sup>15</sup>N HMBC at 400 MHz for <sup>1</sup>H, 25 °C, CD<sub>2</sub>Cl<sub>2</sub>) δ [ppm] = -130.8. <sup>19</sup>F NMR (376 MHz, 25 °C, CD<sub>2</sub>Cl<sub>2</sub>) δ [ppm] = -72.95 (d, *J* = 712.5 Hz, 6F, -PF<sub>6</sub>).

### [Bis(4-methylpyridine)iodine(I)]hexafluorophosphate (**2**).<sup>3</sup>



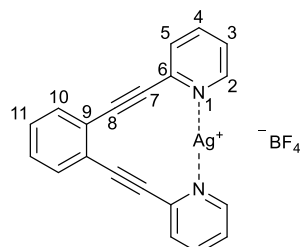
In a glovebox, **1** (0.075 g, 0.17 mmol) was dissolved in dry CH<sub>2</sub>Cl<sub>2</sub> (1 mL) in a dry vial with stirring. Next, I<sub>2</sub> (0.043 g, 0.17 mmol) was dissolved in dry CH<sub>2</sub>Cl<sub>2</sub> (1 mL) and was added dropwise over 10 min to the solution of **1**, until a faint purple colour was observed (indicating a minute excess of I<sub>2</sub>). A yellow precipitate, AgI, was observed immediately upon addition of I<sub>2</sub> solution. The mixture was stirred for a further 20 min before centrifugation for 10 min at 4400 rpm. The resulting supernatant was transferred to another vial, where dry *n*-Hexane (2 mL) was added. The vial was cooled to -35 °C for 30 min to complete precipitation of **2**. Centrifugation of this solution for 10 min at 4400 rpm, followed by removal of supernatant, addition of 2 mL *n*-hexane to wash, further centrifugation for 10 min at 4400 rpm and removal of supernatant, gave a white precipitate. The solid was dried *in vacuo* overnight to yield **2** as a crystalline, white solid (0.066 g, 0.14 mmol, 85 %). <sup>1</sup>H NMR (400 MHz, 25 °C, CD<sub>2</sub>Cl<sub>2</sub>) δ [ppm] = 8.55 (d, *J* = 5.4 Hz, 2H, H2/6), 7.39 (d, *J* = 5.4 Hz, 2H, H3/5), 2.53 (s, 3H, -CH<sub>3</sub>). <sup>13</sup>C NMR (101 MHz, 25 °C, CD<sub>2</sub>Cl<sub>2</sub>) δ [ppm] = 155.8 (C4), 149.0 (C2/6), 129.0 (C3/5), 21.9 (-CH<sub>3</sub>). <sup>15</sup>N NMR (41 MHz, detected *via* <sup>1</sup>H-<sup>15</sup>N HMBC at 400 MHz for <sup>1</sup>H, 25 °C, CD<sub>2</sub>Cl<sub>2</sub>) δ [ppm] = -181.0. <sup>19</sup>F NMR (376 MHz, 25 °C, CD<sub>2</sub>Cl<sub>2</sub>) δ [ppm] = -73.24 (d, *J* = 710.6 Hz, 6F, -PF<sub>6</sub>).

1,2-bis(pyridin-2-ylethynyl)benzene (**3**).<sup>4-6</sup>



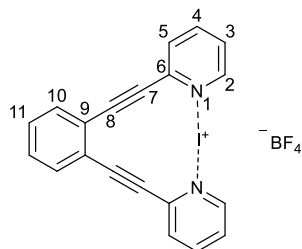
To a 20 mL microwave vial, 1,2-diiodobenzene (2.529 g, 7.67 mmol), 2-ethynylpyridine (1.83 mL, 17.79 mmol), PdPPh<sub>3</sub>Cl<sub>2</sub> (0.538 g, 0.77 mmol), CuI (161 mg, 0.84 mmol), diethylamine (12.00 mL) and dimethylformamide (4 mL) were added, and the vial was sealed. N<sub>2</sub> gas was bubbled through the reaction mixture for 2 min, followed by sonication for 2 min. The mixture was heated under microwave irradiation and stirring at 120 °C for 10 min. Thereafter, the resulting dark brown solution was filtered through a plug of Celite and washed with CH<sub>2</sub>Cl<sub>2</sub> (100 mL). To the filtrate, H<sub>2</sub>O was added and the two phases were separated. The aqueous phase was extracted with CH<sub>2</sub>Cl<sub>2</sub> (3 × 35 mL) and the combined organic phases were dried with anhydrous MgSO<sub>4</sub>, filtered and concentrated *in vacuo*. The brown-black residue was purified by column chromatography two consecutive times using EtOAc/Hexanes (2:3 to 4:1), followed by CH<sub>2</sub>Cl<sub>2</sub>/EtOAc (95:5 to 80:20) as eluents. This yielded the final product **3** (1.462 g, 5.22 mmol, 68 %) as an amber, crystalline solid. <sup>1</sup>H NMR (400 MHz, 25 °C, CD<sub>2</sub>Cl<sub>2</sub>) δ [ppm] = 8.63 (m, 2H, H2), 7.75-7.64 (m, 6H, H5/4/10), 7.42 (BB' part of AA'BB', 2H, H11), 7.28 (ddd, J = 4.8, 4.8, 2.4 Hz, 2H, H3). <sup>13</sup>C NMR (101 MHz, 25 °C, CD<sub>2</sub>Cl<sub>2</sub>) δ [ppm] = 150.6 (C2), 143.7 (C6), 136.5 (C4), 132.6 (C10), 129.3 (C11), 128.1 (C5), 125.7 (C3), 123.4 (C9), 93.5 (C7), 87.5 (C8).

[(1,2-bis(pyridin-2-ylethynyl)benzene)silver(I)]tetrafluoroborate (**4**).<sup>4-6</sup>



In a glovebox, **3** (0.008 g, 0.029 mmol) and AgBF<sub>4</sub> (0.006 mg, 0.029 mmol) were dissolved in dry CH<sub>2</sub>Cl<sub>2</sub> with stirring for 5 min. Thereafter, dry *n*-Hexane (2 mL) was added to precipitate the Ag<sup>+</sup> complex. The mixture was then centrifuged for 10 min at 4400 rpm, the supernatant removed and the white solid dried *in vacuo* overnight. The product, **4**, a white powder (0.012 g, 0.025 mmol, 87 %) was obtained. <sup>1</sup>H NMR (400 MHz, 25 °C, CD<sub>2</sub>Cl<sub>2</sub>) δ [ppm] = 8.85 (dd, J = 5.4, 1.7 Hz, 2H, H2), 7.92 (dd, J = 7.9, 7.9 Hz, 2H, H4), 7.74 (d, J = 7.9 Hz, 2H, H5), 7.61 (AA' part of AA'BB', 2H, H10), 7.51 (dd, J = 7.7, 5.4, 1.4 Hz, 2H, H3), 7.39 (BB' part of AA'BB', 2H, H11). <sup>13</sup>C NMR (101 MHz, 25 °C, CD<sub>2</sub>Cl<sub>2</sub>) δ [ppm] = 153.4 (C2) 143.6 (C6), 139.9 (C4), 133.4 (C10), 130.5 (C11), 128.8 (C5), 125.6 (C3), 123.8 (C9), 92.4 (C7), 91.1 (C8).

[(1,2-bis(pyridin-2-ylethynyl)benzene)iodine(I)]tetrafluoroborate (**5**).<sup>4-6</sup>



In a glovebox, **4** (0.012 g, 0.025 mmol) was dissolved in dry CH<sub>2</sub>Cl<sub>2</sub> in a dry vial with stirring for 5 min. I<sub>2</sub> (0.007 g, 0.027 mmol) was dissolved in dry CH<sub>2</sub>Cl<sub>2</sub> (0.5 mL) and this solution was added dropwise over 10 min to the solution of **4**, until a faint purple colour was observed (indicating a minute excess of I<sub>2</sub>). A yellow precipitate, AgI, was observed immediately upon addition of I<sub>2</sub> solution. The mixture was stirred for a further 20 min before centrifugation for 10 min at 4400 rpm. The resulting supernatant was transferred to another vial, where dry *n*-Hexane (1 mL) was added. The vial was cooled to -35 °C for 30 min to complete precipitation of **5**. Centrifugation of this solution for 10 min at 4400 rpm, followed by removal of supernatant, addition of 1 mL *n*-Hexane to wash, further centrifugation for 10 min at 4400 rpm and removal of supernatant, gave a white precipitate. The solid was dried *in vacuo* overnight to yield **5** as a crystalline, white solid (0.012 g, 0.024 mmol, 98 %). <sup>1</sup>H NMR (400 MHz, 25 °C, CD<sub>2</sub>Cl<sub>2</sub>) δ [ppm] = 8.83 (ddd, *J* = 5.7, 1.6 Hz, 2H, H2), 8.17 (ddd, *J* = 7.8, 7.8, 1.5 Hz, 2H, H4), 7.89 (dd, *J* = 7.9, 1.4 Hz, 2H, H5), 7.76 (AA' part of AA'BB', 2H, H10), 7.57 (BB' part of AA'BB', 2H, H11), 7.48 (ddd, *J* = 7.6, 5.6, 1.4 Hz, 2H, H3). <sup>13</sup>C NMR (101 MHz, 25 °C, CD<sub>2</sub>Cl<sub>2</sub>) δ [ppm] = 151.1 (C2), 143.0 (C6), 142.6 (C4), 134.7 (C10), 131.3 (C11), 130.7 (C5), 126.9 (C3), 124.5 (C9), 98.9 (C8), 91.0 (C7).

### 1.3 <sup>19</sup>F DOSY Data

**Table S1.** <sup>19</sup>F NMR translational diffusion coefficients of the PF<sub>6</sub><sup>-</sup> counter-anion of [bis(4-methylpyridine)-iodine(I)]<sup>+</sup> and [bis(4-methylpyridine)silver(I)]<sup>+</sup> complexes at different molar ratios yet at a constant overall concentration (44.4 mM, below given as 4 eq).

Molar Equivalents		D × 10 <sup>-10</sup> m/s <sup>2</sup>
[Ag(PMe <sub>2</sub> Py) <sub>2</sub> ] <sup>+</sup>	[I(PMe <sub>2</sub> Py) <sub>2</sub> ] <sup>+</sup>	PF <sub>6</sub> <sup>-</sup>
0	4	10.4
1	3	10.5
2	2	10.6
3	1	10.8
4	0	10.9

## 2. NMR Spectra

### 2.1 Synthesised Compounds

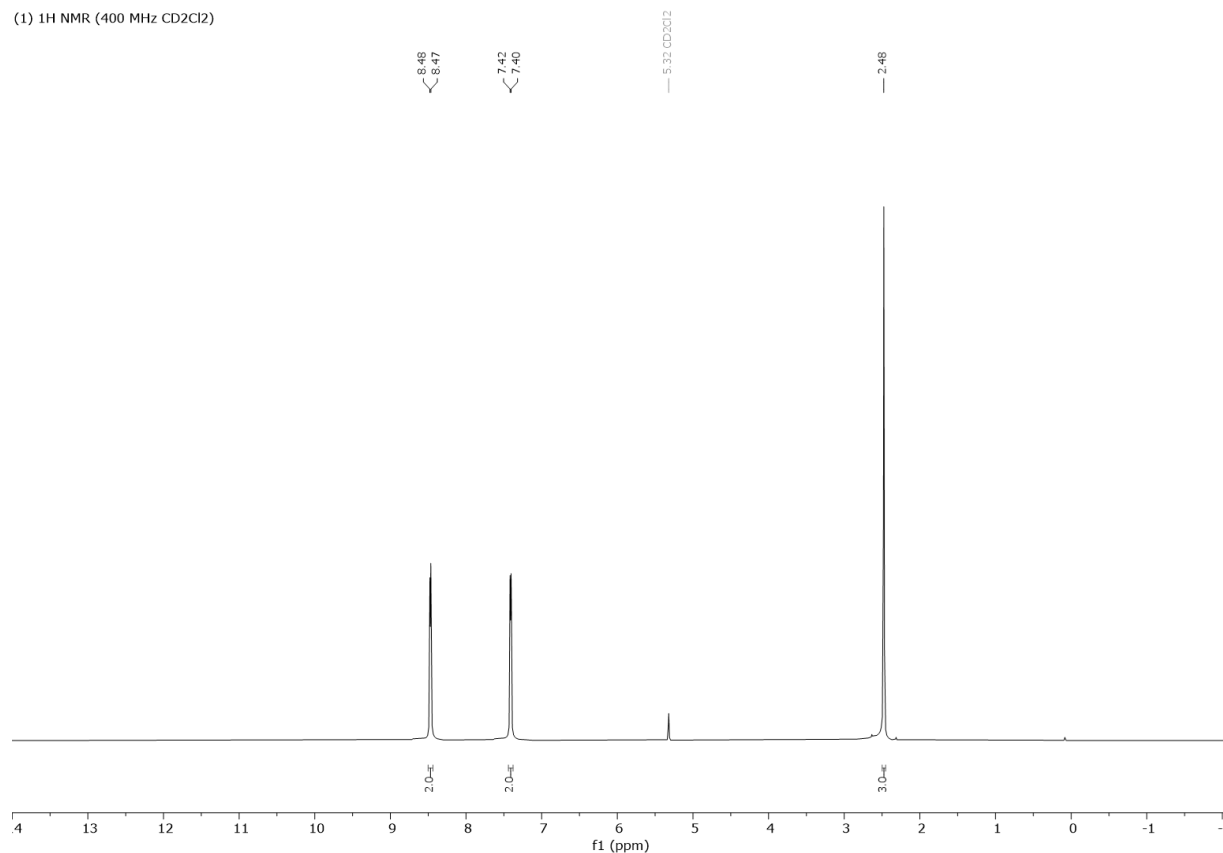


**Figure S1.**  $^1\text{H}$  NMR spectrum of [bis(4-methylpyridine)silver(I)]hexafluorophosphate (**1**) (400 MHz,  $\text{CD}_2\text{Cl}_2$ , 25°C).

(1)  $^{13}\text{C}$  NMR (101 MHz  $\text{CD}_2\text{Cl}_2$ )

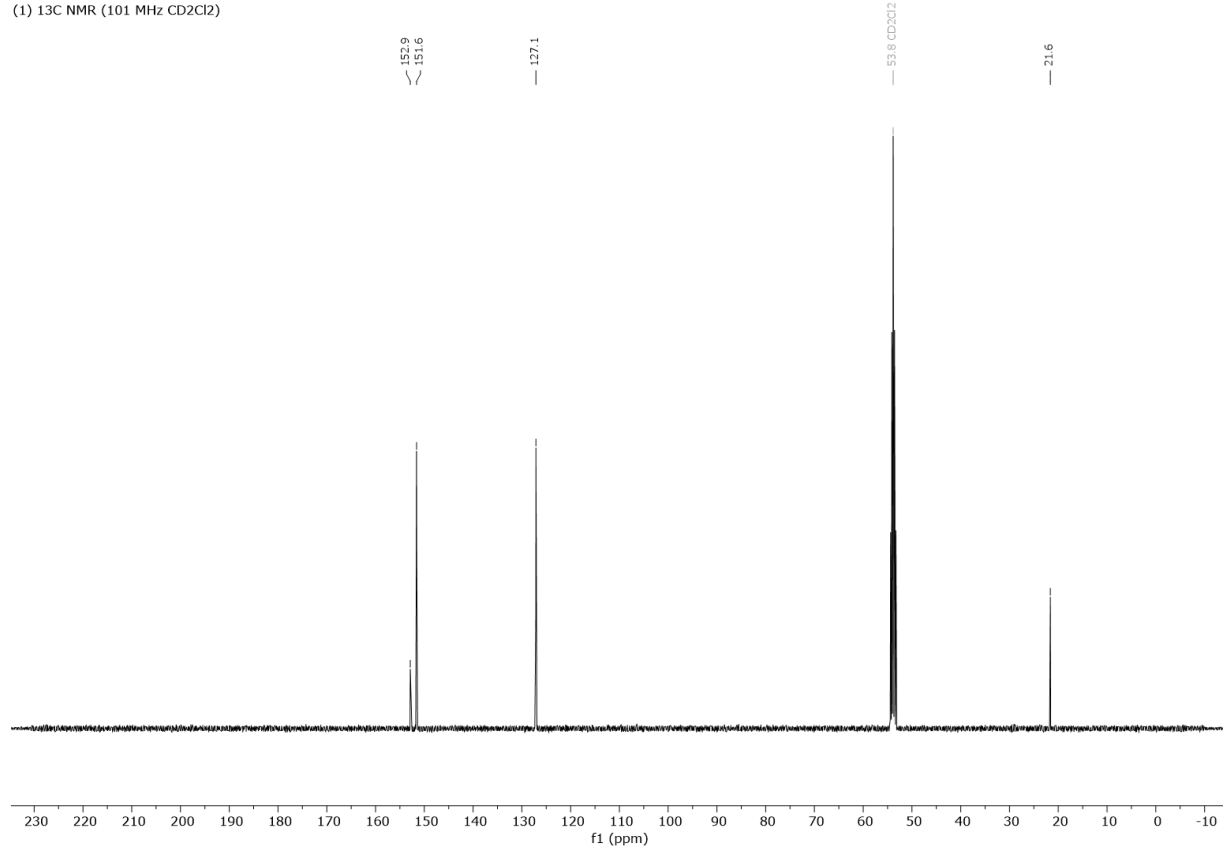


**Figure S2.**  $^{13}\text{C}$  NMR spectrum of [bis(4-methylpyridine)silver(I)]hexafluorophosphate (**1**) (101 MHz,  $\text{CD}_2\text{Cl}_2$ , 25°C).

(1) 1H (for1H-15N HMBC) (400 & 41 MHz CD<sub>2</sub>Cl<sub>2</sub>)

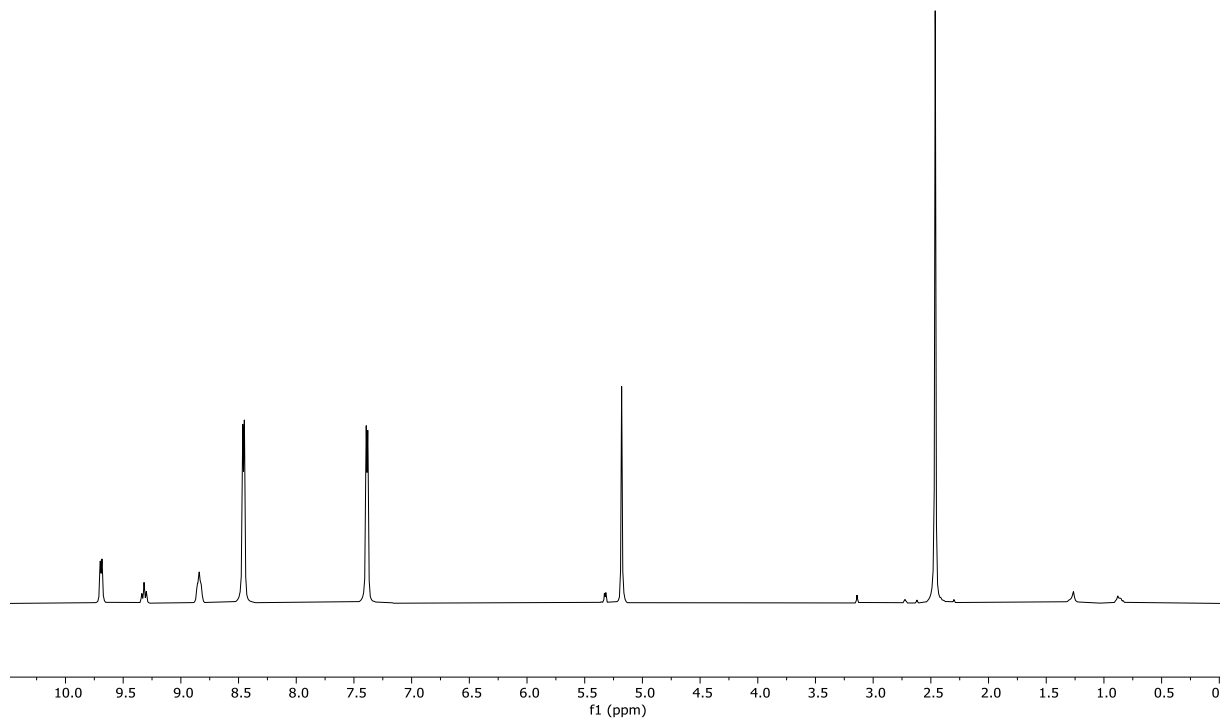


**Figure S3.** <sup>1</sup>H NMR spectrum of [bis(4-methylpyridine)silver(I)]hexafluorophosphate (**1**) with capillary of 1-Methylpyridinium iodide in CD<sub>3</sub>CN (400 MHz, CD<sub>2</sub>Cl<sub>2</sub>, 25°C).

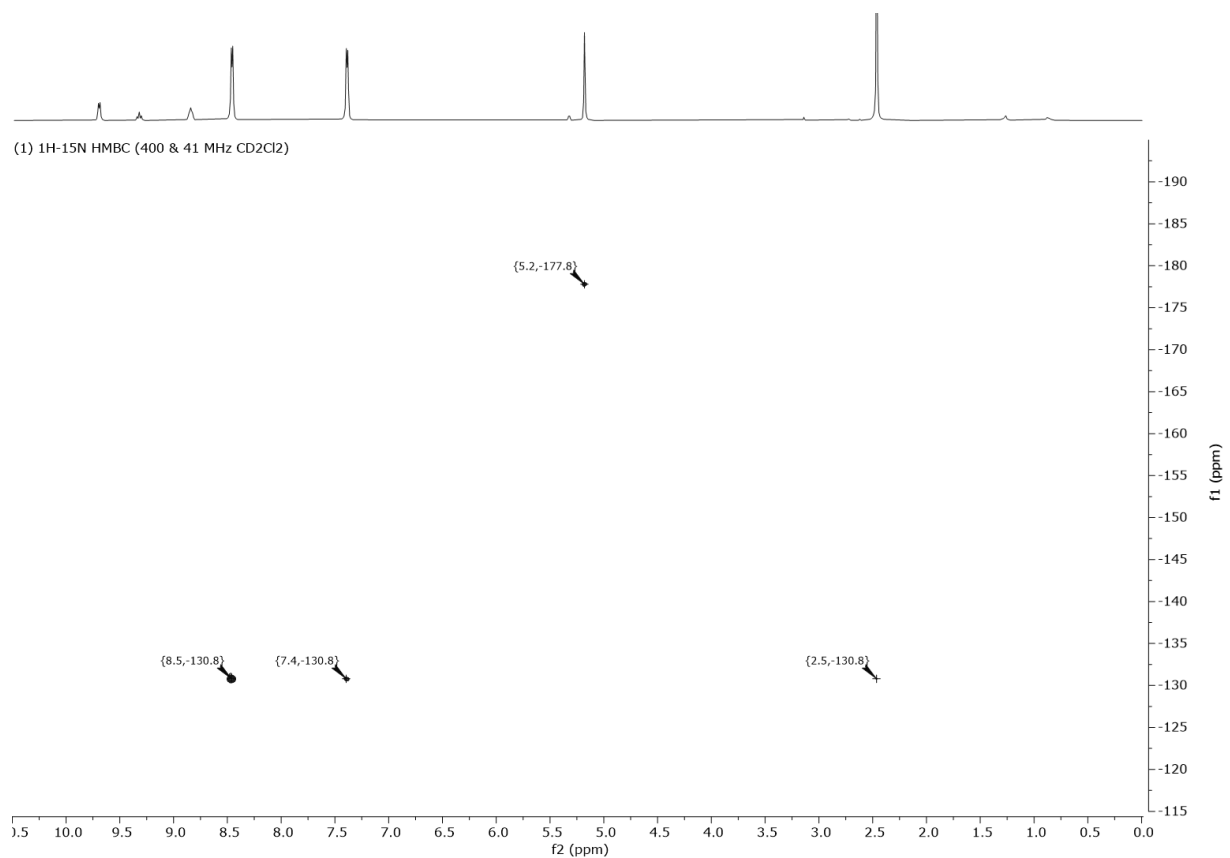


**Figure S4.** <sup>1</sup>H-<sup>15</sup>N HMBC NMR spectrum of [bis(4-methylpyridine)silver(I)]hexafluorophosphate (**1**), with capillary of 1-Methylpyridinium iodide in CD<sub>3</sub>CN (400 & 41 MHz, CD<sub>2</sub>Cl<sub>2</sub>, 25°C).

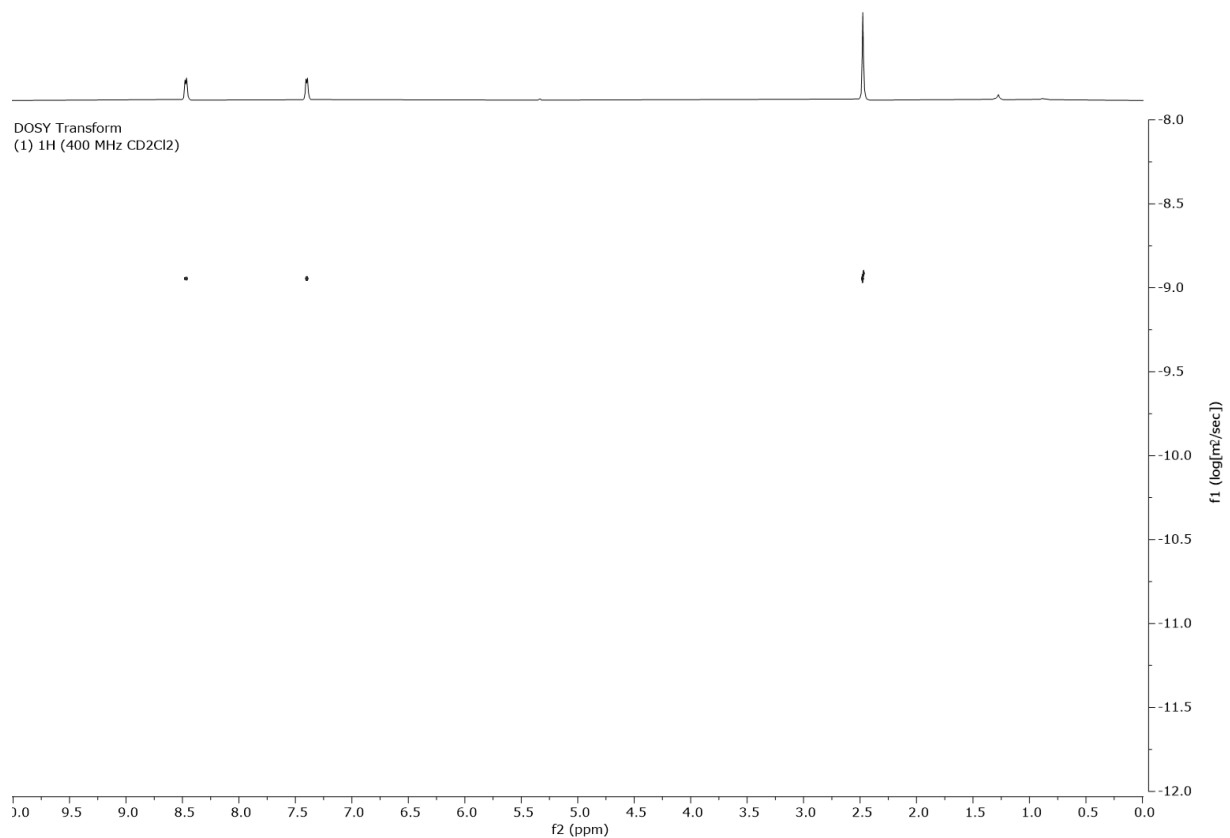


**Figure S5.**  ${}^1\text{H}$  DOSY Transform NMR spectrum of [bis(4-methylpyridine)silver(I)]hexafluorophosphate (**1**) (400 MHz,  $\text{CD}_2\text{Cl}_2$ , 25°C).

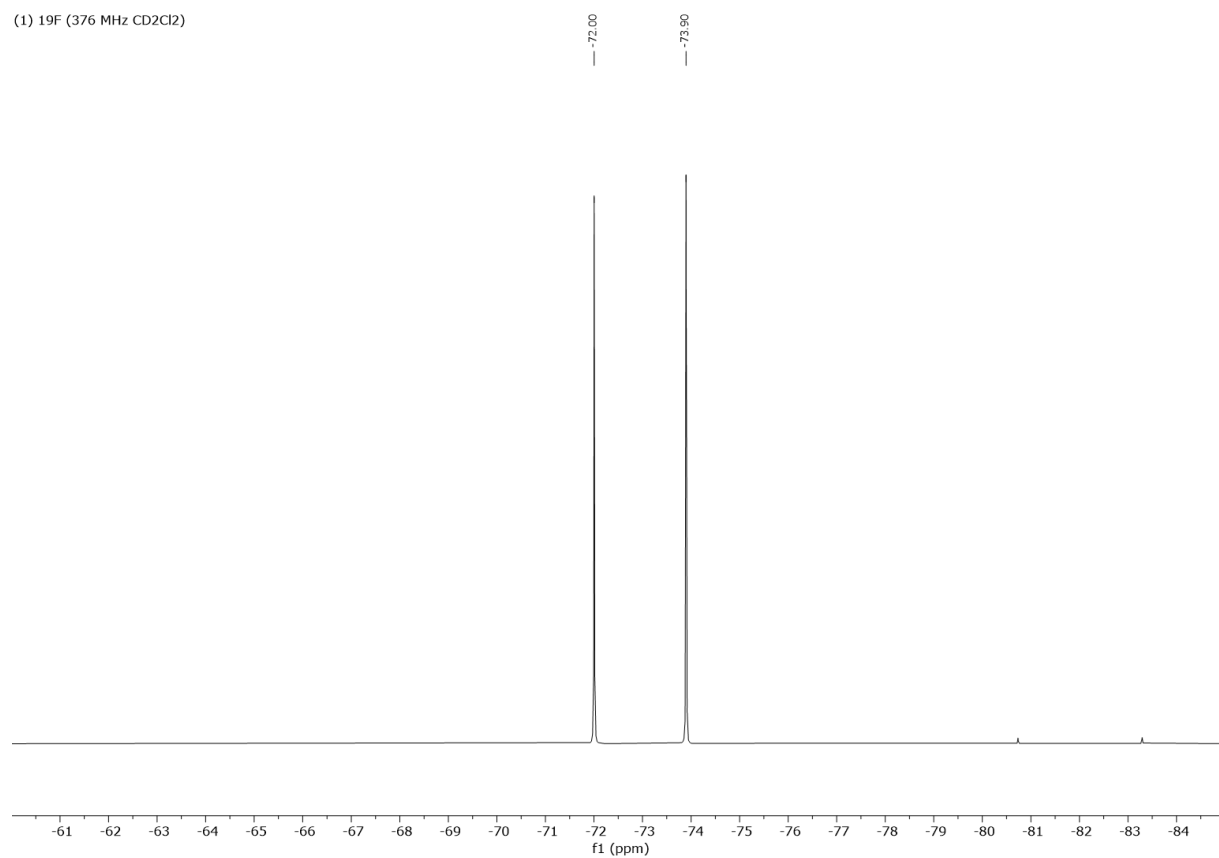


**Figure S6.**  $^{19}\text{F}$  NMR spectrum of [bis(4-methylpyridine)silver(I)]hexafluorophosphate (**1**) (376 MHz,  $\text{CD}_2\text{Cl}_2$ , 25 °C).

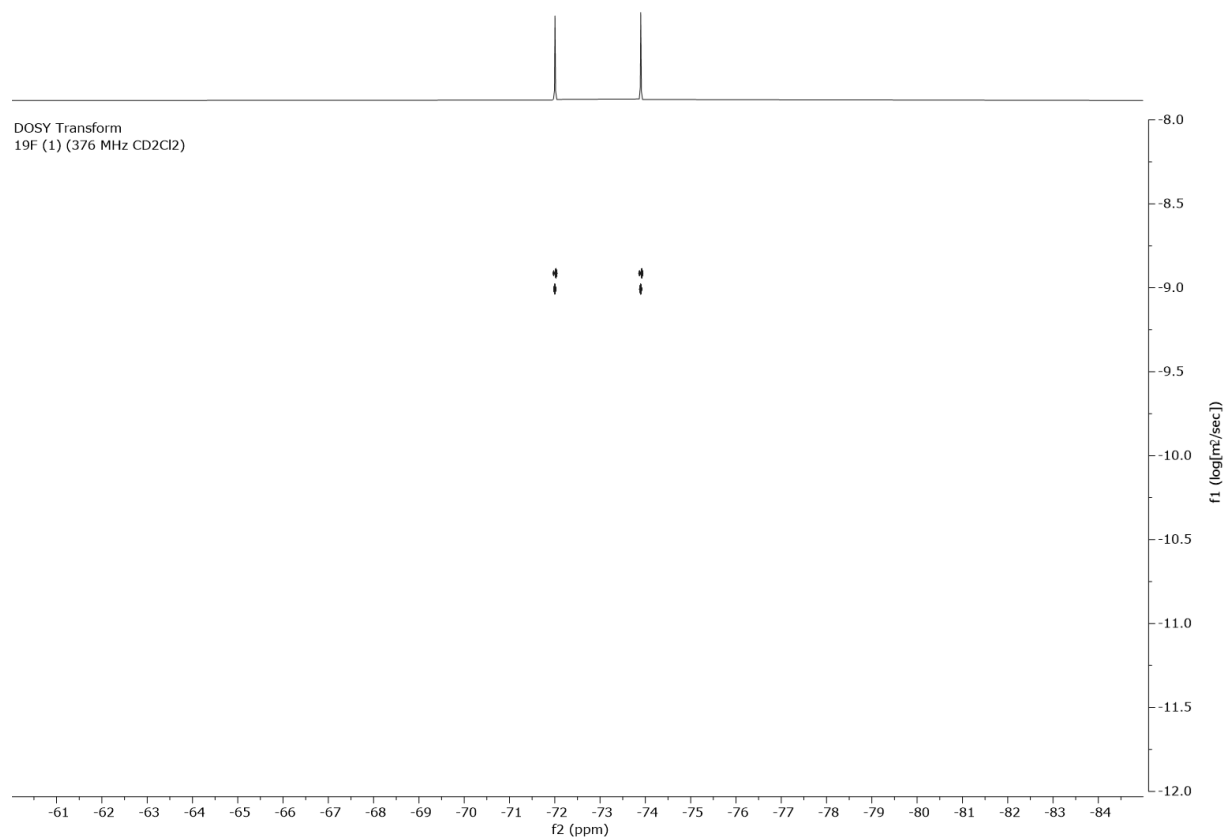


**Figure S7.**  $^{19}\text{F}$  DOSY Transform NMR spectrum of [bis(4-methylpyridine)silver(I)]hexafluorophosphate (**1**) (376 MHz,  $\text{CD}_2\text{Cl}_2$ , 25°C).

(2)  $^1\text{H}$  NMR (400 MHz  $\text{CD}_2\text{Cl}_2$ )

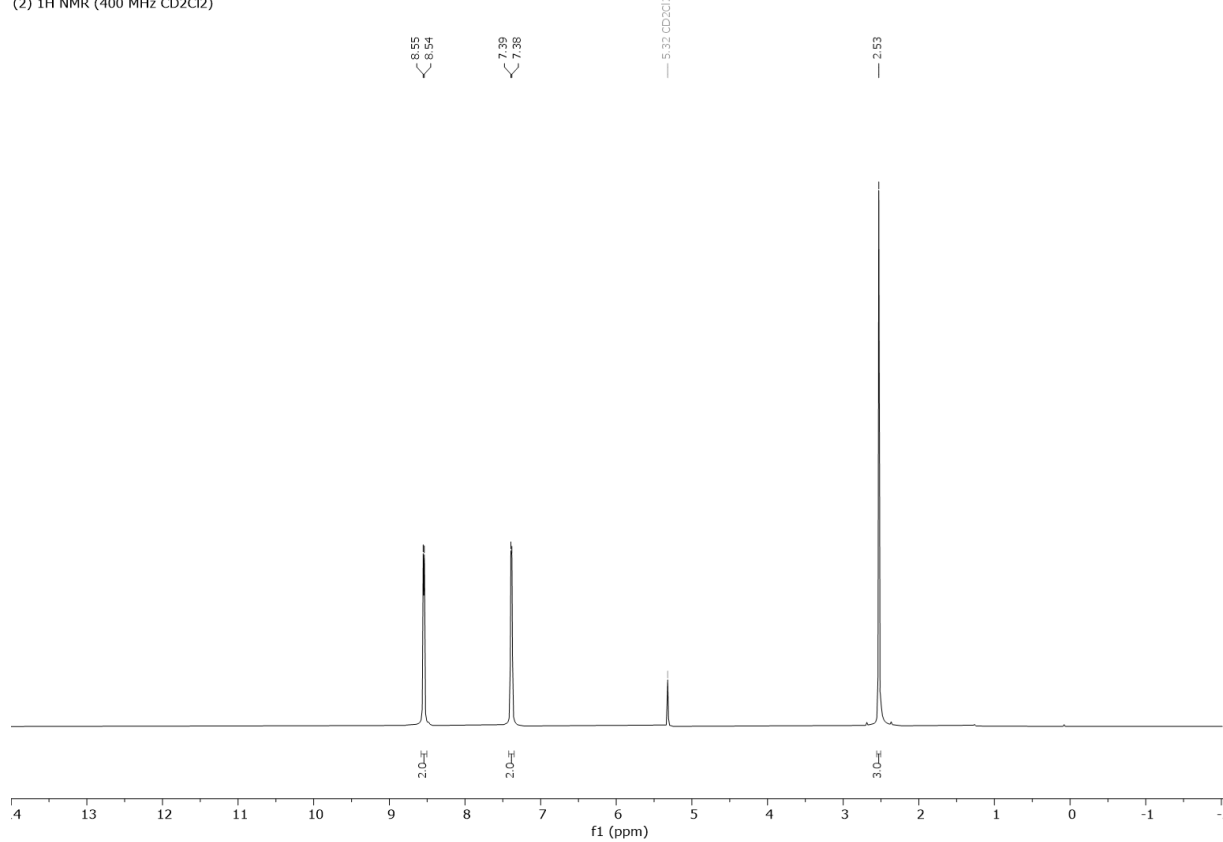


**Figure S8.**  $^1\text{H}$  NMR spectrum of [bis(4-methylpyridine)iodine(I)]hexafluorophosphate (**2**) (400 MHz,  $\text{CD}_2\text{Cl}_2$ , 25°C).

(2)  $^{13}\text{C}$  NMR (101 MHz  $\text{CD}_2\text{Cl}_2$ )

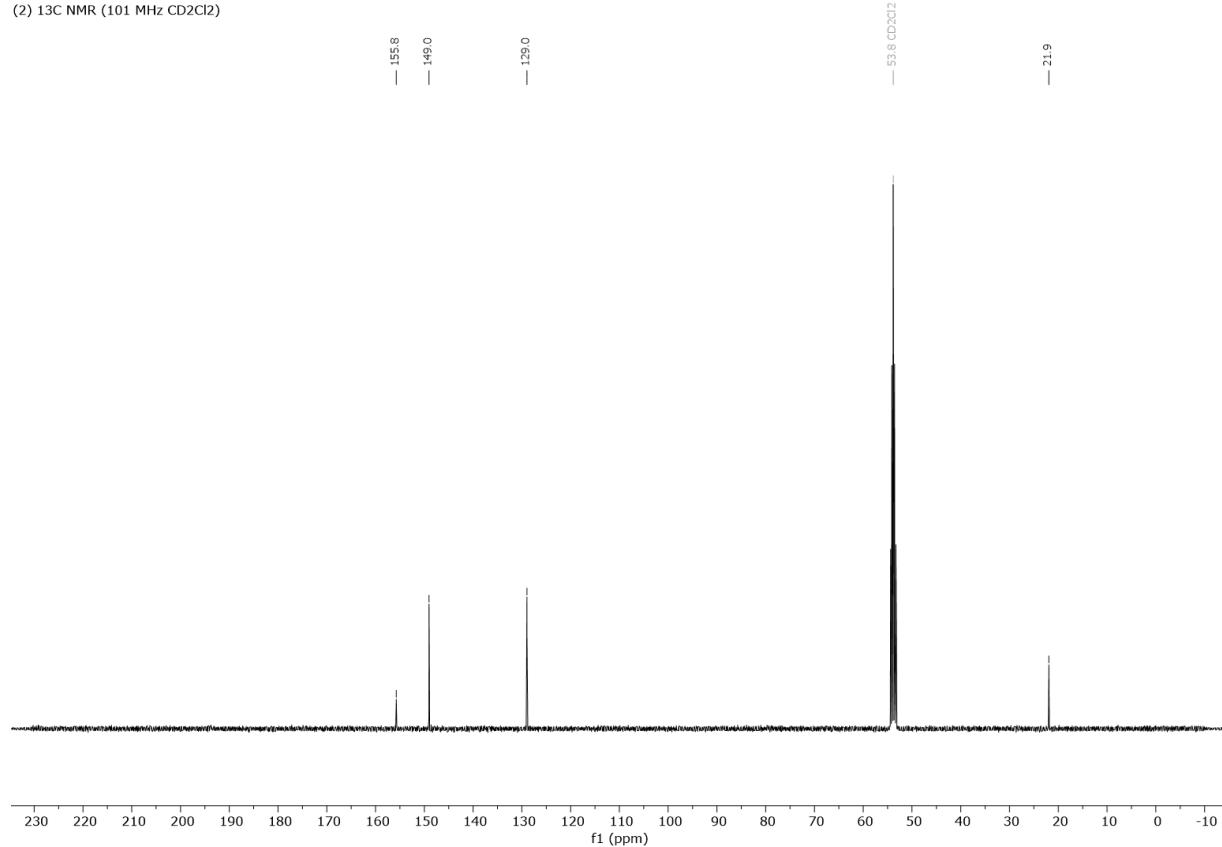


**Figure S9.**  $^{13}\text{C}$  NMR spectrum of [bis(4-methylpyridine)iodine(I)]hexafluorophosphate (**2**) (101 MHz,  $\text{CD}_2\text{Cl}_2$ , 25°C).

(2)  $^1\text{H}$  NMR (for  $^1\text{H}$ - $^{15}\text{N}$  HMBC) (400 MHz  $\text{CD}_2\text{Cl}_2$ )

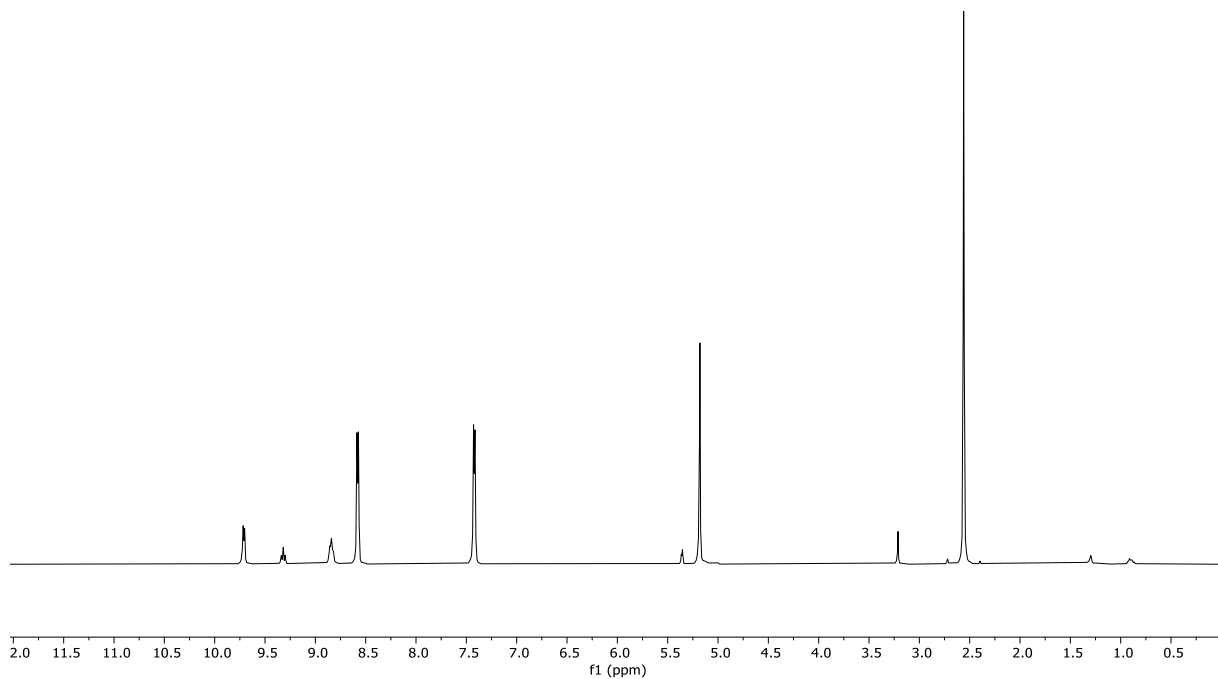


**Figure S10.**  $^1\text{H}$  NMR spectrum of [bis(4-methylpyridine)iodine(I)]hexafluorophosphate (**2**), with capillary of 1-methylpyridinium iodide in  $\text{CD}_3\text{CN}$  (400 MHz,  $\text{CD}_2\text{Cl}_2$ , 25°C).

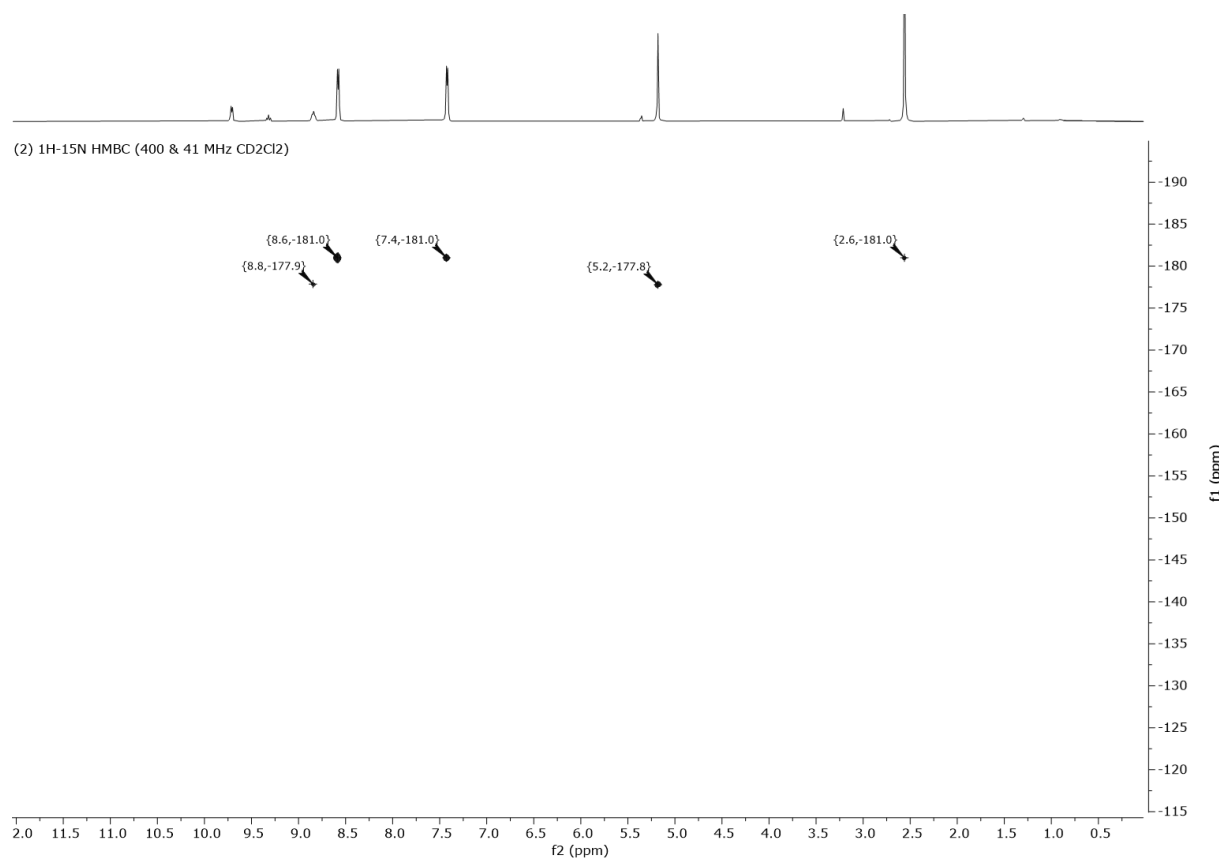


**Figure S11.** <sup>1</sup>H-<sup>15</sup>N HMBC NMR spectrum of [bis(4-methylpyridine)iodine(I)]hexafluorophosphate (**2**), with capillary of 1-methylpyridinium iodide in CD<sub>3</sub>CN (400 & 41 MHz, CD<sub>2</sub>Cl<sub>2</sub>, 25°C).

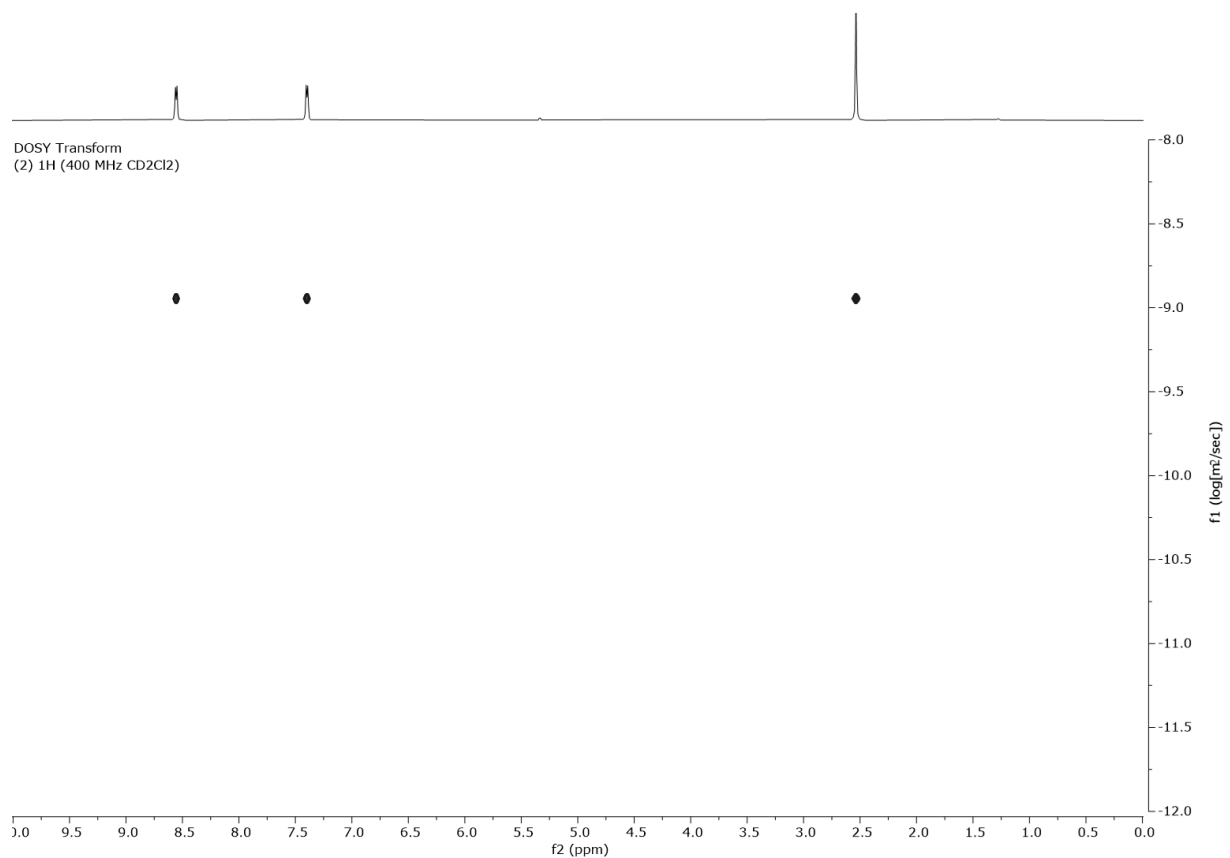


**Figure S12.** <sup>1</sup>H DOSY Transform NMR spectrum of [bis(4-methylpyridine)iodine(I)]hexafluorophosphate (**2**) (400 MHz, CD<sub>2</sub>Cl<sub>2</sub>, 25°C).

(2)  $^{19}\text{F}$  NMR (376 MHz  $\text{CD}_2\text{Cl}_2$ )

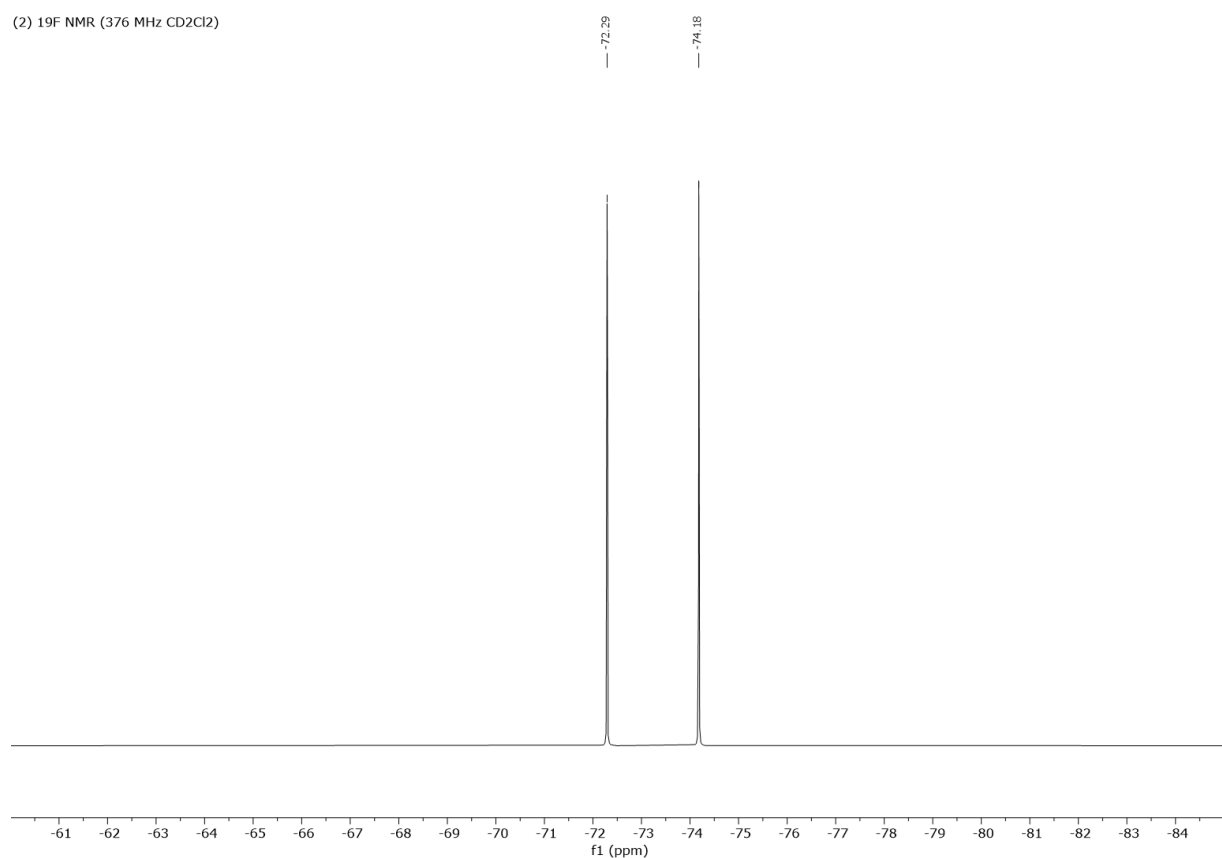


**Figure S13.**  $^{19}\text{F}$  NMR spectrum of [bis(4-methylpyridine)iodine(I)]hexafluorophosphate (**2**) (376 MHz,  $\text{CD}_2\text{Cl}_2$ , 25°C).

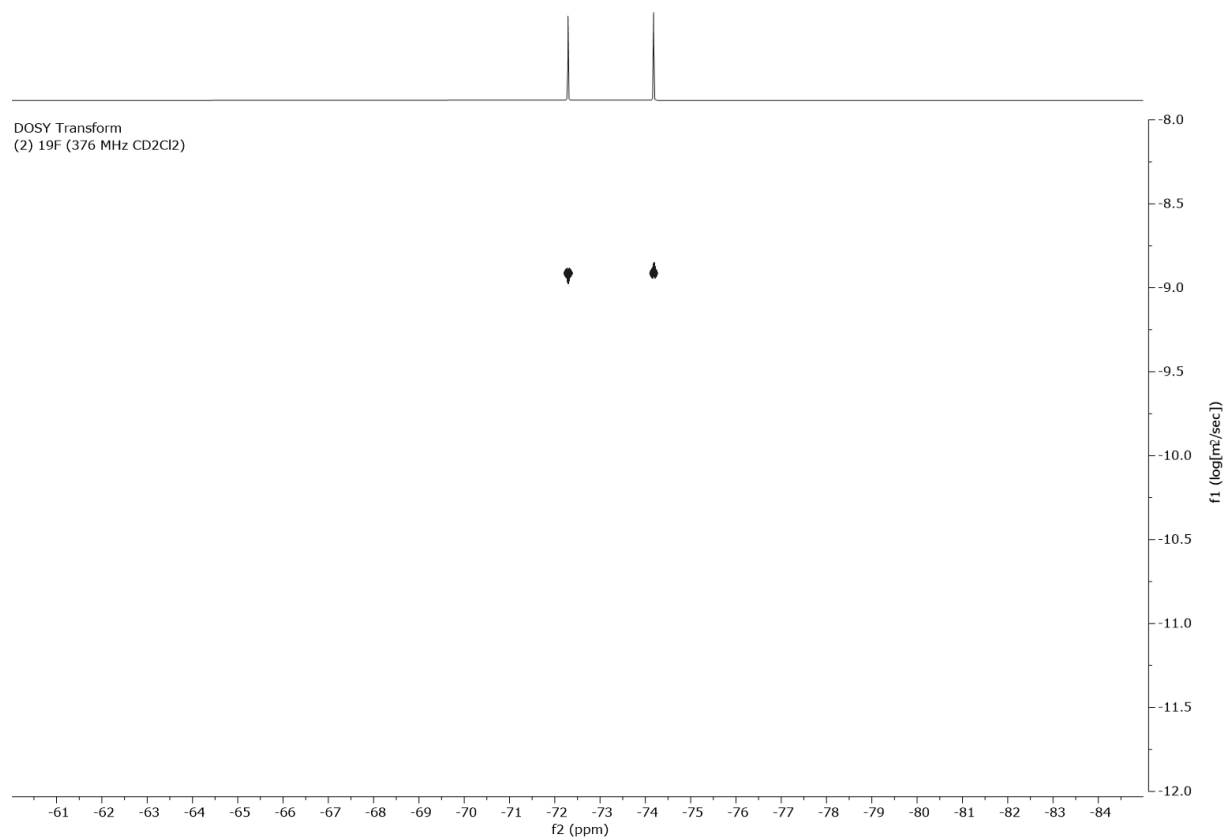


**Figure S14.**  $^{19}\text{F}$  DOSY Transform NMR spectrum of [bis(4-methylpyridine)iodine(I)]hexafluorophosphate (**2**) (376 MHz,  $\text{CD}_2\text{Cl}_2$ , 25°C).

(3)  $^1\text{H}$  NMR (400 MHz  $\text{CD}_2\text{Cl}_2$ )

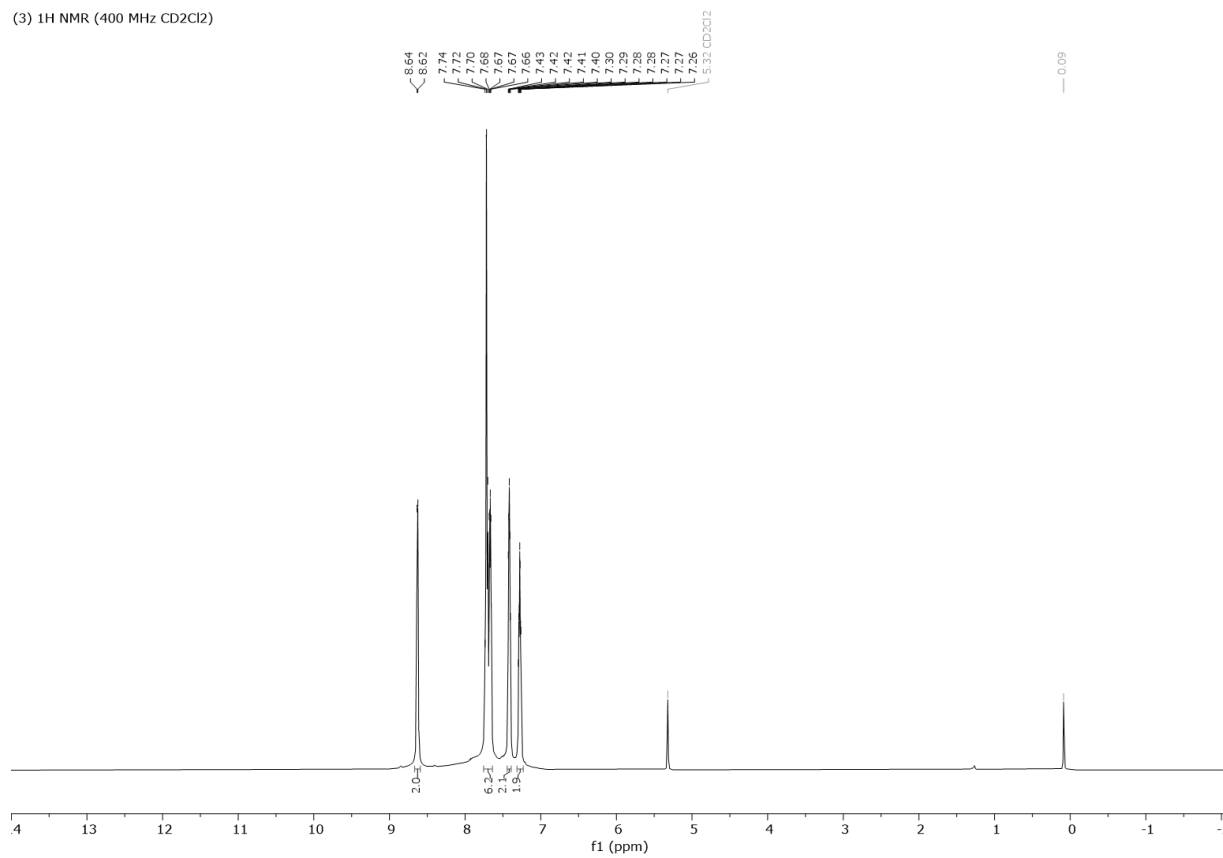


**Figure S15.**  $^1\text{H}$  NMR spectrum of 1,2-bis(pyridin-2-ylethynyl)benzene (**3**) (400 MHz,  $\text{CD}_2\text{Cl}_2$ , 25 °C).

(3)  $^{13}\text{C}$  NMR (101 MHz  $\text{CD}_2\text{Cl}_2$ )

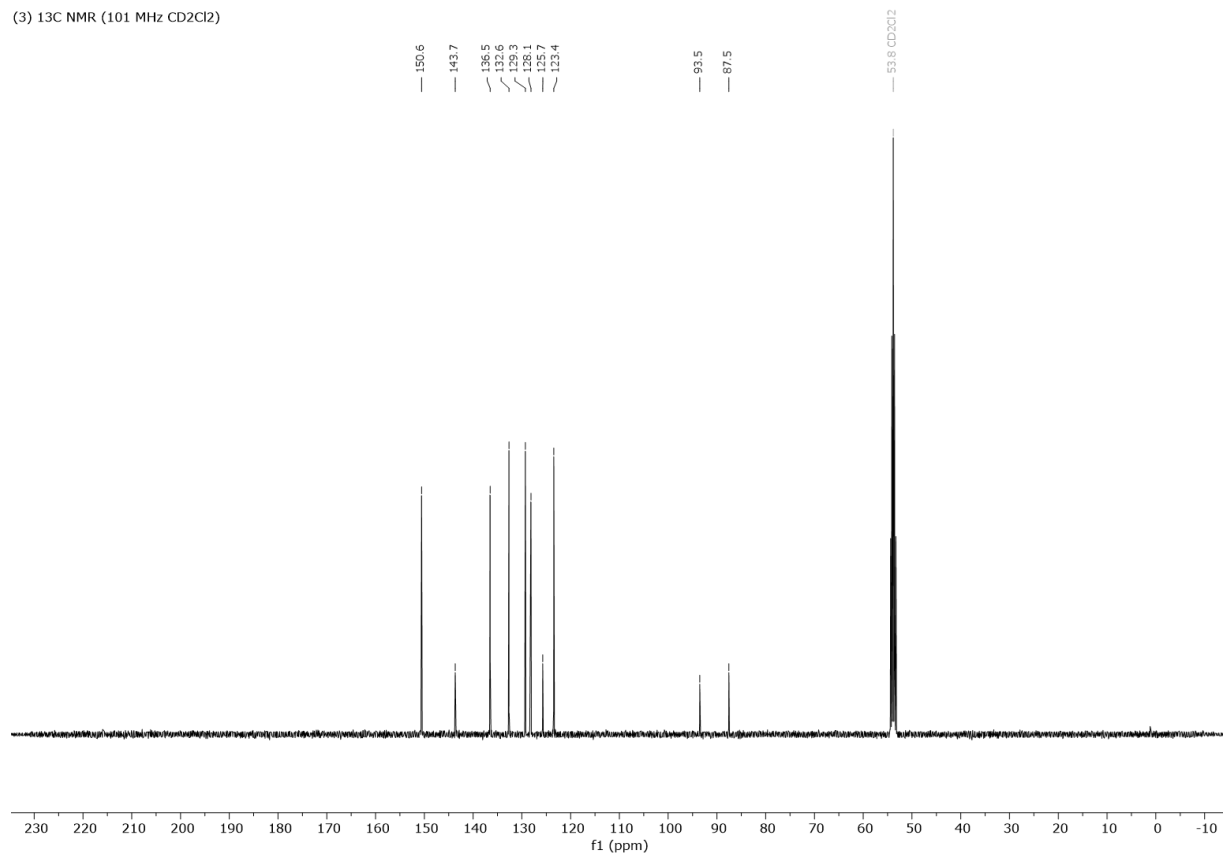


**Figure S16.**  $^{13}\text{C}$  NMR spectrum of 1,2-bis(pyridin-2-ylethynyl)benzene (3) (101 MHz,  $\text{CD}_2\text{Cl}_2$ , 25°C).

(4)  $^1\text{H}$  NMR (400 MHz  $\text{CD}_2\text{Cl}_2$ )

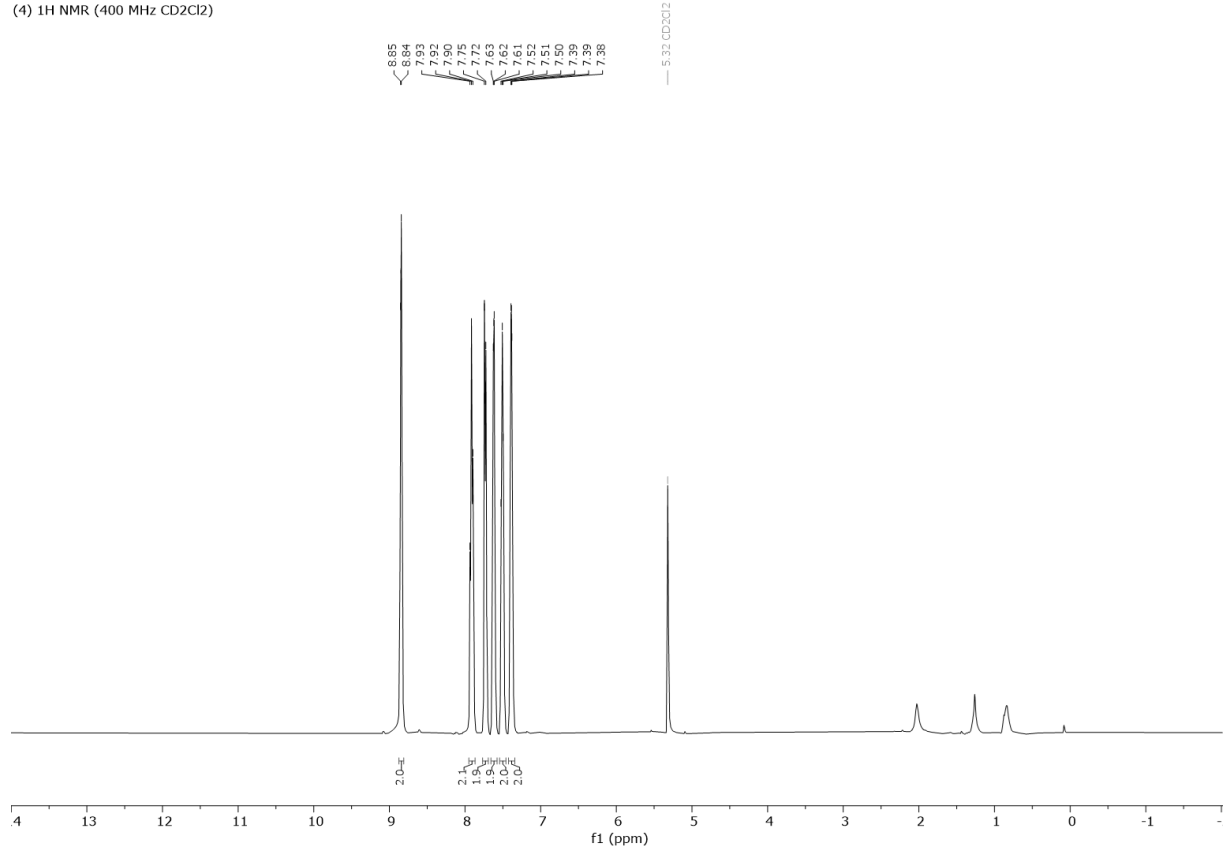


**Figure S17.**  $^1\text{H}$  NMR spectrum of  $[(1,2\text{-bis}(\text{pyridin}-2\text{-ylethynyl})\text{benzene})\text{silver}(\text{I})]\text{tetrafluoroborate}$  (4) (400 MHz,  $\text{CD}_2\text{Cl}_2$ , 25°C).

(4)  $^{13}\text{C}$  NMR (101 MHz  $\text{CD}_2\text{Cl}_2$ )

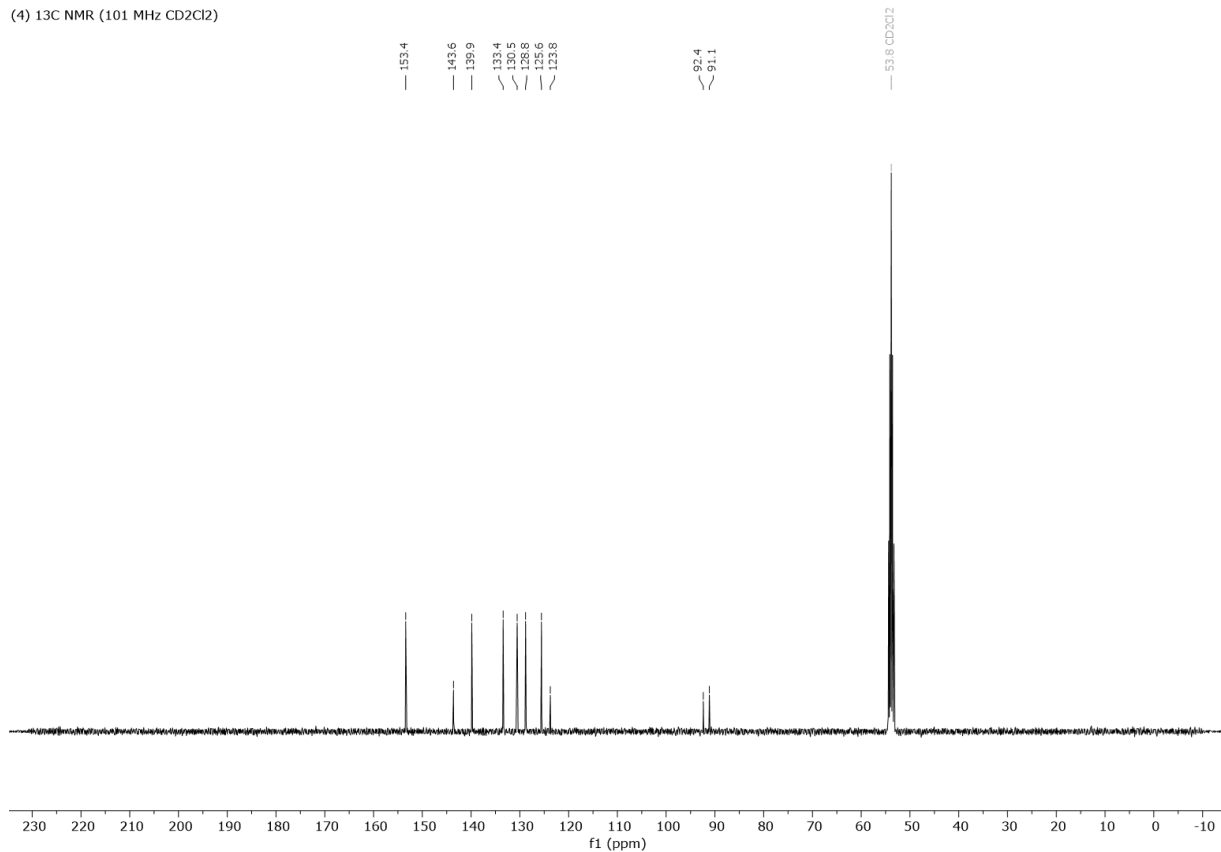


**Figure S18.**  $^{13}\text{C}$  NMR spectrum of  $[(1,2\text{-bis}(\text{pyridin}-2\text{-ylethynyl})\text{benzene})\text{silver}(\text{I})]\text{tetrafluoroborate}$  (4) (101 MHz,  $\text{CD}_2\text{Cl}_2$ , 25°C).

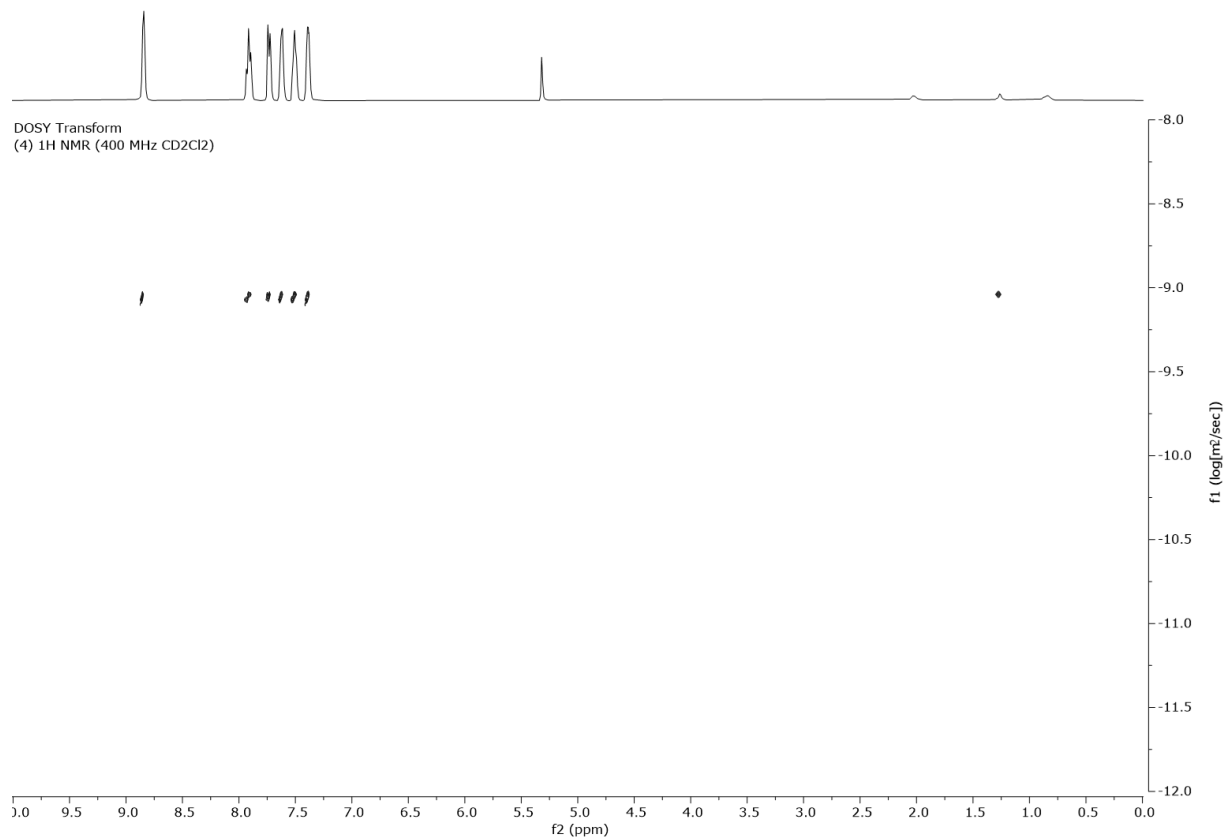


**Figure S19.**  $^1\text{H}$  DOSY Transform NMR spectrum of [(1,2-bis(pyridin-2-ylethynyl)benzene)silver(I)]tetrafluoroborate (**4**) (400 MHz,  $\text{CD}_2\text{Cl}_2$ , 25°C).

(5)  $^1\text{H}$  NMR (400 MHz CD<sub>2</sub>Cl<sub>2</sub>)

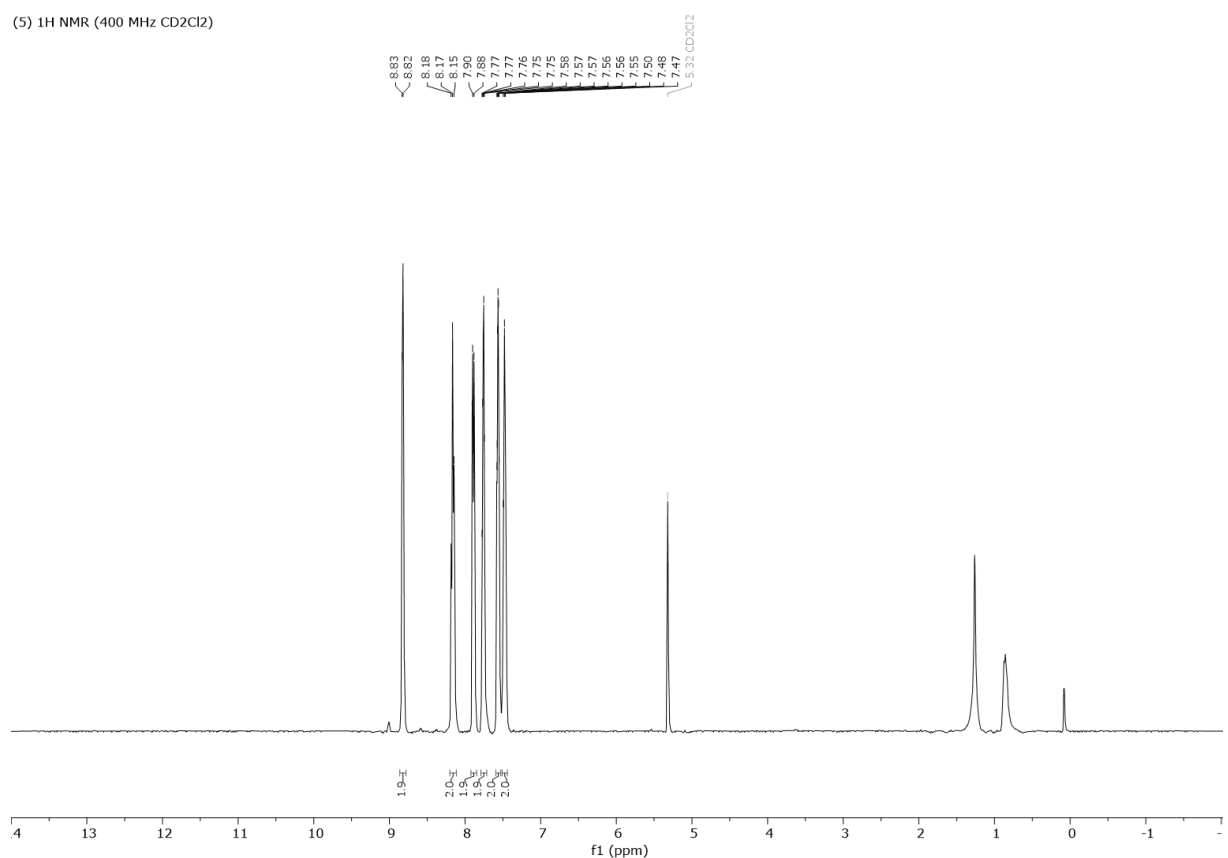


**Figure S20.**  $^1\text{H}$  NMR spectrum of [(1,2-bis(pyridin-2-ylethynyl)benzene)iodine(I)]tetrafluoroborate (**5**) (400 MHz,  $\text{CD}_2\text{Cl}_2$ , 25°C).

(5)  $^{13}\text{C}$  NMR (101 MHz  $\text{CD}_2\text{Cl}_2$ )

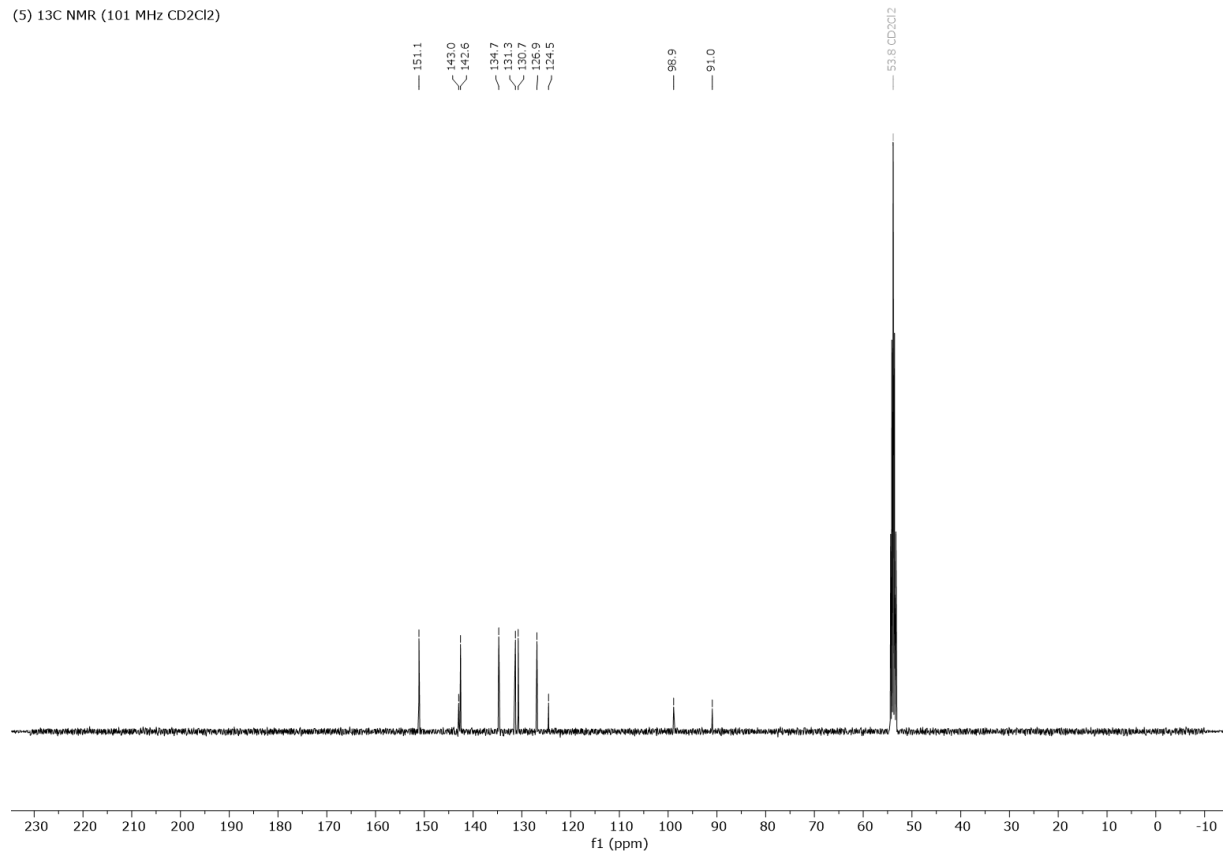


**Figure S21.**  $^{13}\text{C}$  NMR spectrum of  $[(1,2\text{-bis}(\text{pyridin}-2\text{-ylethynyl})\text{benzene})\text{iodine}(I)]\text{tetrafluoroborate}$  (5) (101 MHz,  $\text{CD}_2\text{Cl}_2$ , 25°C).

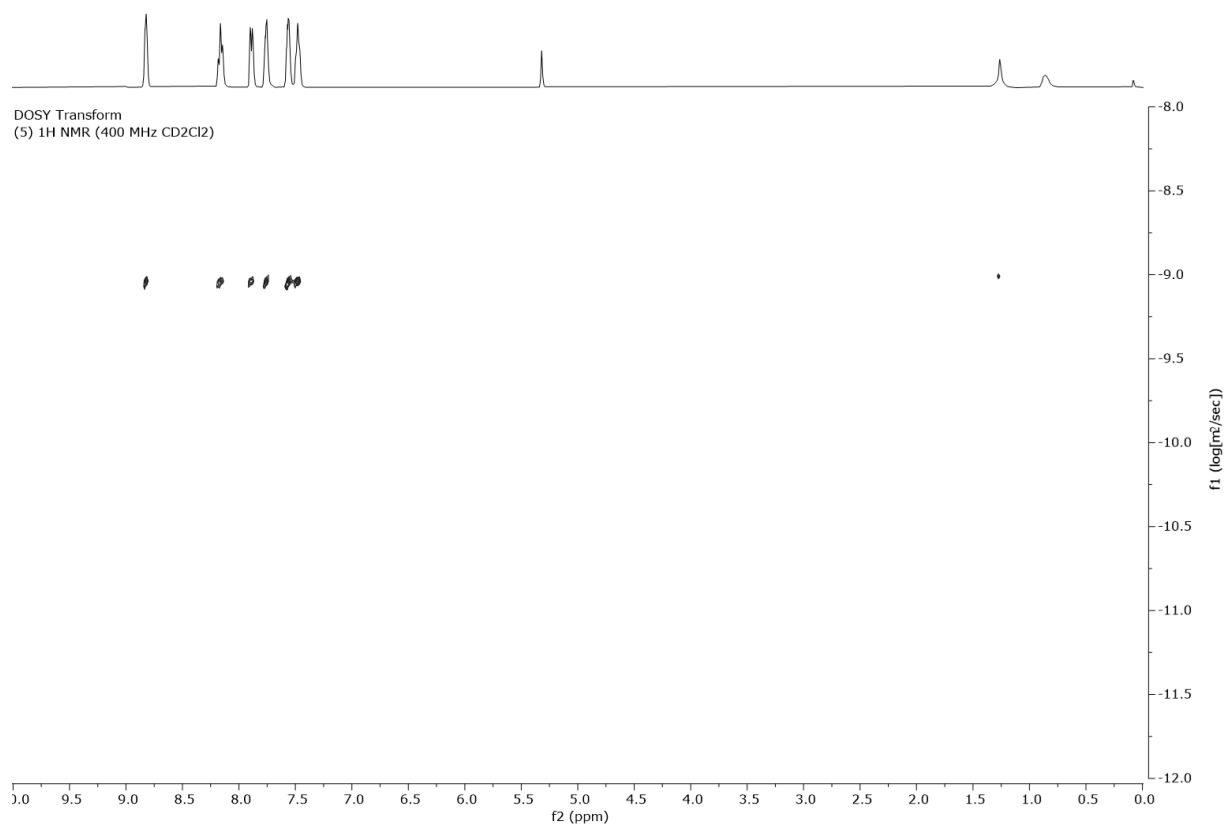


**Figure S22.**  $^1\text{H}$  DOSY Transform NMR spectrum of [(1,2-bis(pyridin-2-ylethynyl)benzene)iodine(I)] tetrafluoroborate (**5**) (400 MHz,  $\text{CD}_2\text{Cl}_2$ , 25°C).

## 2.2 Mixtures of Complexes & Addition of Reagents

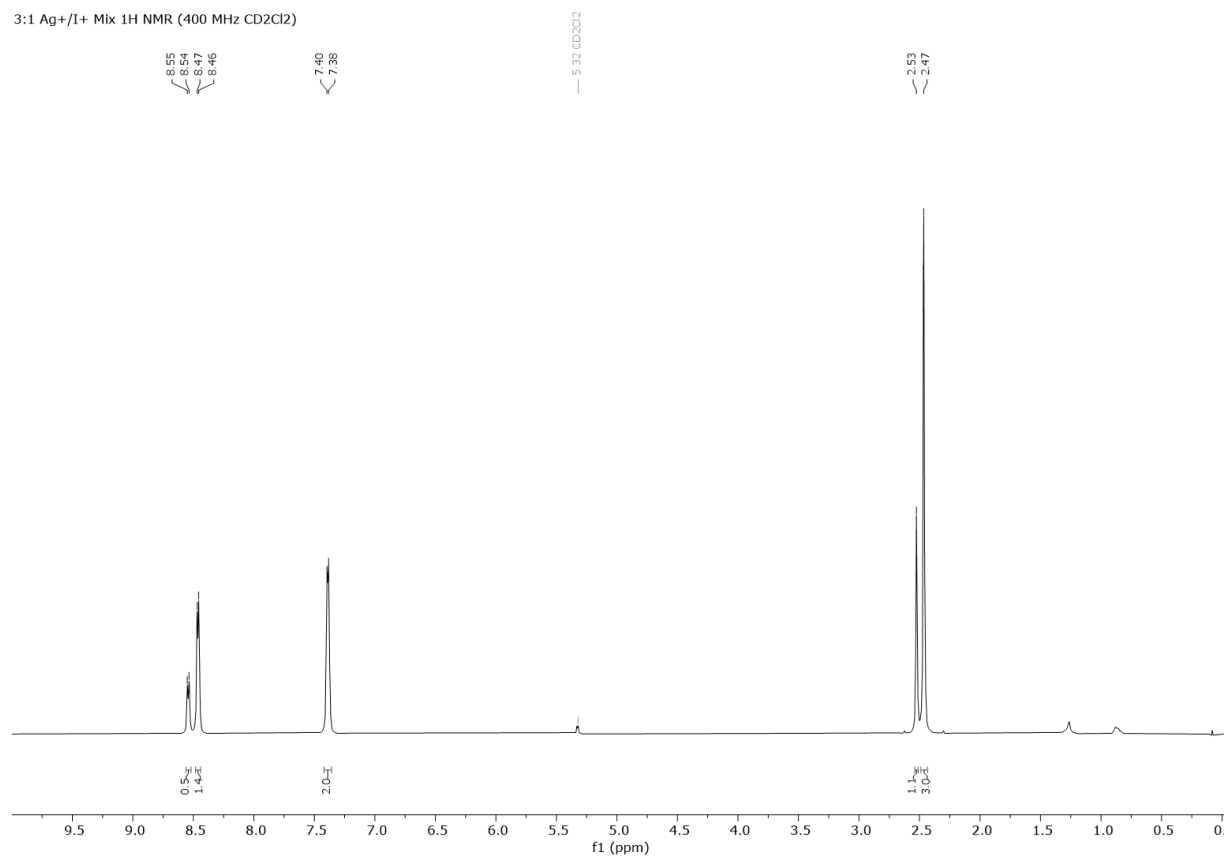


**Figure S23.** <sup>1</sup>H NMR spectrum of a 3:1 mixture of [bis(4-methylpyridine)silver(I)]hexafluorophosphate (**1**) and [Bis(4-methylpyridine)iodine(I)]hexafluorophosphate (**2**) (400 MHz, CD<sub>2</sub>Cl<sub>2</sub>, 25°C).

3:1 Ag+/I+ Mix 1H (for 1H-15N HMBC) (400 & 41 MHz CD<sub>2</sub>Cl<sub>2</sub>)

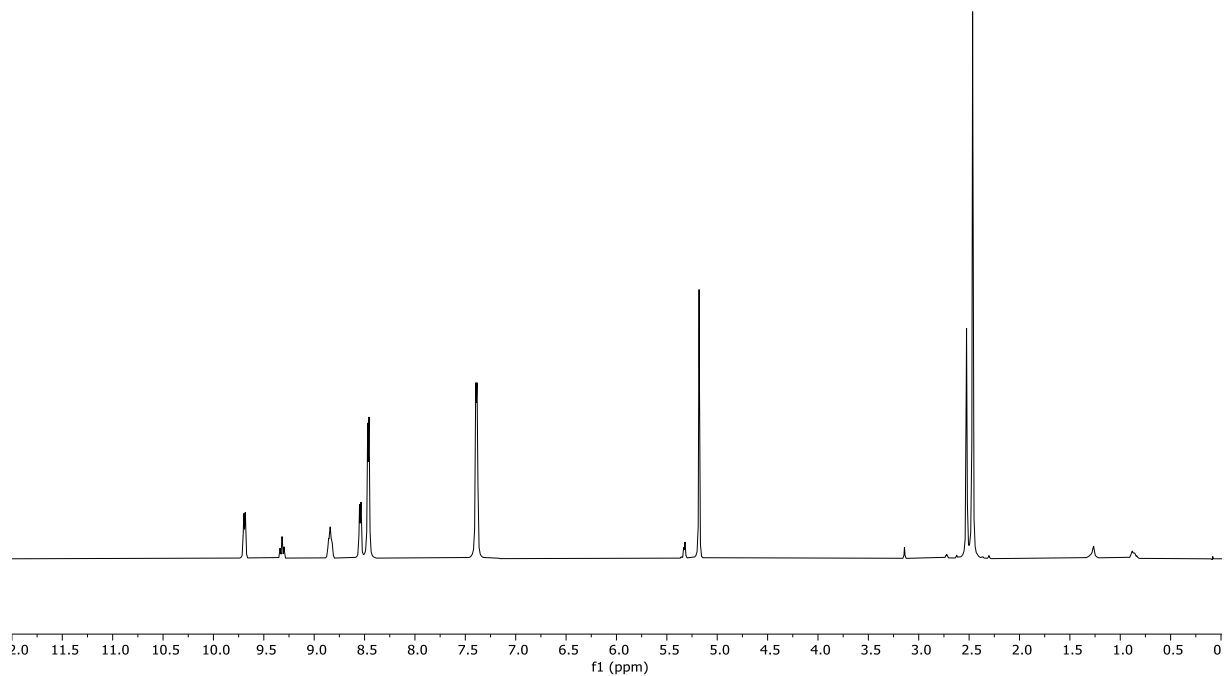


**Figure S24.** <sup>1</sup>H NMR spectrum of a 3:1 mixture of [bis(4-methylpyridine)silver(I)]hexafluorophosphate (**1**) and [bis(4-methylpyridine)iodine(I)]hexafluorophosphate (**2**), with capillary of 1-methylpyridinium iodide in CD<sub>3</sub>CN (400 MHz, CD<sub>2</sub>Cl<sub>2</sub>, 25°C).

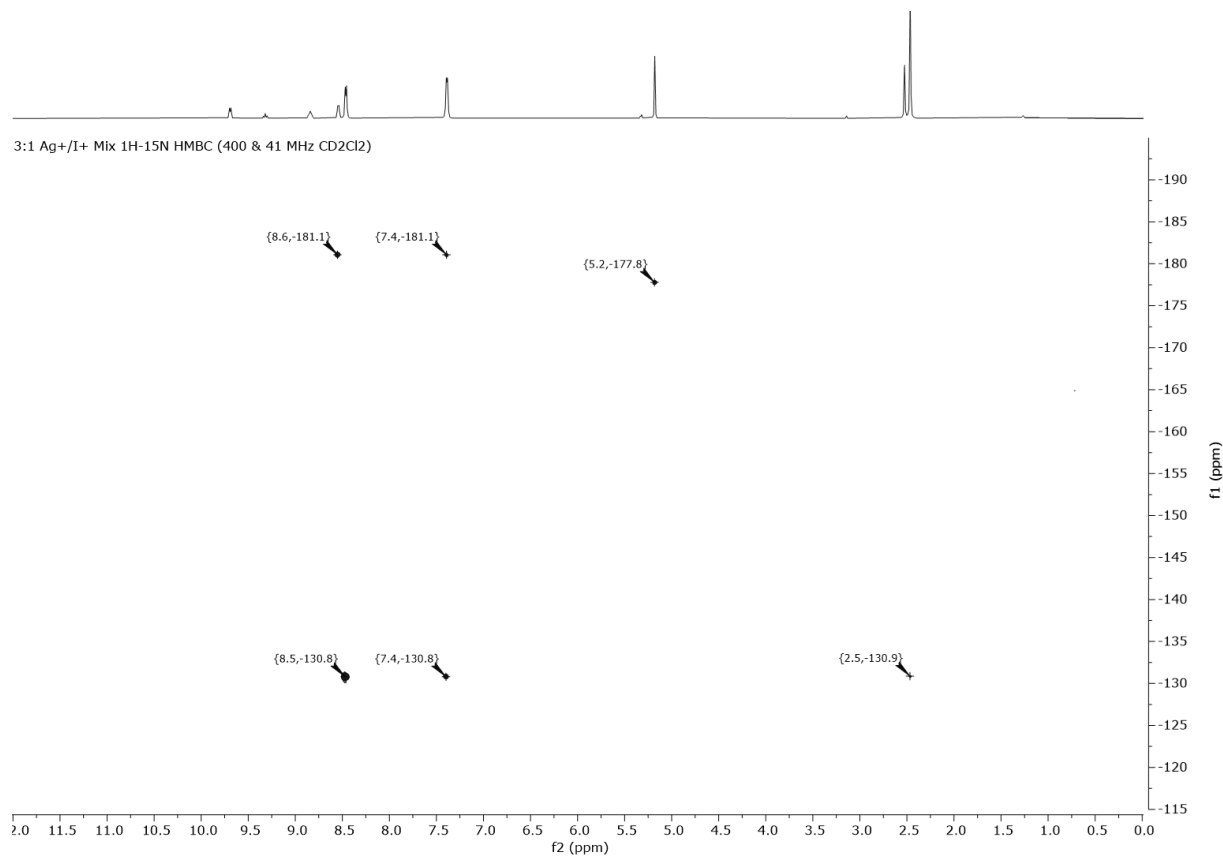


**Figure S25.** <sup>1</sup>H-<sup>15</sup>N HMBC NMR spectrum of a 3:1 mixture of [bis(4-methylpyridine)silver(I)]hexafluorophosphate (**1**) and [bis(4-methylpyridine)iodine(I)]hexafluorophosphate (**2**), with capillary of 1-methylpyridinium iodide in CD<sub>3</sub>CN (400 & 41 MHz, CD<sub>2</sub>Cl<sub>2</sub>, 25°C).

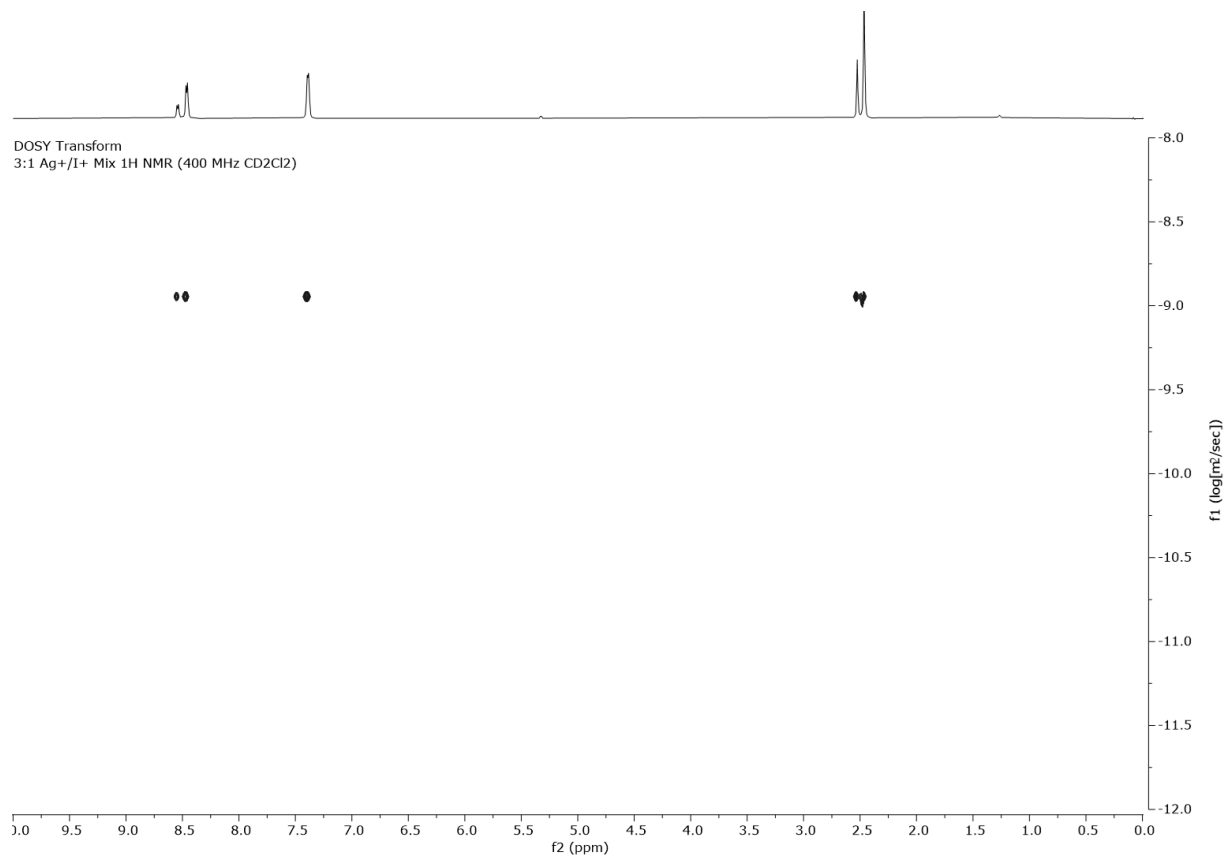


**Figure S26.** <sup>1</sup>H DOSY Transform NMR spectrum of a 3:1 mixture of [bis(4-methylpyridine)silver(I)] hexafluorophosphate (**1**) and [bis(4-methylpyridine)iodine(I)]hexafluorophosphate (**2**) (400 MHz, CD<sub>2</sub>Cl<sub>2</sub>, 25°C).

3:1 Mix Ag+/I+  $^{19}\text{F}$  NMR (376 MHz  $\text{CD}_2\text{Cl}_2$ )

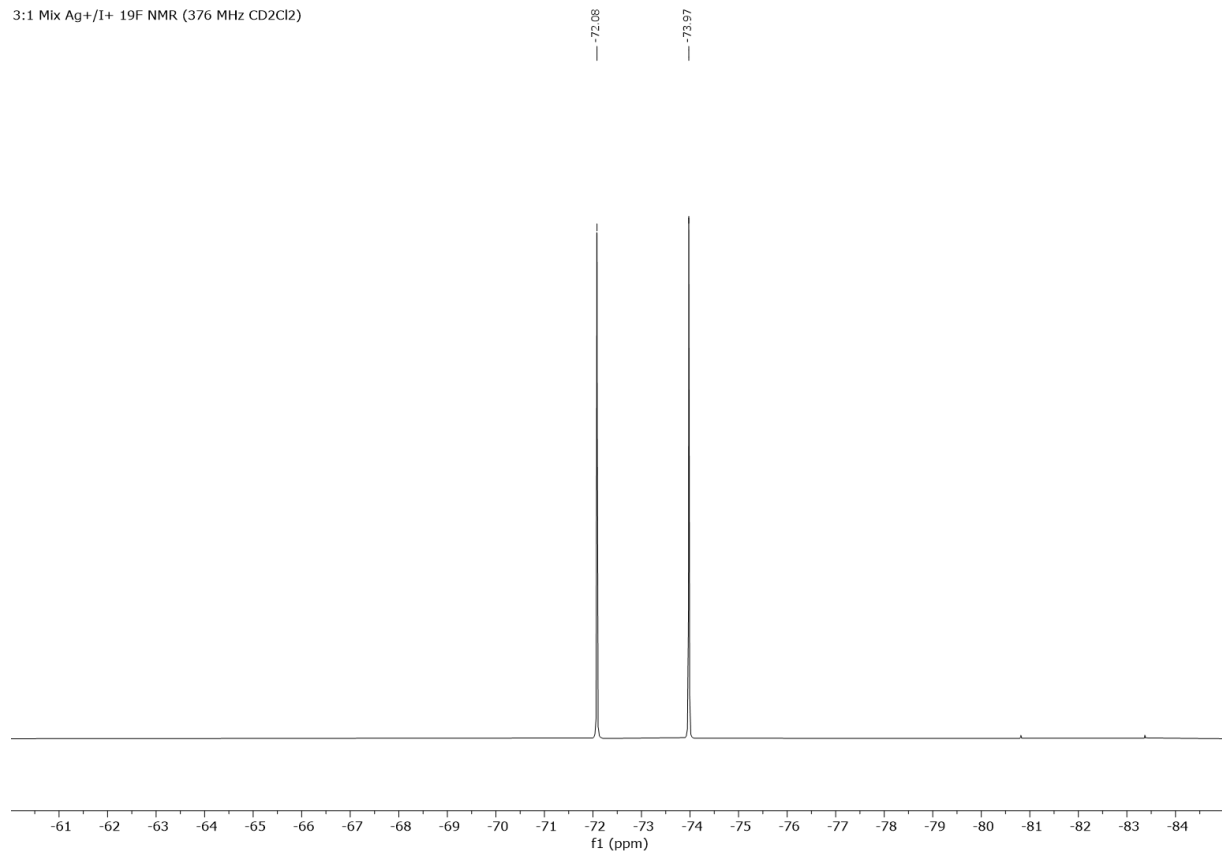


**Figure S27.**  $^{19}\text{F}$  NMR spectrum of a 3:1 mixture of [bis(4-methylpyridine)silver(I)]hexafluorophosphate (**1**) and [bis(4-methylpyridine)iodine(I)]hexafluorophosphate (**2**) (376 MHz,  $\text{CD}_2\text{Cl}_2$ , 25°C).

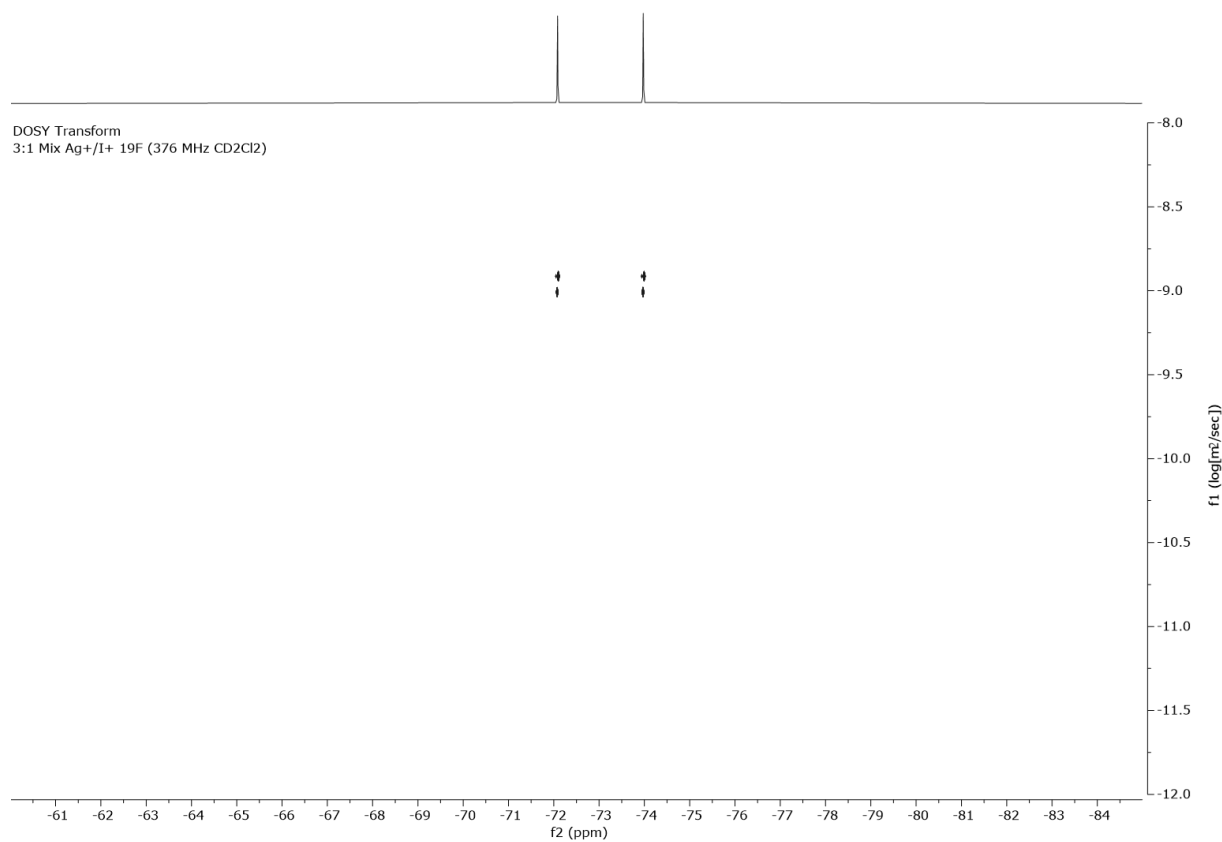


**Figure S28.** <sup>19</sup>F DOSY Transform NMR spectrum of a 3:1 mixture of [bis(4-methylpyridine)silver(I)] hexafluorophosphate (**1**) and [bis(4-methylpyridine)iodine(I)]hexafluorophosphate (**2**) (376 MHz, CD<sub>2</sub>Cl<sub>2</sub>, 25°C).

2:2 Ag+/I+ Mix 1H (400 MHz CD<sub>2</sub>Cl<sub>2</sub>)

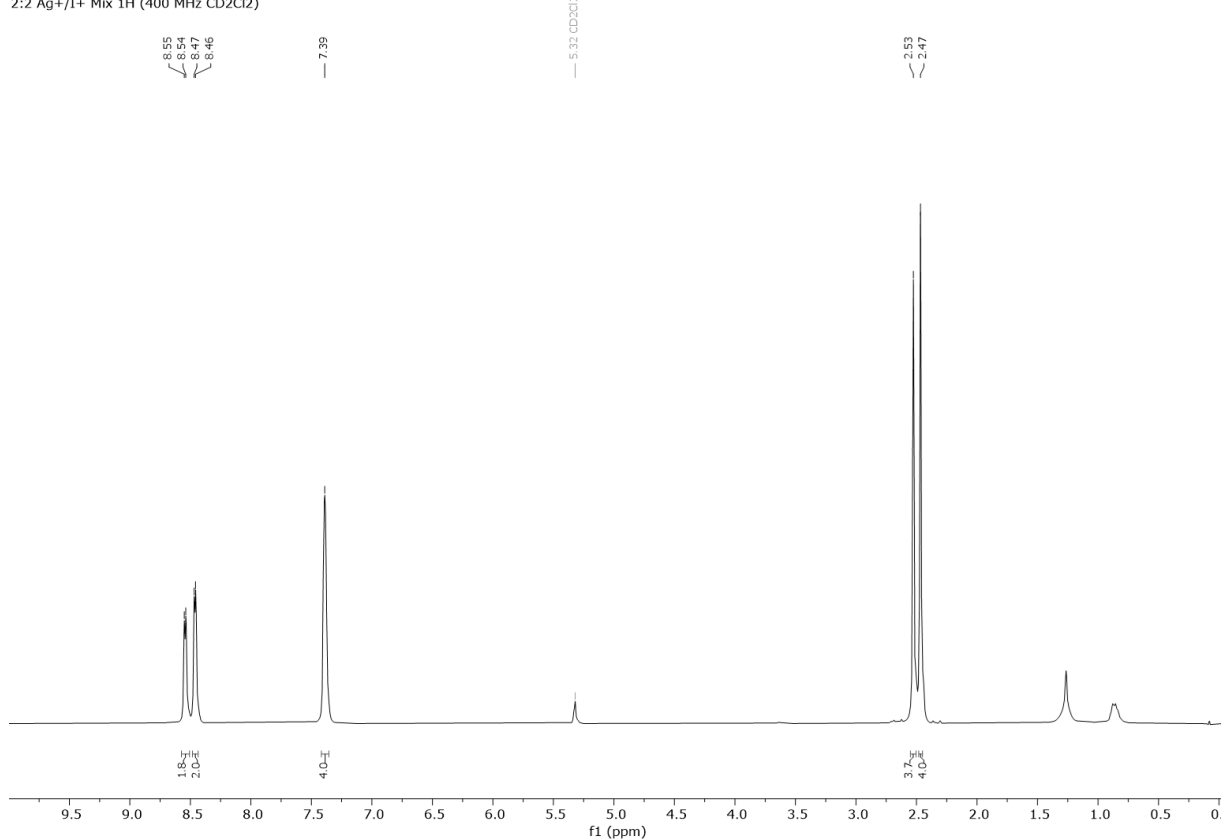


**Figure S29.** <sup>1</sup>H NMR spectrum of a 2:2 mixture of [bis(4-methylpyridine)silver(I)]hexafluorophosphate (**1**) and [bis(4-methylpyridine)iodine(I)]hexafluorophosphate (**2**) (400 MHz, CD<sub>2</sub>Cl<sub>2</sub>, 25°C).

2:2 Ag+/I+ Mix 1H (for 1H-15N HMBC) (400 & 41 MHz CD<sub>2</sub>Cl<sub>2</sub>)

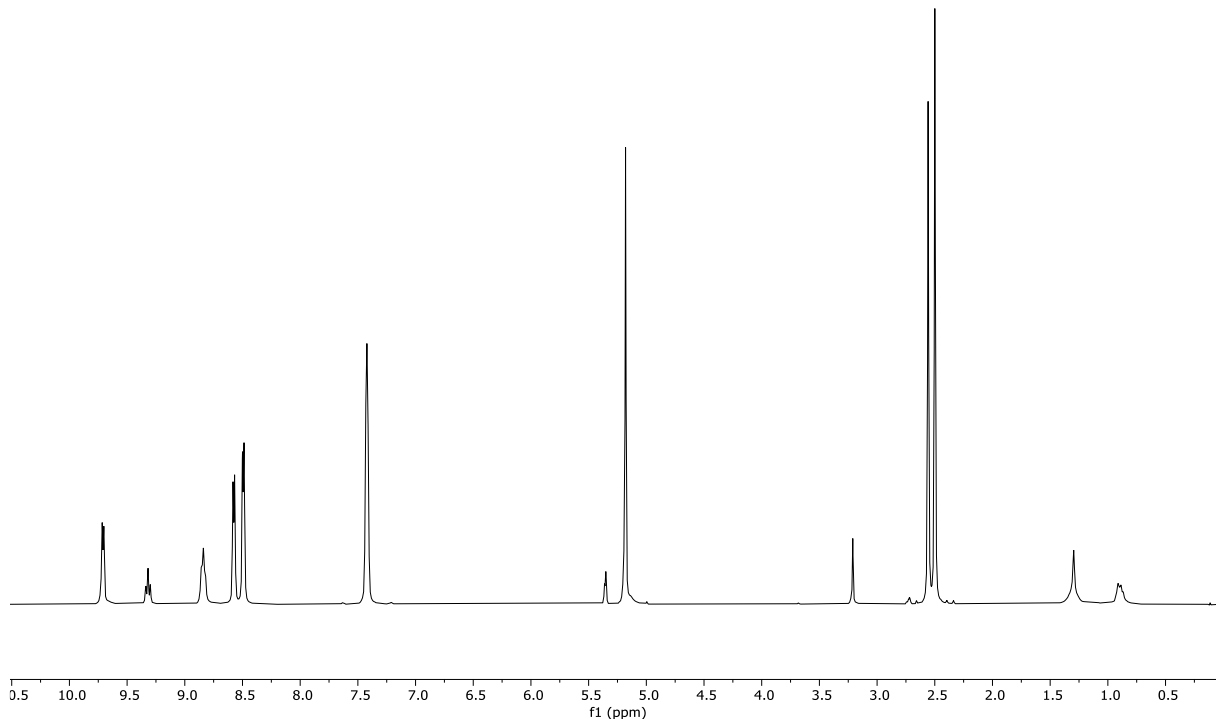


**Figure S30.**  $^1\text{H}$ - $^{15}\text{N}$  HMBC NMR spectrum of a 2:2 mixture of [bis(4-methylpyridine)silver(I)]hexafluorophosphate (**1**) and [bis(4-methylpyridine)iodine(I)]hexafluorophosphate (**2**), with capillary of 1-methylpyridinium iodide in CD<sub>3</sub>CN (400 MHz, CD<sub>2</sub>Cl<sub>2</sub>, 25°C).

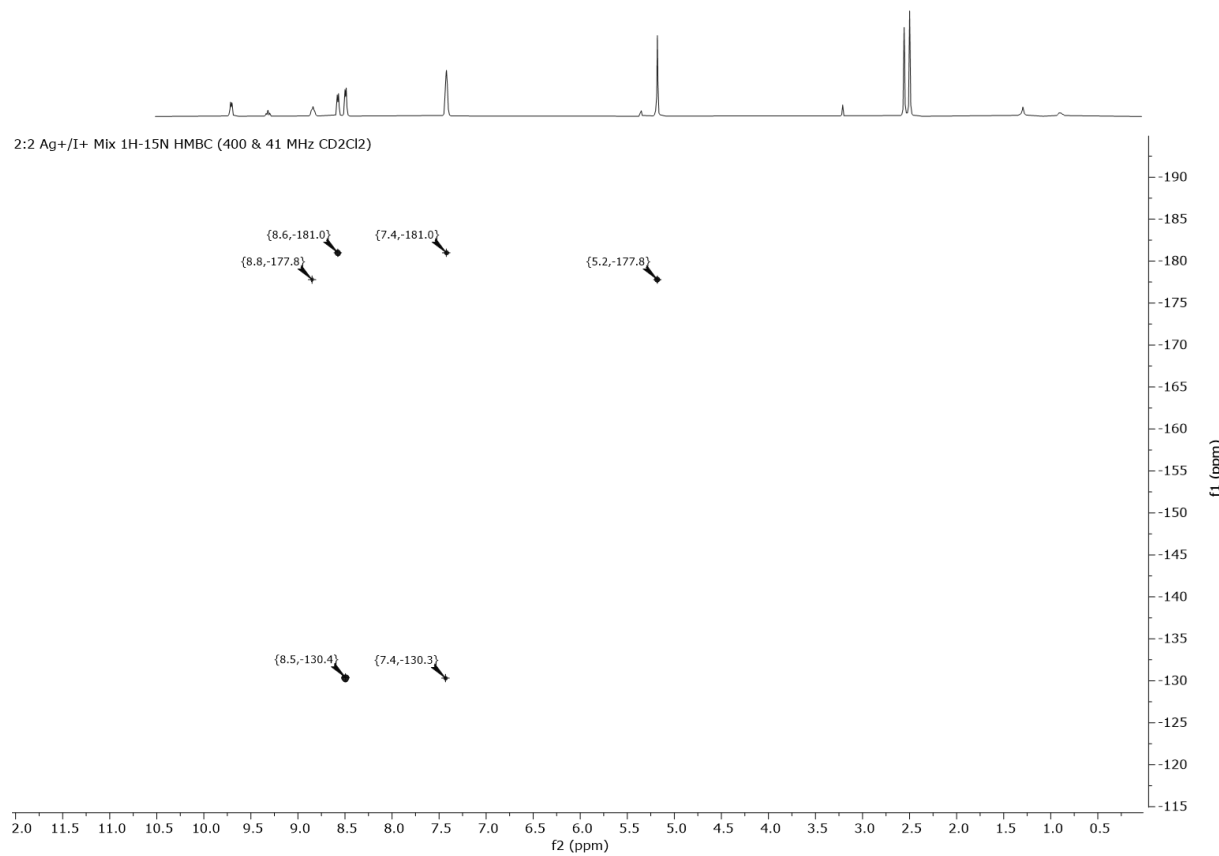


**Figure S31.**  $^1\text{H}$ - $^{15}\text{N}$  HMBC NMR spectrum of a 2:2 mixture of [bis(4-methylpyridine)silver(I)]hexafluorophosphate (**1**) and [bis(4-methylpyridine)iodine(I)]hexafluorophosphate (**2**), with capillary of 1-methylpyridinium iodide in  $\text{CD}_3\text{CN}$  (400 & 41 MHz,  $\text{CD}_2\text{Cl}_2$ , 25°C).

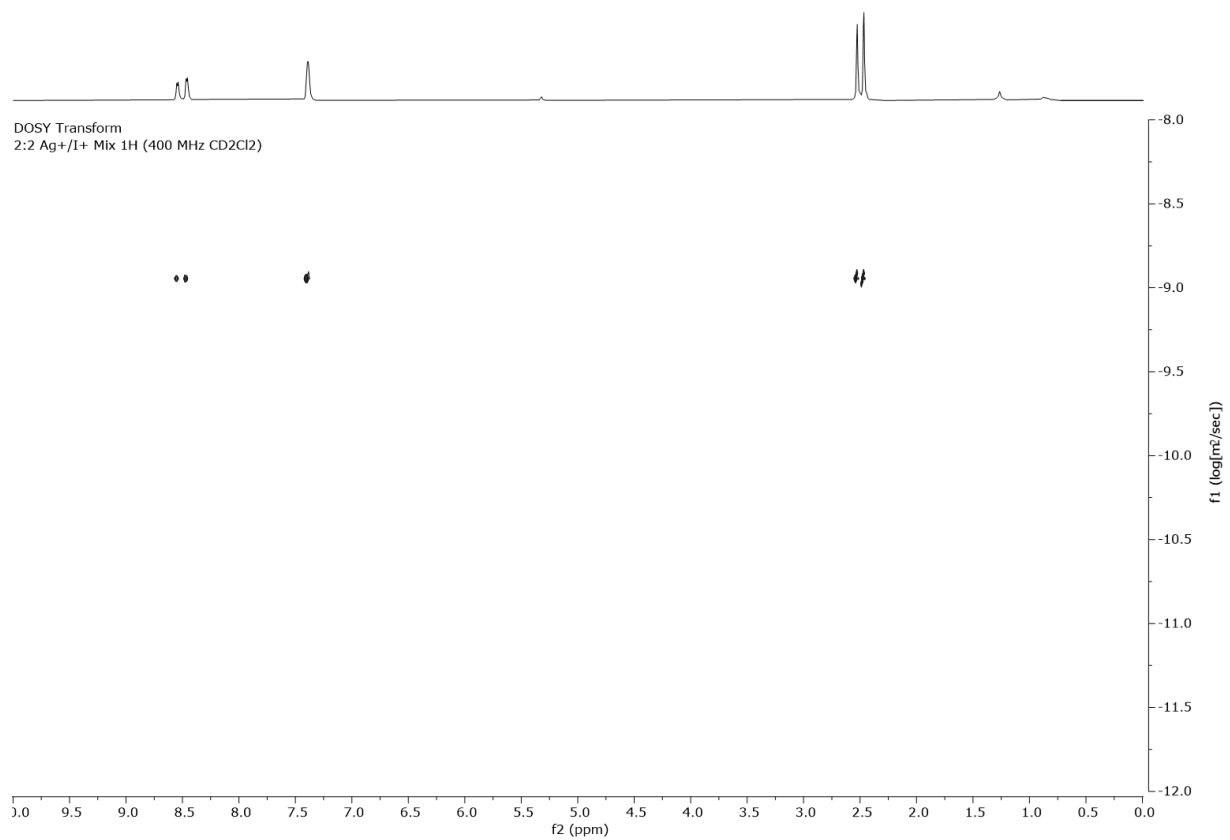


**Figure S32.**  $^1\text{H}$  DOSY Transform NMR spectrum of a 2:2 mixture of [bis(4-methylpyridine)silver(I)]hexafluorophosphate (**1**) and [bis(4-methylpyridine)iodine(I)]hexafluorophosphate (**2**) (400 MHz,  $\text{CD}_2\text{Cl}_2$ , 25°C).

2:2 Mix Ag+/I+  $^{19}\text{F}$  NMR (376 MHz  $\text{CD}_2\text{Cl}_2$ )

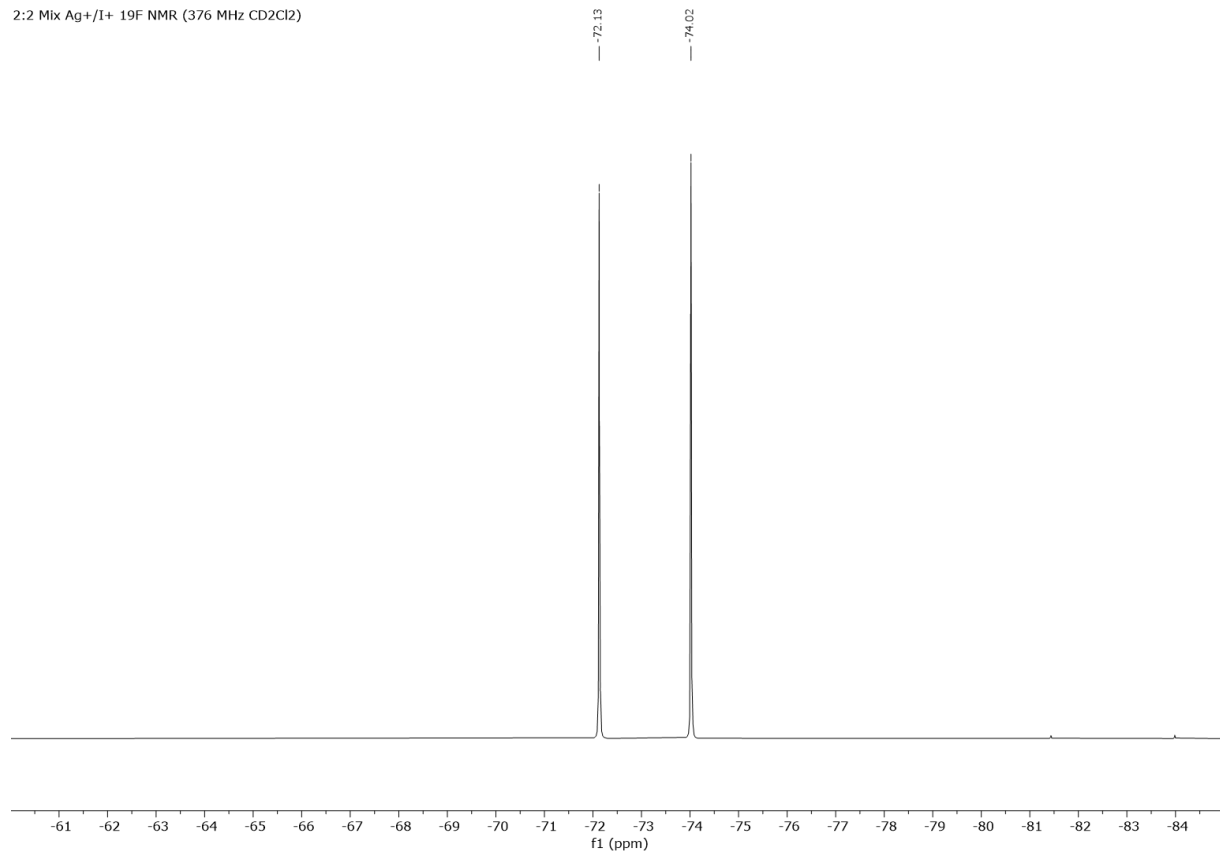


**Figure S33.**  $^{19}\text{F}$  NMR spectrum of a 2:2 mixture of [bis(4-methylpyridine)silver(I)]hexafluorophosphate (**1**) and [bis(4-methylpyridine)iodine(I)]hexafluorophosphate (**2**) (376 MHz,  $\text{CD}_2\text{Cl}_2$ , 25°C).

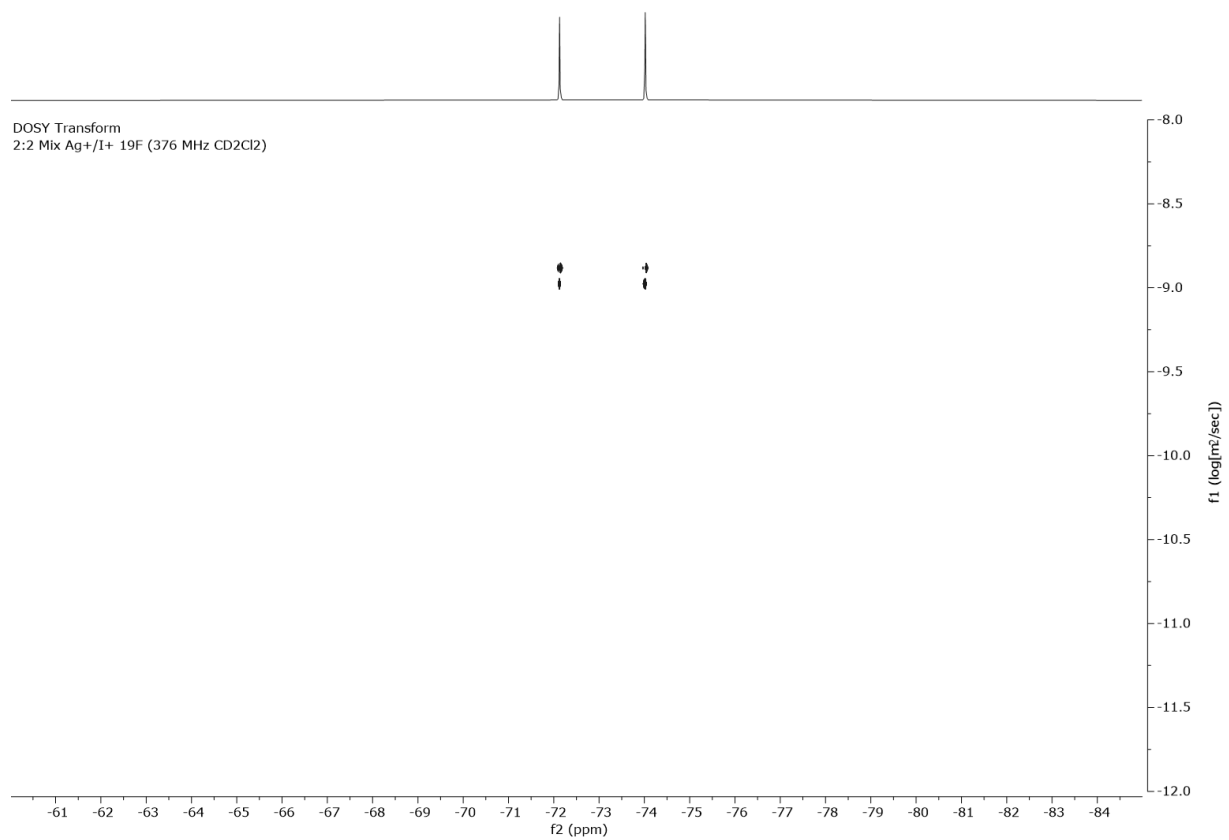


**Figure S34.** <sup>19</sup>F DOSY Transform NMR spectrum of a 2:2 mixture of [bis(4-methylpyridine)silver(I)]hexafluorophosphate (**1**) and [bis(4-methylpyridine)iodine(I)]hexafluorophosphate (**2**) (376 MHz, CD<sub>2</sub>Cl<sub>2</sub>, 25 °C).

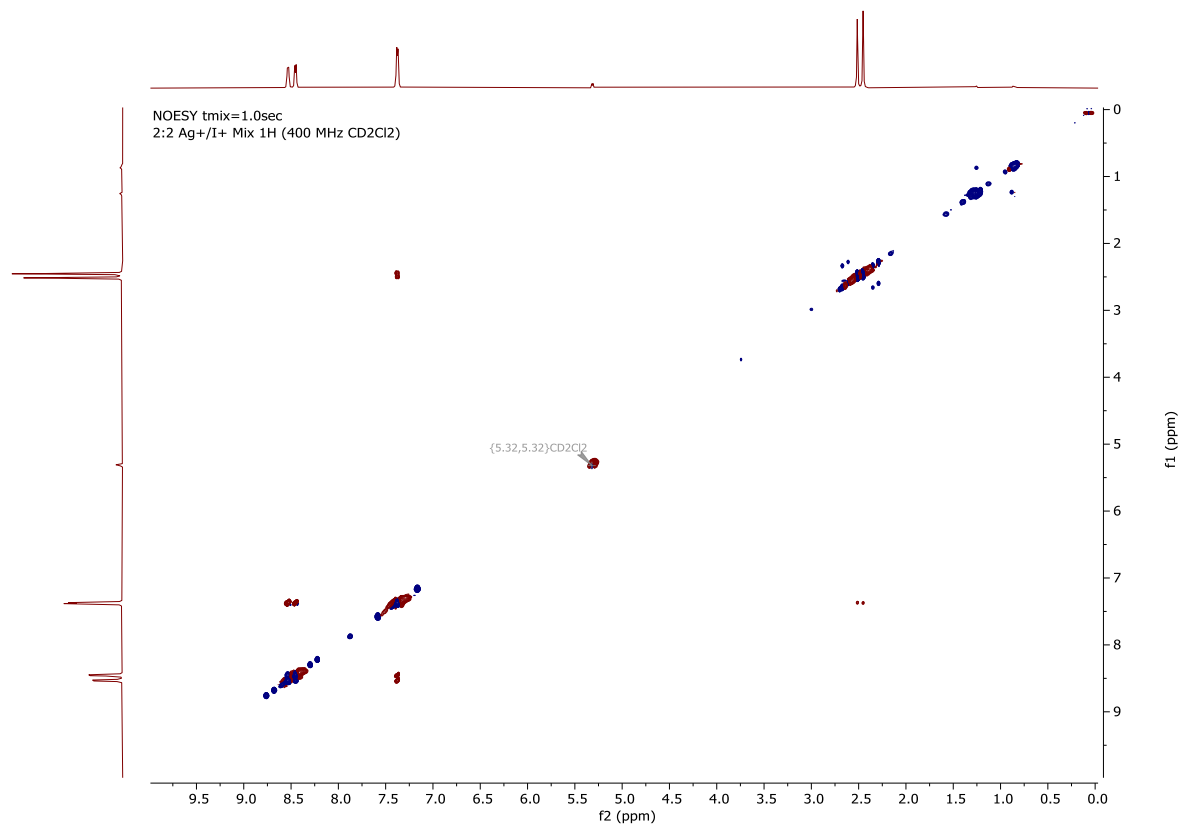


**Figure S35.**  $^1\text{H}$ - $^1\text{H}$  NOESY spectrum of a 2:2 mixture of [bis(4-methylpyridine)silver(I)]hexafluorophosphate (**1**) and [bis(4-methylpyridine)iodine(I)]hexafluorophosphate (**2**),  $t_{\text{mix}} = 1$  s (400 MHz,  $\text{CD}_2\text{Cl}_2$ ,  $25^\circ\text{C}$ ,  $t_{\text{mix}} = 1$  s).

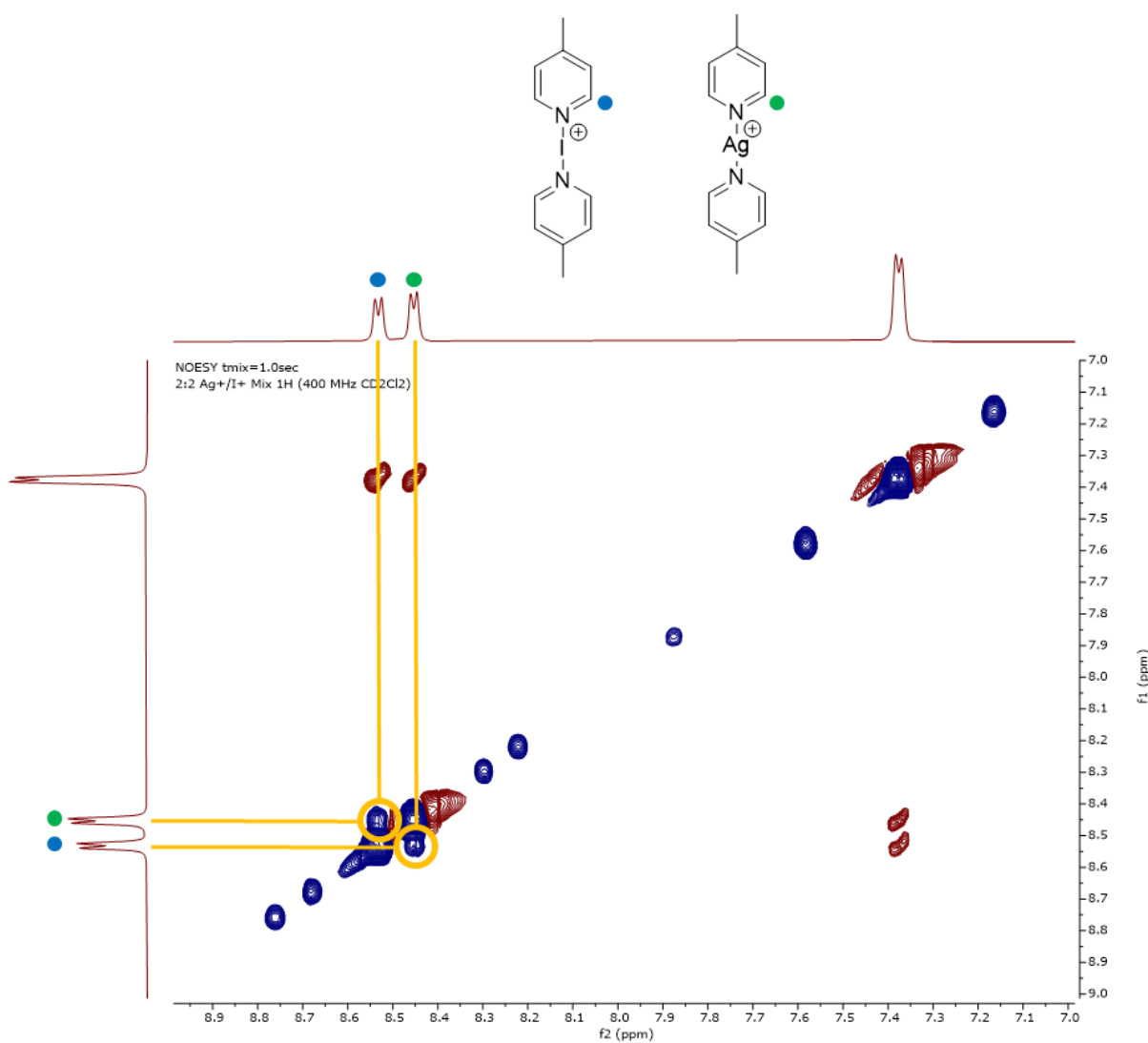


**Figure S36.** Expansion of Fig. S35 showing an EXSY cross-peak between H-2 signals of an equimolar mixture of the two species in solution (400 MHz,  $\text{CD}_2\text{Cl}_2$ , 25 °C,  $t_{mix} = 1\text{ s}$ ). The EXSY cross-peak between the signals of the two complexes reveals 4-methylpyridine exchange during the mixing time.

1:3 Ag+/I+ Mix 1H (400 MHz CD<sub>2</sub>Cl<sub>2</sub>)

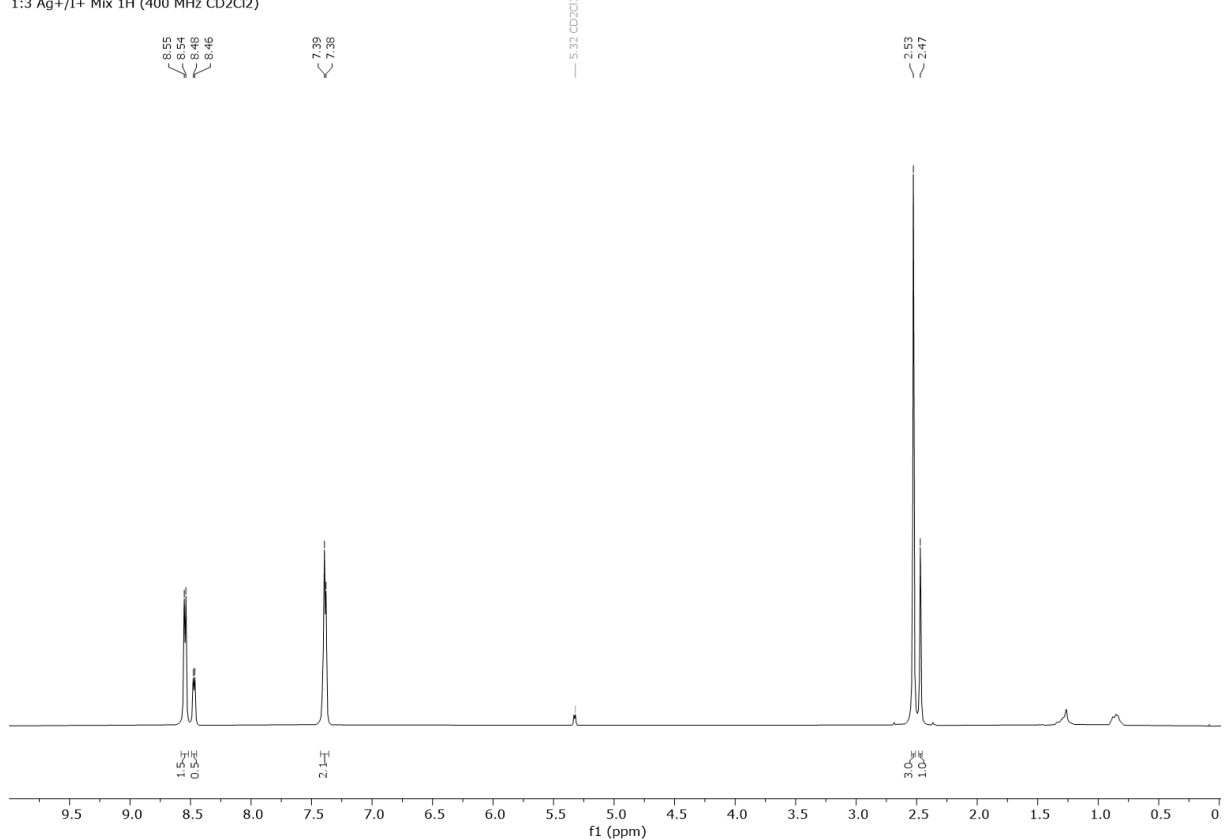


**Figure S36.** <sup>1</sup>H NMR spectrum of a 1:3 mixture of [bis(4-methylpyridine)silver(I)]hexafluorophosphate (**1**) and [bis(4-methylpyridine)iodine(I)]hexafluorophosphate (**2**) (400 MHz, CD<sub>2</sub>Cl<sub>2</sub>, 25°C).

1:3 Ag+/I+ Mix 1H (for 1H-15N HMBC) (400 & 41 MHz CD<sub>2</sub>Cl<sub>2</sub>)

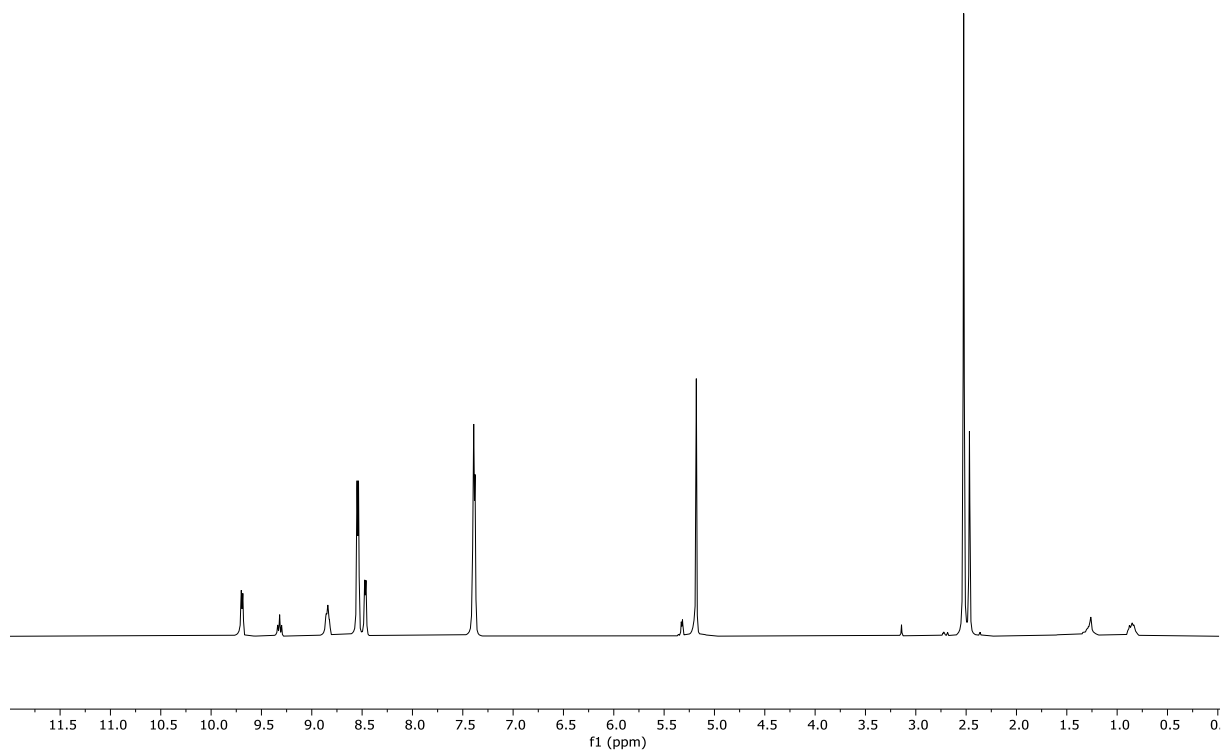


**Figure S37.** <sup>1</sup>H NMR spectrum of a 1:3 mixture of [bis(4-methylpyridine)silver(I)]hexafluorophosphate (**1**) and [bis(4-methylpyridine)iodine(I)]hexafluorophosphate (**2**), with capillary of 1-Methylpyridinium iodide in CD<sub>3</sub>CN (400 MHz, CD<sub>2</sub>Cl<sub>2</sub>, 25°C).

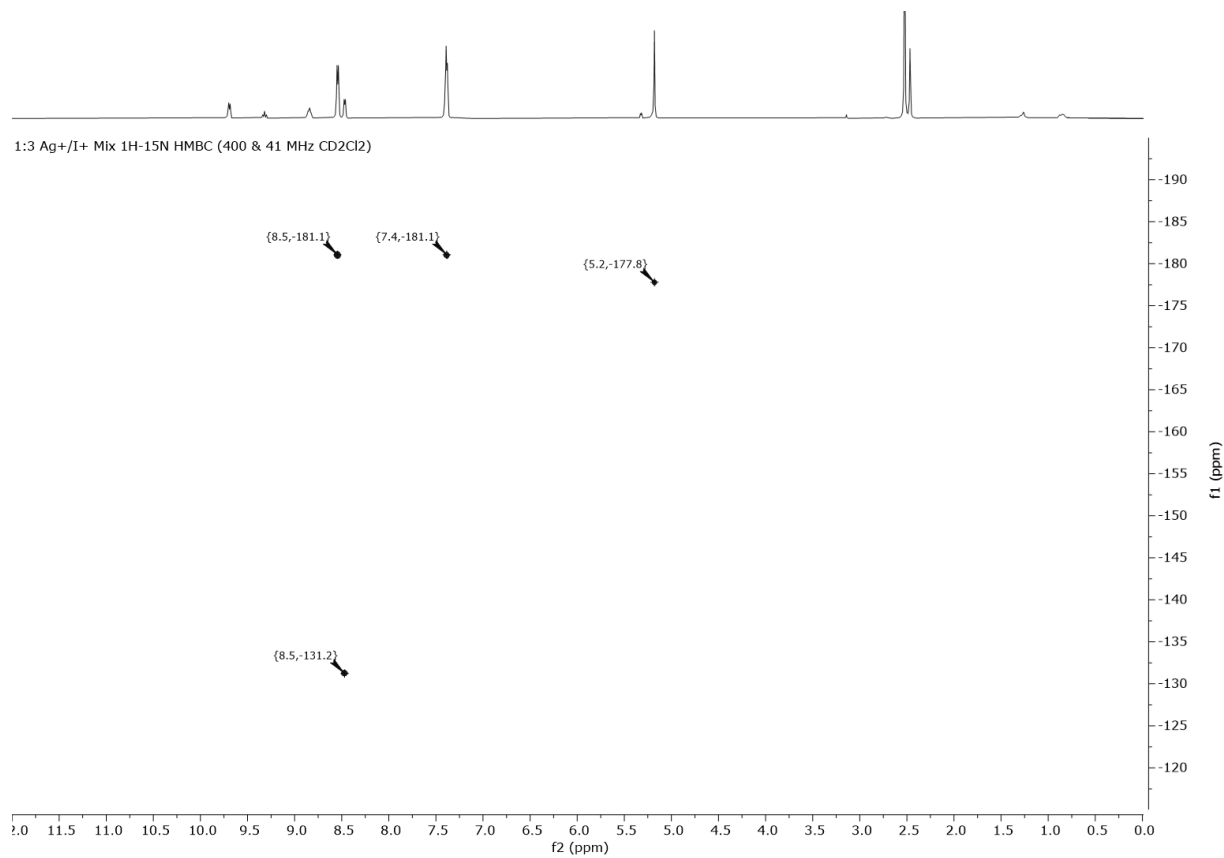


**Figure S38.** <sup>1</sup>H-<sup>15</sup>N HMBC NMR spectrum of a 1:3 mixture of [bis(4-methylpyridine)silver(I)]hexafluorophosphate (**1**) and [bis(4-methylpyridine)iodine(I)]hexafluorophosphate (**2**), with capillary of 1-methylpyridinium iodide in  $\text{CD}_3\text{CN}$  (400 & 41 MHz,  $\text{CD}_2\text{Cl}_2$ , 25°C).

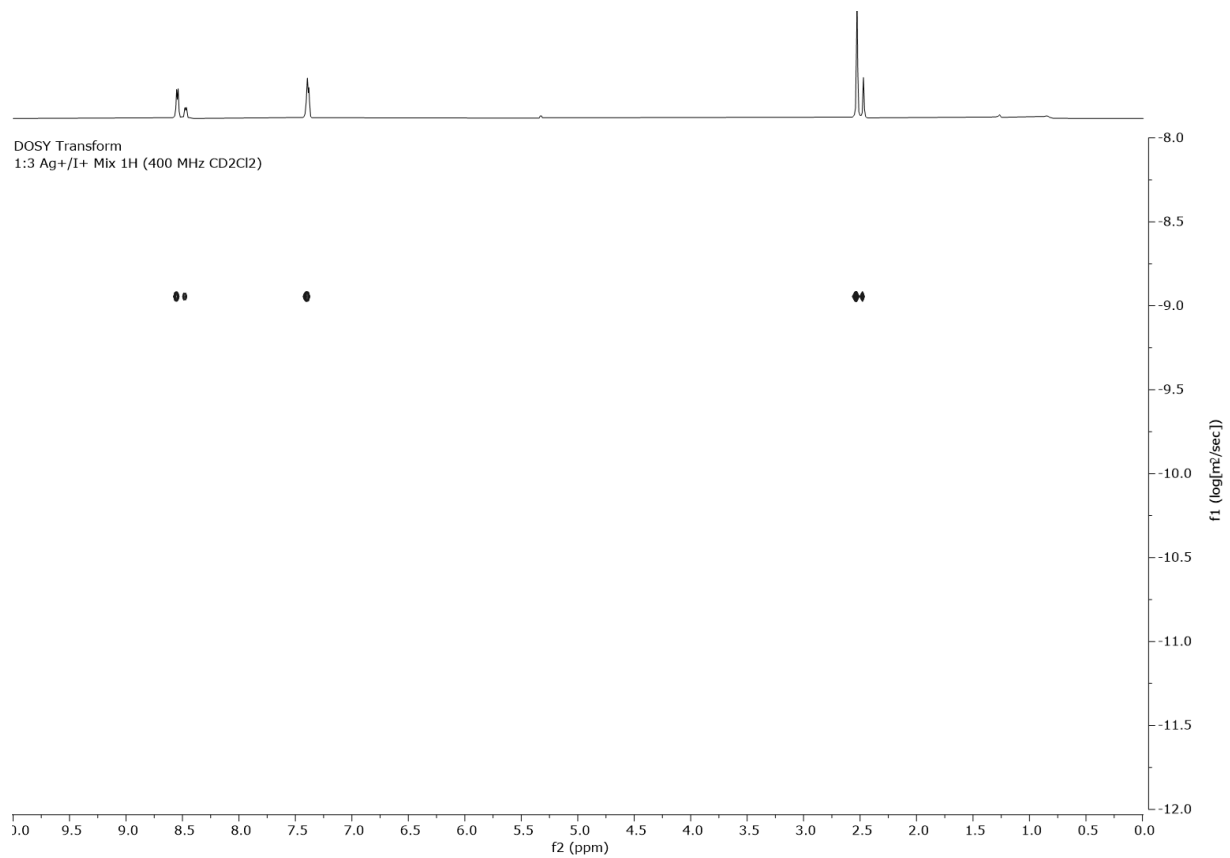


**Figure S39.** <sup>1</sup>H DOSY Transform NMR spectrum of a 1:3 mixture of [bis(4-methylpyridine)silver(I)]hexafluorophosphate (**1**) and [bis(4-methylpyridine)iodine(I)]hexafluorophosphate (**2**) (400 MHz, CD<sub>2</sub>Cl<sub>2</sub>, 25°C).

1:3 Mix Ag+/I+  $^{19}\text{F}$  NMR (376 MHz  $\text{CD}_2\text{Cl}_2$ )

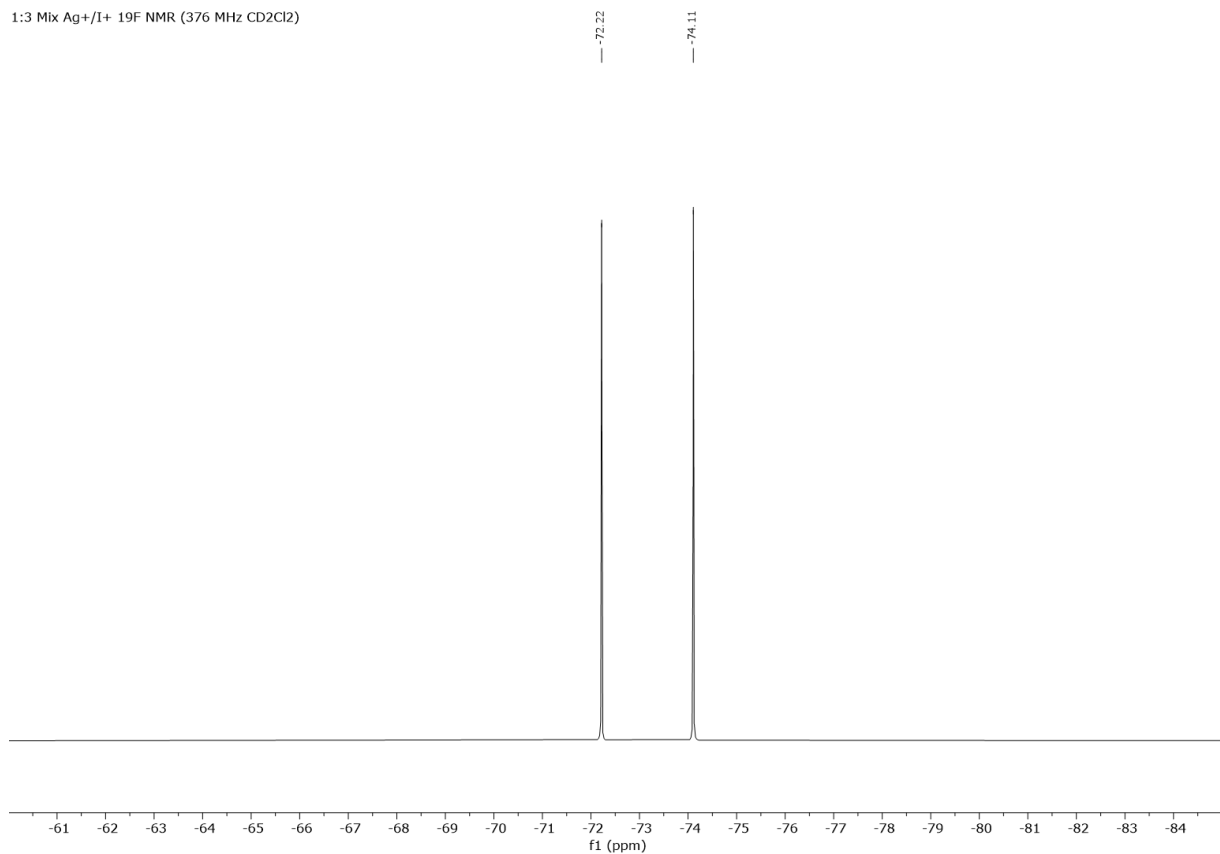


**Figure S40.**  $^{19}\text{F}$  NMR spectrum of a 1:3 mixture of [bis(4-methylpyridine)silver(I)]hexafluorophosphate (**1**) and [bis(4-methylpyridine)iodine(I)]hexafluorophosphate (**2**) (376 MHz,  $\text{CD}_2\text{Cl}_2$ , 25°C).

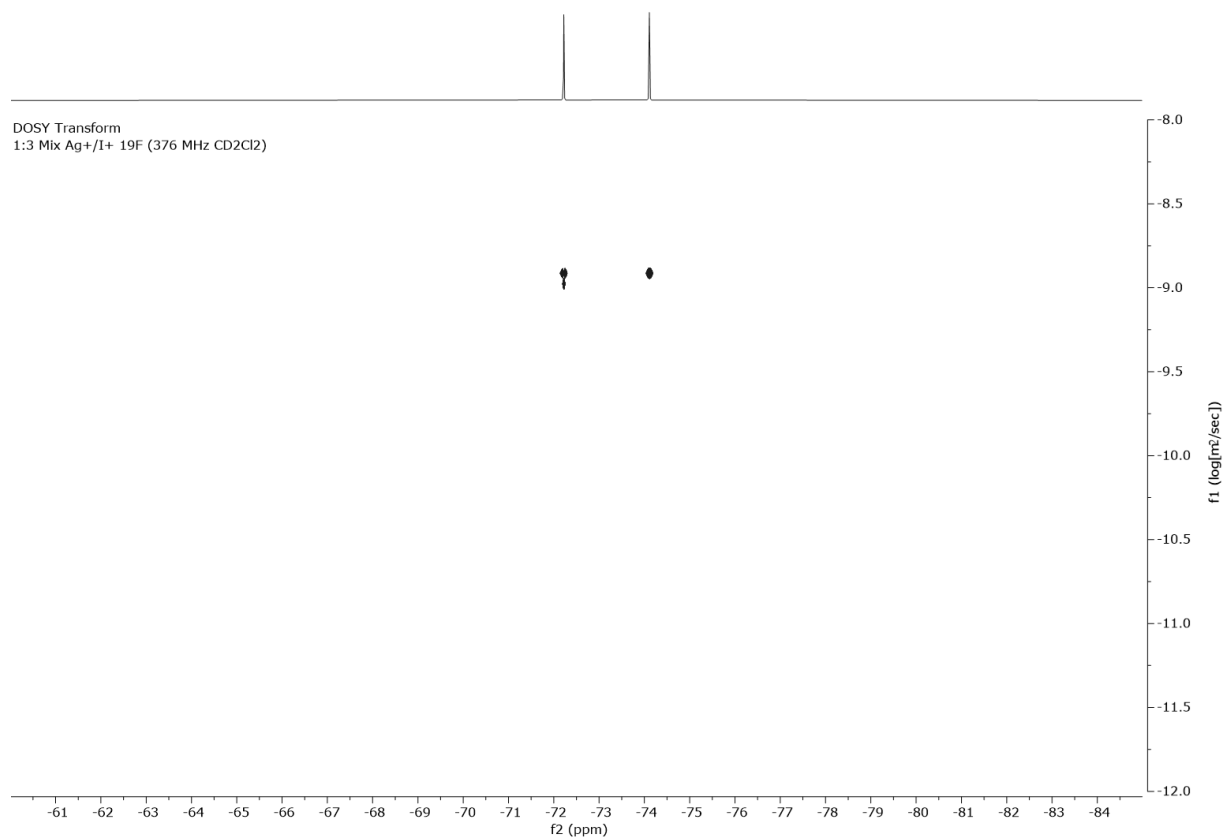


**Figure S41.** <sup>19</sup>F DOSY Transform NMR spectrum of a 1:3 mixture of [bis(4-methylpyridine)silver(I)]hexafluorophosphate (**1**) and [bis(4-methylpyridine)iodine(I)]hexafluorophosphate (**2**) (376 MHz, CD<sub>2</sub>Cl<sub>2</sub>, 25°C).

(1) + 100% H<sub>2</sub>O 1H (for 1H-15N HMBC) (400 MHz CD<sub>2</sub>Cl<sub>2</sub>)

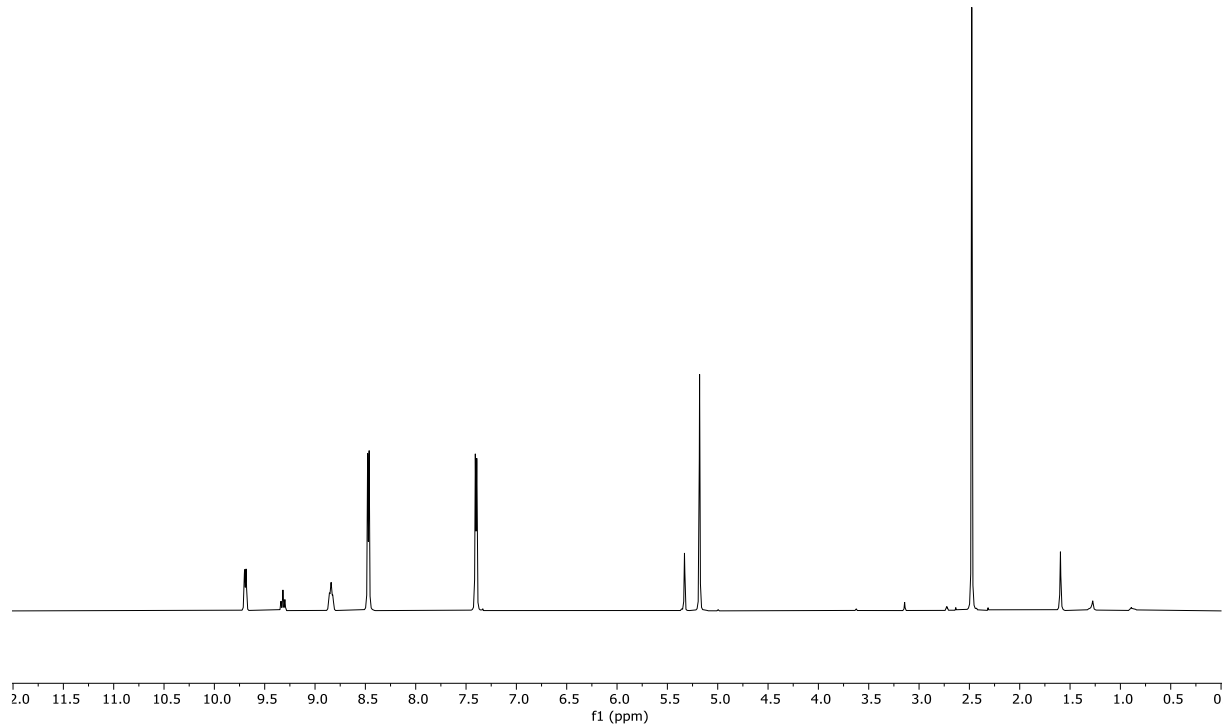


**Figure S42.** <sup>1</sup>H NMR spectrum of [bis(4-methylpyridine)silver(I)]hexafluorophosphate (**1**) with added H<sub>2</sub>O (100 mol%), with capillary of 1-methylpyridinium iodide in CD<sub>3</sub>CN (400 MHz, CD<sub>2</sub>Cl<sub>2</sub>, 25°C).

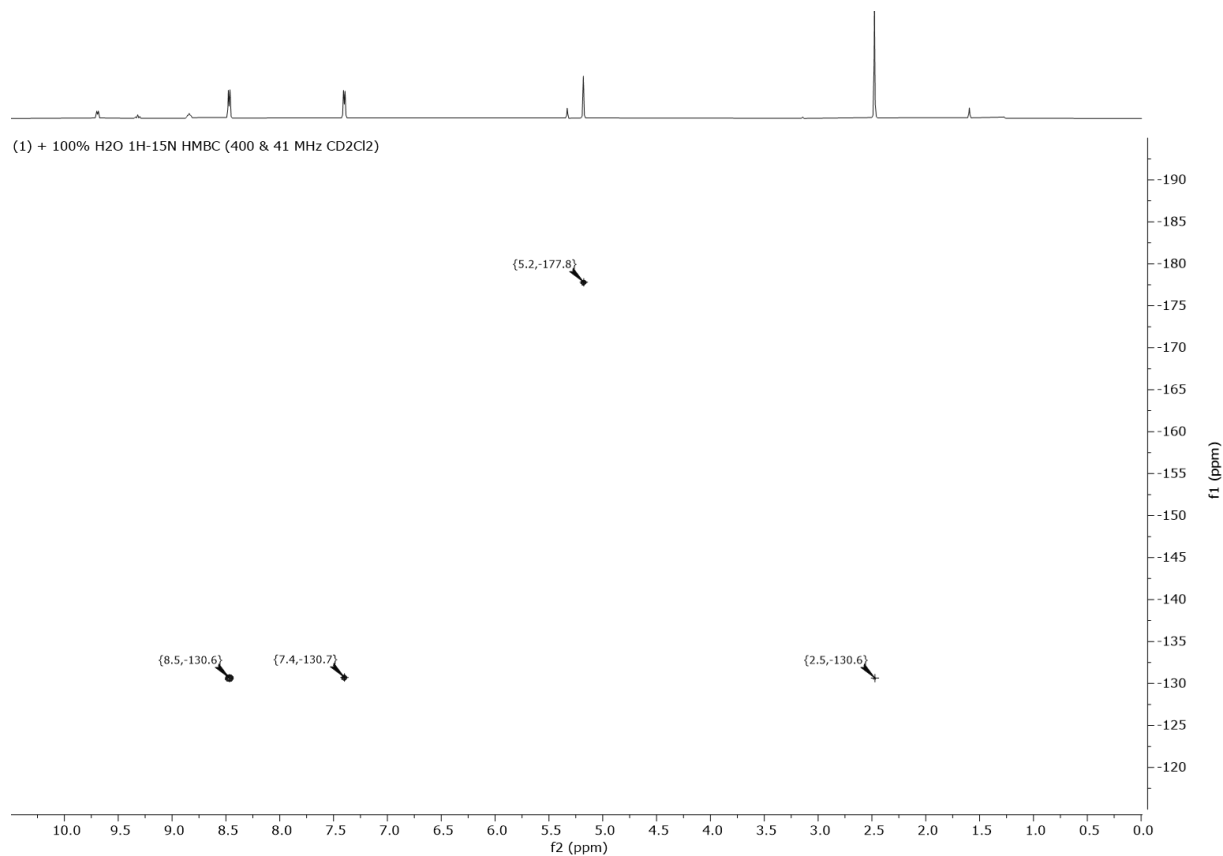


**Figure S43.**  $^1\text{H}$ - $^{15}\text{N}$  HMBC NMR spectrum of [bis(4-methylpyridine)silver(I)]hexafluorophosphate (**1**) with added H<sub>2</sub>O (100 mol%), with capillary of 1-methylpyridinium iodide in CD<sub>3</sub>CN (400 & 41 MHz, CD<sub>2</sub>Cl<sub>2</sub>, 25°C).

(1) + 8% 4-MePy 1H (for 1H-15N HMBC) (400 MHz CD<sub>2</sub>Cl<sub>2</sub>)

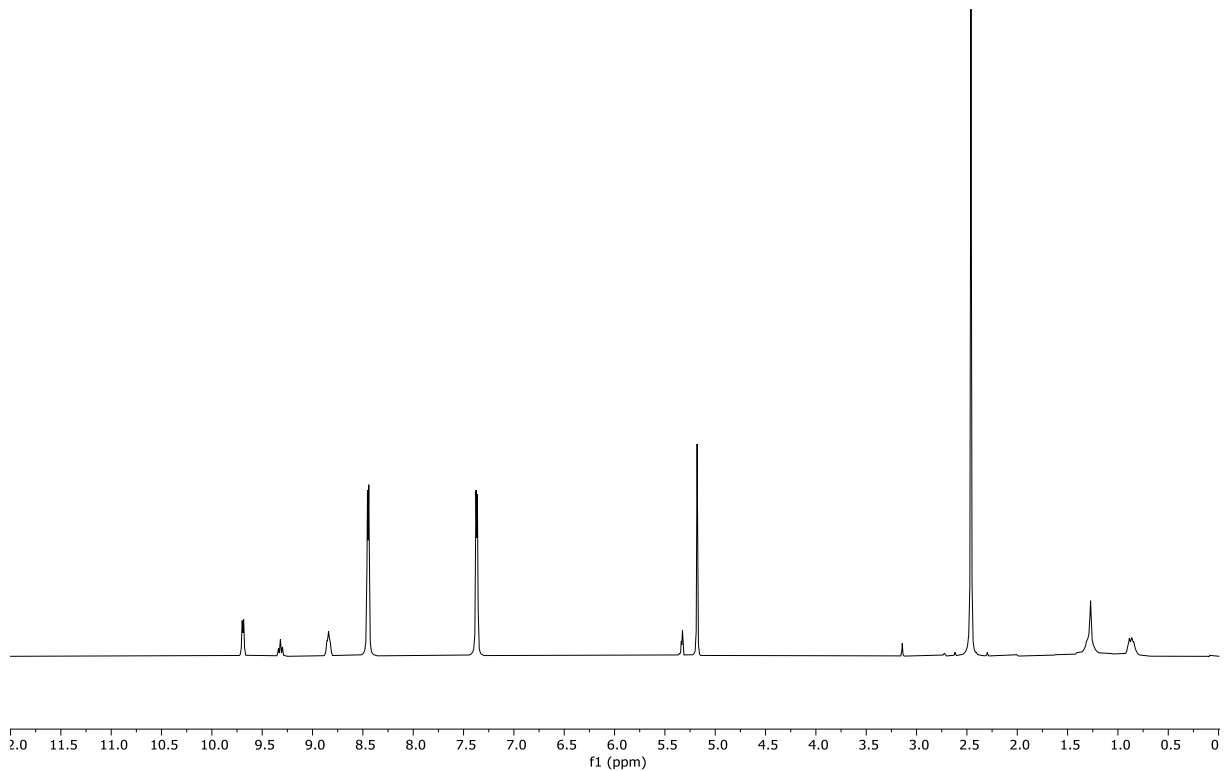


**Figure S44.** <sup>1</sup>H NMR spectrum of [bis(4-methylpyridine)silver(I)]hexafluorophosphate (**1**) with added 4-Methylpyridine (8 mol%), with capillary of 1-methylpyridinium iodide in CD<sub>3</sub>CN (400 MHz, CD<sub>2</sub>Cl<sub>2</sub>, 25°C).

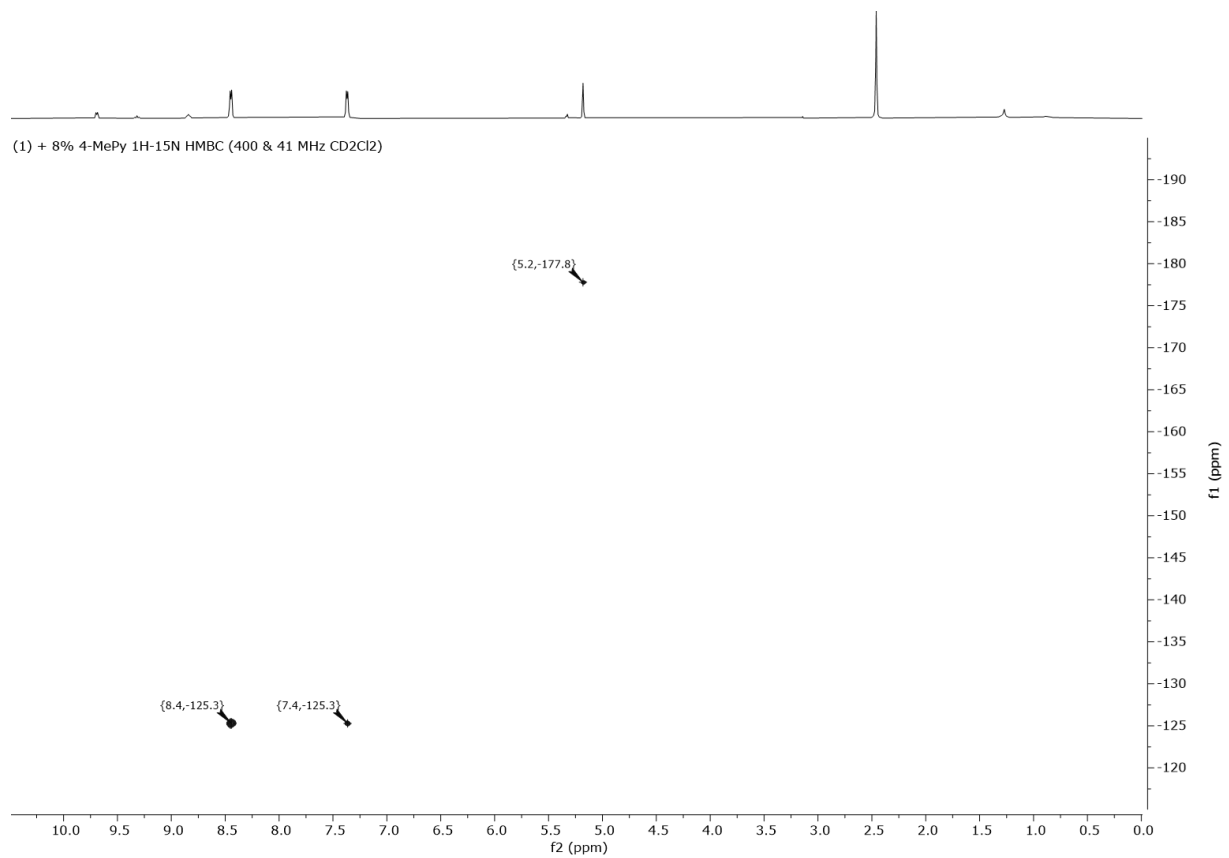


**Figure S45.**  $^1\text{H}$ - $^{15}\text{N}$  HMBC NMR spectrum of [bis(4-methylpyridine)silver(I)]hexafluorophosphate (**1**) with added 4-methylpyridine (8 mol%), with capillary of 1-methylpyridinium iodide in CD<sub>3</sub>CN (400 & 41 MHz, CD<sub>2</sub>Cl<sub>2</sub>, 25°C).

(1) + 20% 4-MePy 1H (for 1H-15N HMBC) (400 MHz CD<sub>2</sub>Cl<sub>2</sub>)

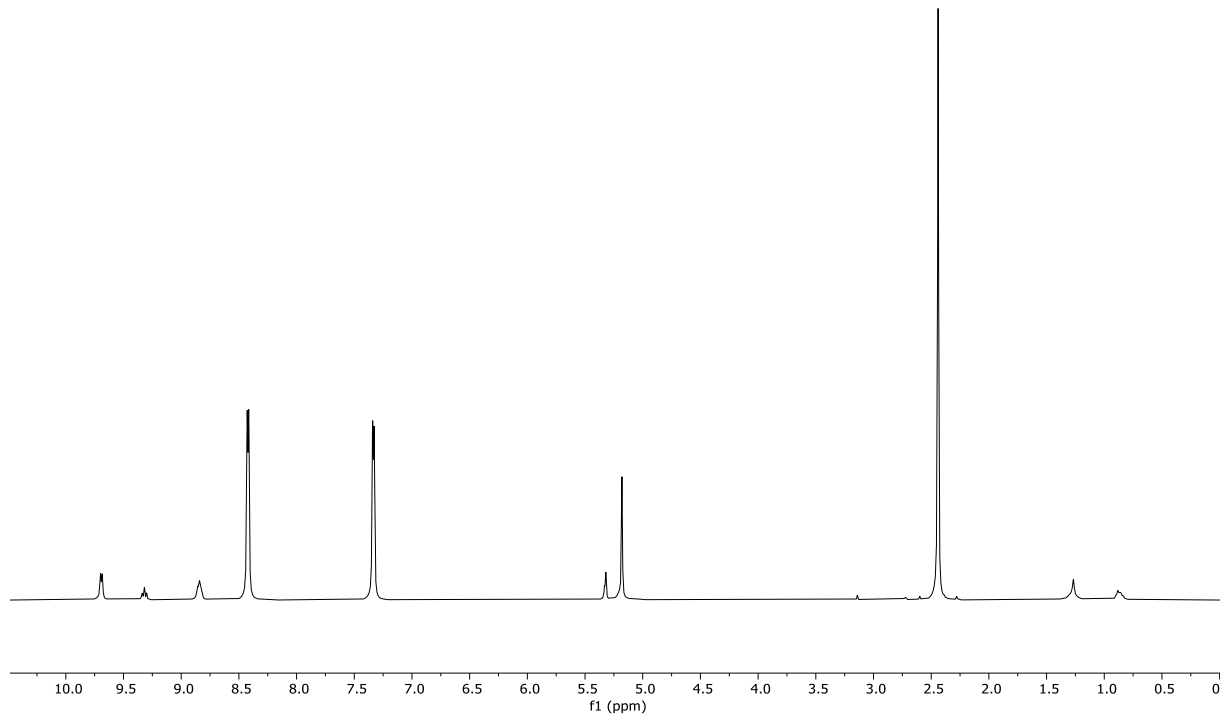


**Figure S46.** <sup>1</sup>H NMR spectrum of [bis(4-methylpyridine)silver(I)]hexafluorophosphate (**1**) with added 4-methylpyridine (20 mol%), with capillary of 1-methylpyridinium iodide in CD<sub>3</sub>CN (400 MHz, CD<sub>2</sub>Cl<sub>2</sub>, 25°C).

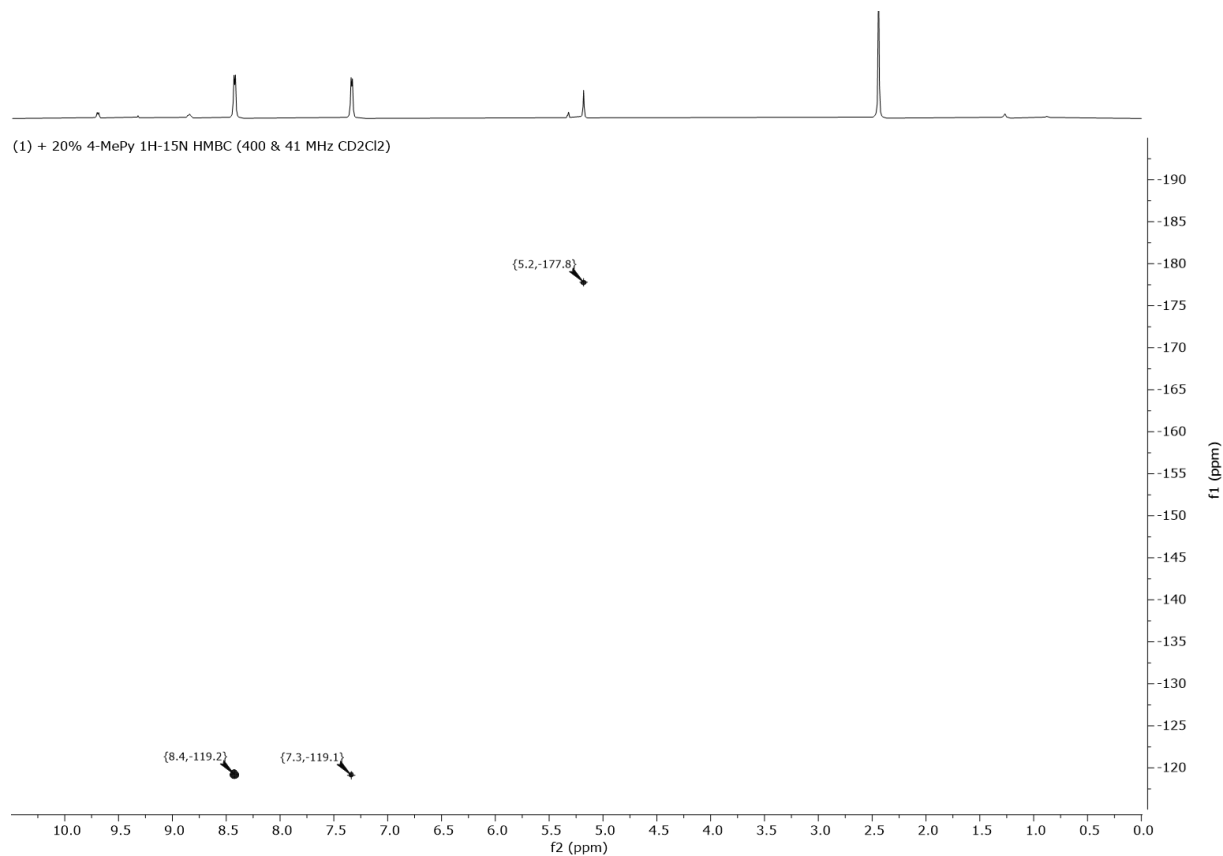


**Figure S47.**  $^1\text{H}$ - $^{15}\text{N}$  HMBC NMR spectrum of [bis(4-methylpyridine)silver(I)]hexafluorophosphate (**1**) with added 4-methylpyridine (20 mol%), with capillary of 1-methylpyridinium iodide in  $\text{CD}_3\text{CN}$  (400 & 41 MHz,  $\text{CD}_2\text{Cl}_2$ , 25°C).

(1) + 25% TFA 1H NMR (for 1H-15N HMBC) (400 MHz CD<sub>2</sub>Cl<sub>2</sub>)

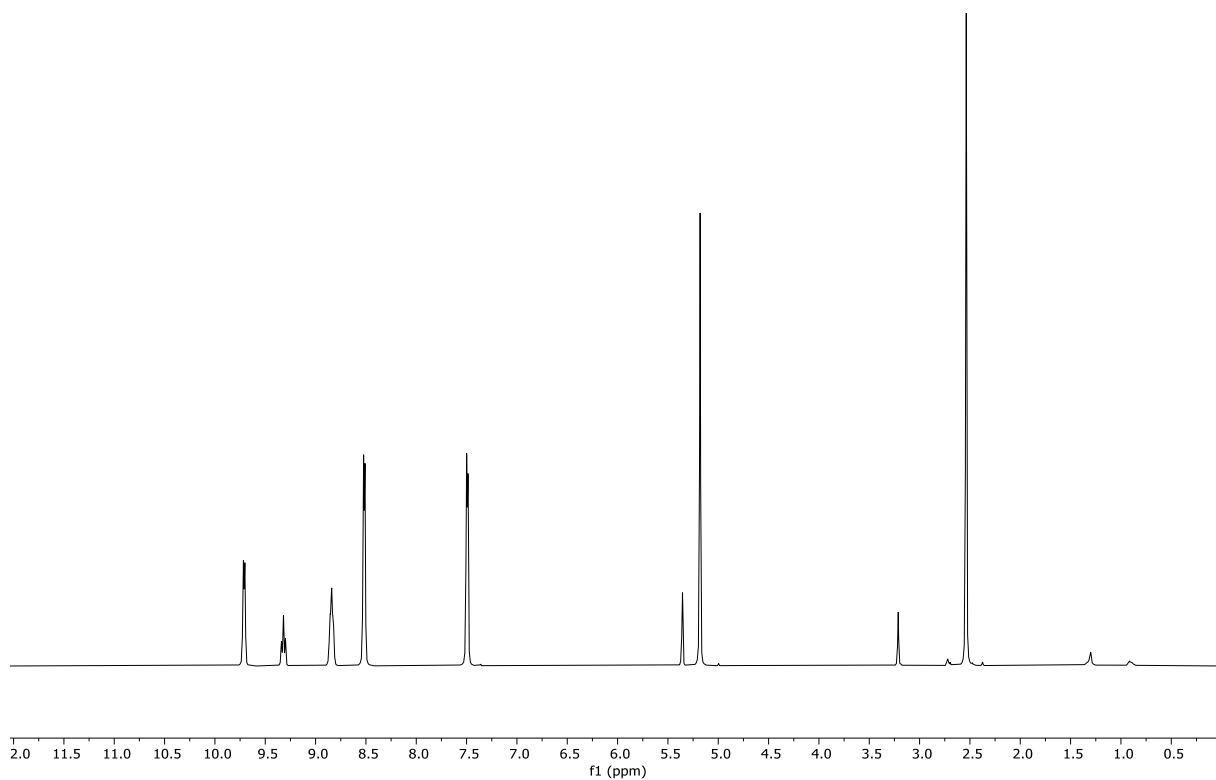


**Figure S48.** <sup>1</sup>H NMR spectrum of [bis(4-methylpyridine)silver(I)]hexafluorophosphate (**1**) with added trifluoroacetic acid (25 mol%), with capillary of 1-methylpyridinium iodide in CD<sub>3</sub>CN (400 MHz, CD<sub>2</sub>Cl<sub>2</sub>, 25°C).

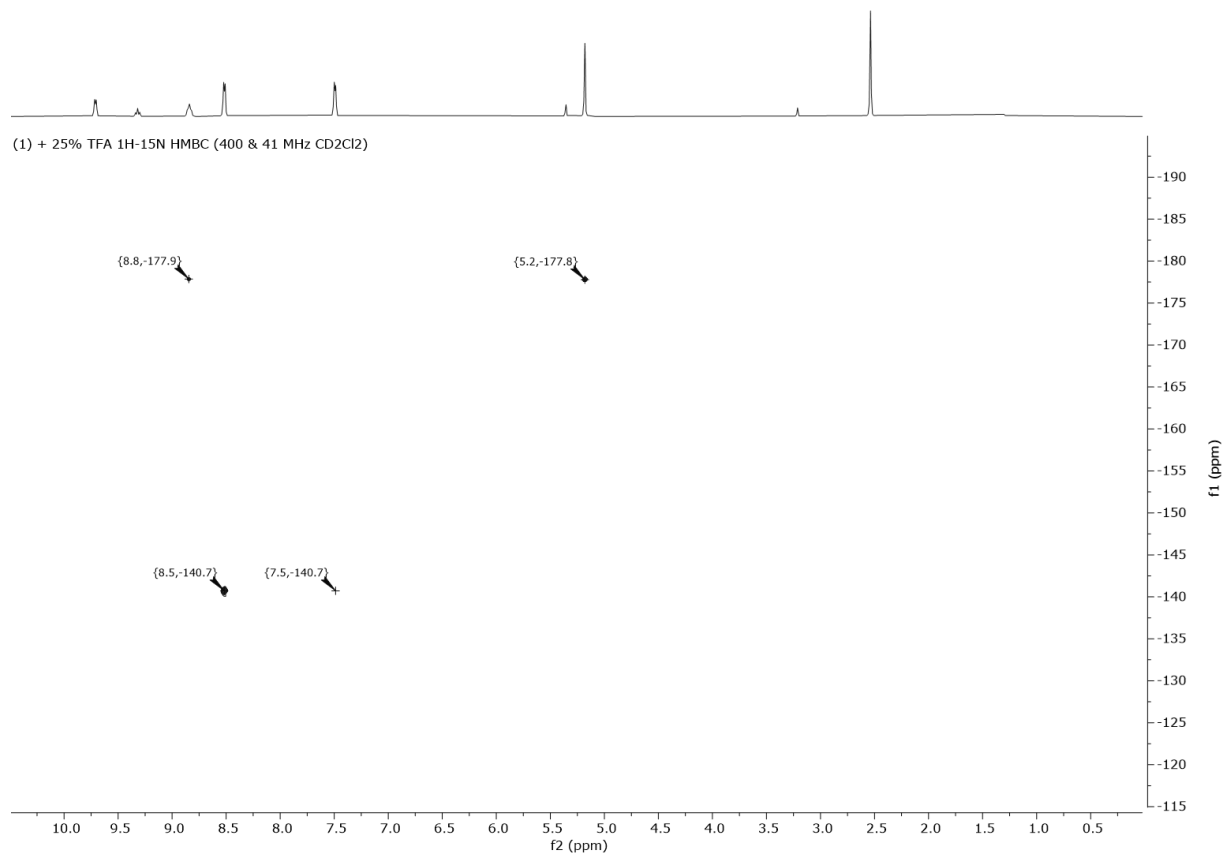


**Figure S49.**  $^1\text{H}$ - $^{15}\text{N}$  HMBC NMR spectrum of [bis(4-methylpyridine)silver(I)]hexafluorophosphate (**1**) with added trifluoroacetic acid (25 mol%), with capillary of 1-methylpyridinium iodide in CD<sub>3</sub>CN (400 & 41 MHz, CD<sub>2</sub>Cl<sub>2</sub>, 25°C).

(1) + 4-Methylpyridine (8 mol%) + TFA (8 mol%) 1H (for 1H-15N HMBC) (400 MHz CD<sub>2</sub>Cl<sub>2</sub>)

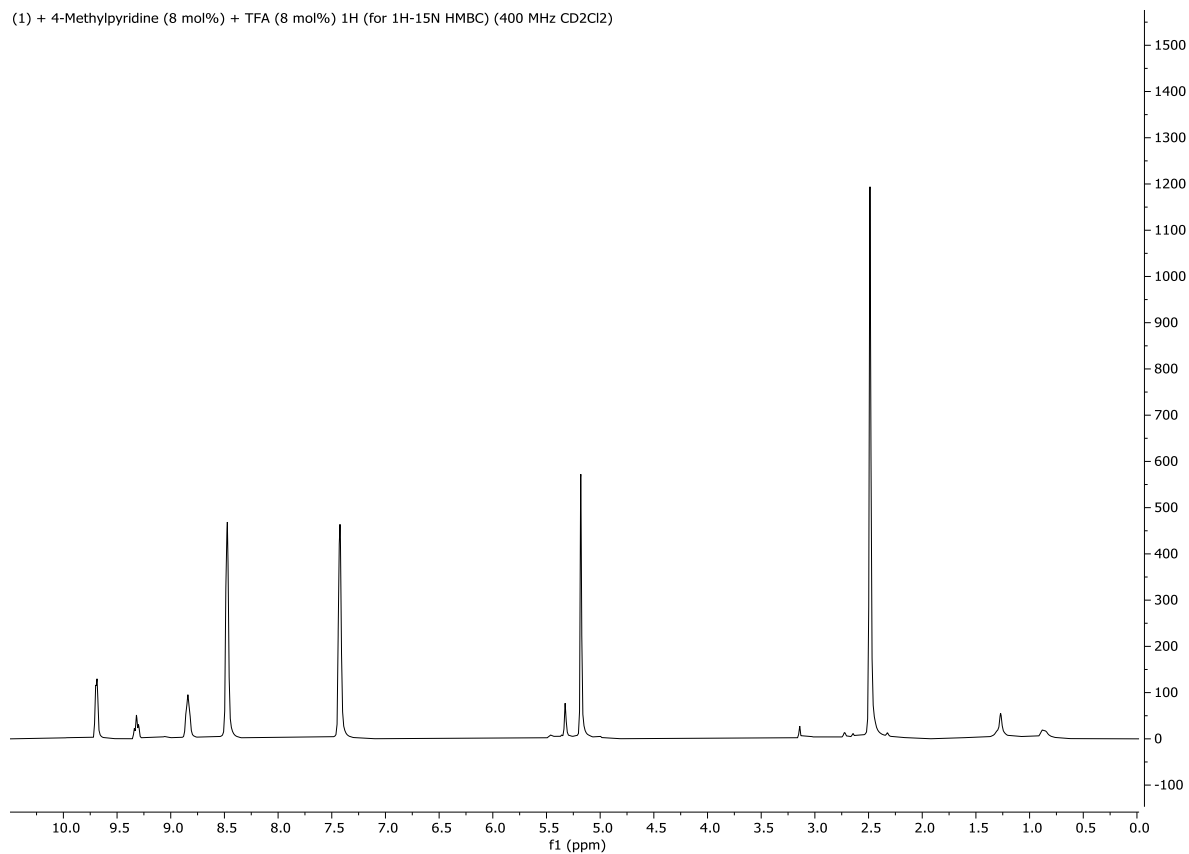


**Figure S50.** <sup>1</sup>H NMR spectrum of [bis(4-methylpyridine)silver(I)]hexafluorophosphate (**1**) with added mixture of 4-methylpyridine (8 mol%) and trifluoroacetic acid (8 mol%), with capillary of 1-methylpyridinium iodide in CD<sub>3</sub>CN (400 MHz, CD<sub>2</sub>Cl<sub>2</sub>, 25°C).

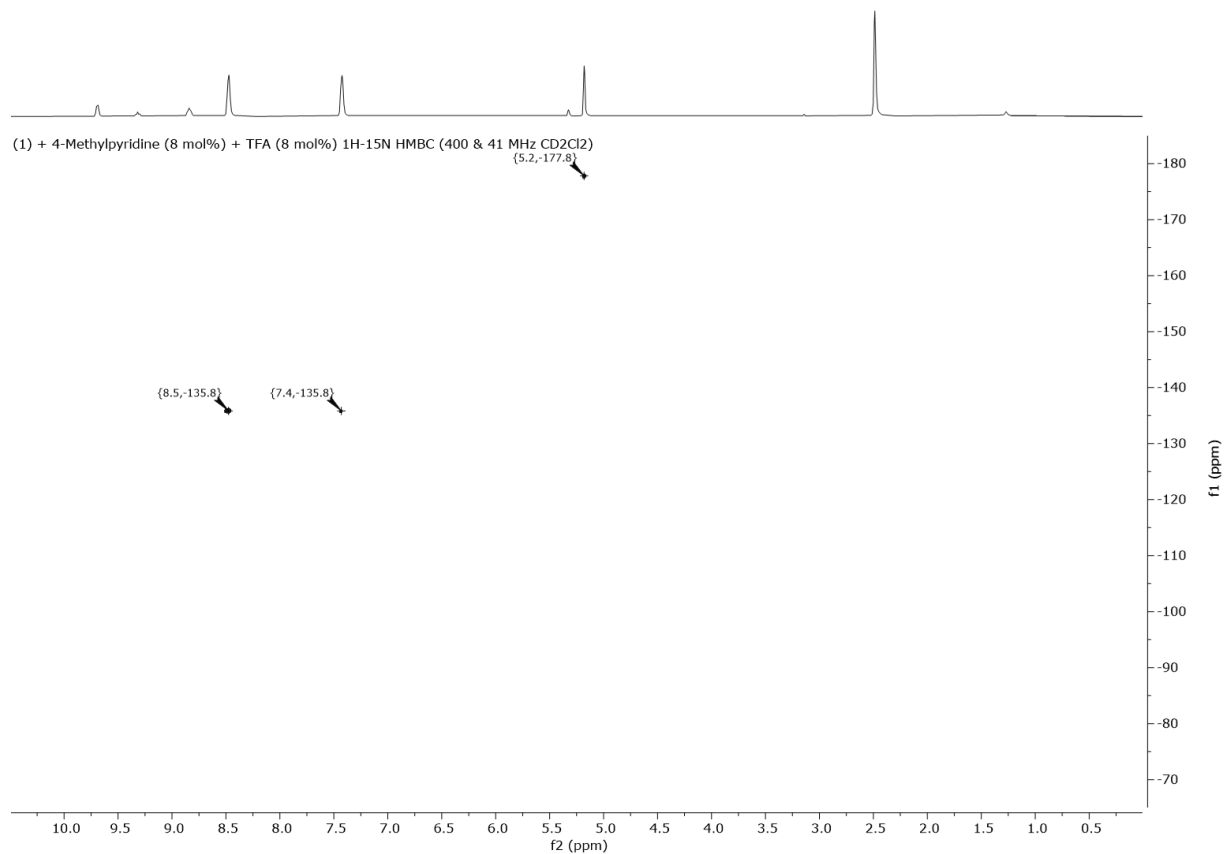


**Figure S51.**  $^1\text{H}$ - $^{15}\text{N}$  HMBC NMR spectrum of [bis(4-methylpyridine)silver(I)]hexafluorophosphate (**1**) with added mixture of 4-methylpyridine (8 mol%) and Trifluoroacetic acid (8 mol%), with capillary of 1-methylpyridinium iodide in  $\text{CD}_3\text{CN}$  (400 & 41 MHz,  $\text{CD}_2\text{Cl}_2$ , 25°C).

(1) + 4-Methylpyridine (100 mol%) + TFA (100 mol%) 1H (for 1H-15N HMBC) (400 MHz CD<sub>2</sub>Cl<sub>2</sub>)

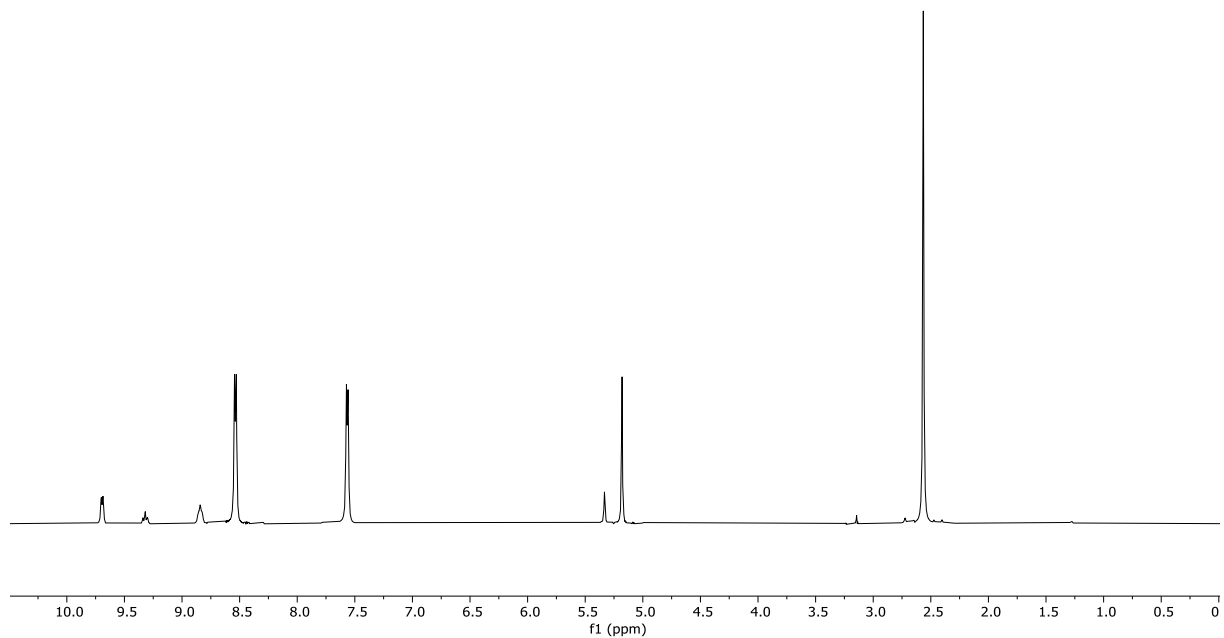


**Figure S52.** <sup>1</sup>H NMR spectrum of [bis(4-methylpyridine)silver(I)]hexafluorophosphate (**1**) with added mixture of 4-methylpyridine (100 mol%) and trifluoroacetic acid (100 mol%), with capillary of 1-methylpyridinium iodide in CD<sub>3</sub>CN (400 MHz, CD<sub>2</sub>Cl<sub>2</sub>, 25°C).

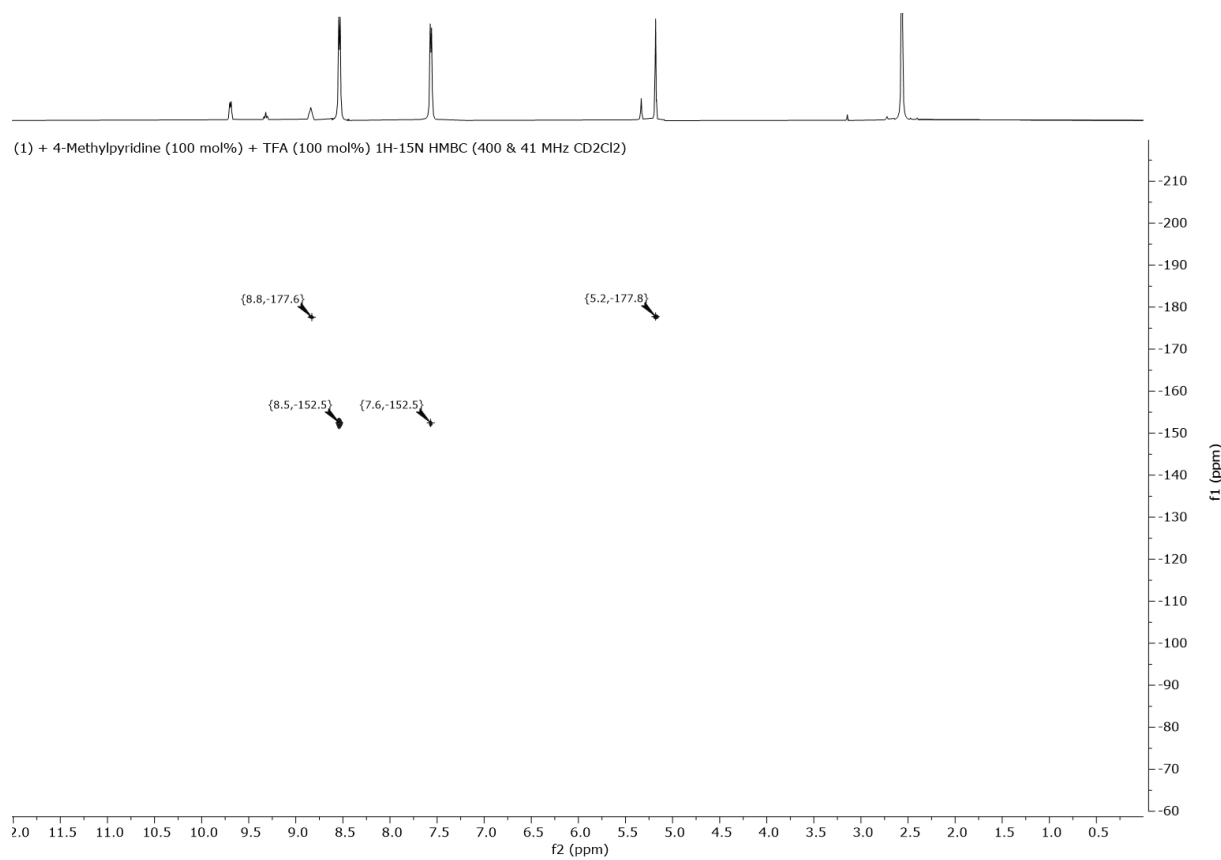


**Figure S53.**  $^1\text{H}$ - $^{15}\text{N}$  HMBC NMR spectrum of [bis(4-methylpyridine)silver(I)]hexafluorophosphate (**1**) with added mixture of 4-methylpyridine (100 mol%) and trifluoroacetic acid (100 mol%), with capillary of 1-methylpyridinium iodide in CD<sub>3</sub>CN (400 & 41 MHz, CD<sub>2</sub>Cl<sub>2</sub>, 25°C).

1:1 Mix 4-Methylpyridine/TFA 1H (for 1H-15N HMBC) (400 MHz CD<sub>2</sub>Cl<sub>2</sub>)

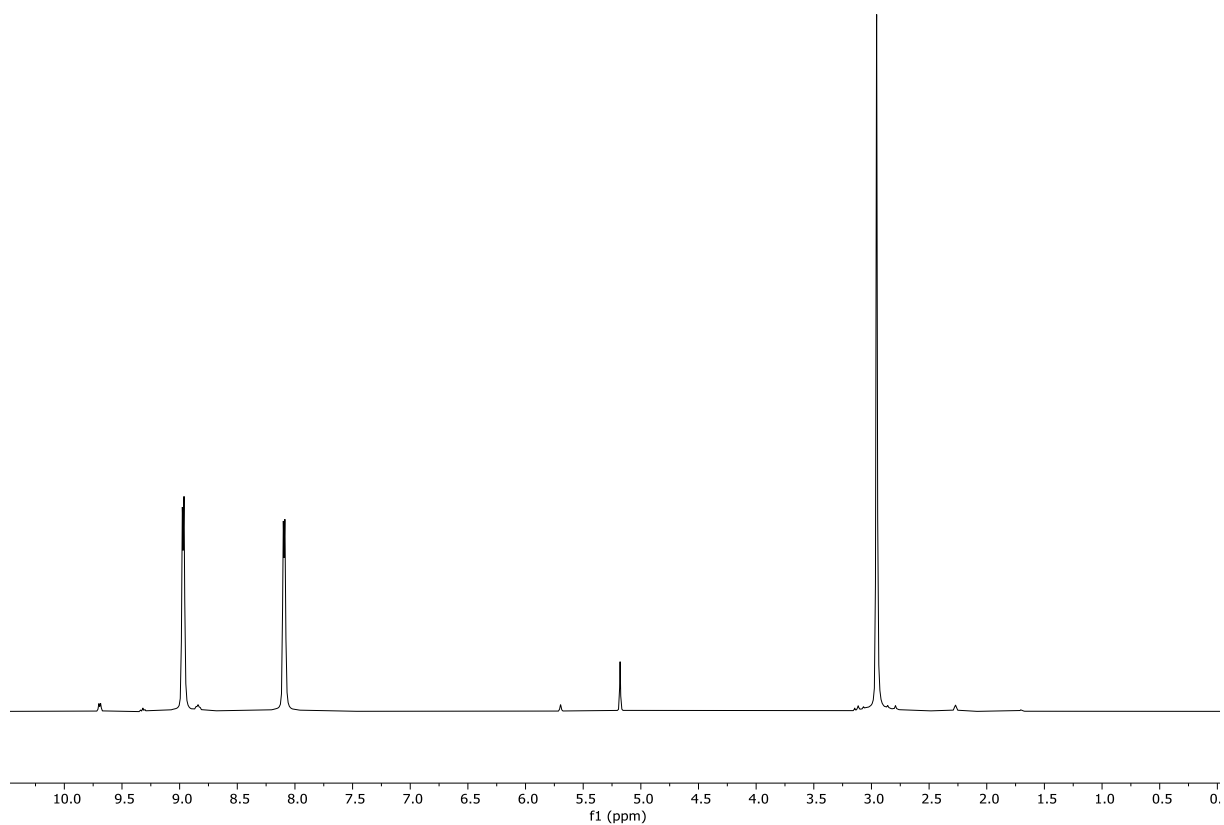


**Figure S54.** <sup>1</sup>H NMR spectrum of 4-methylpyridine with added trifluoroacetic acid (120 mol%), with capillary of 1-methylpyridinium iodide in CD<sub>3</sub>CN (400 MHz, CD<sub>2</sub>Cl<sub>2</sub>, 25°C).

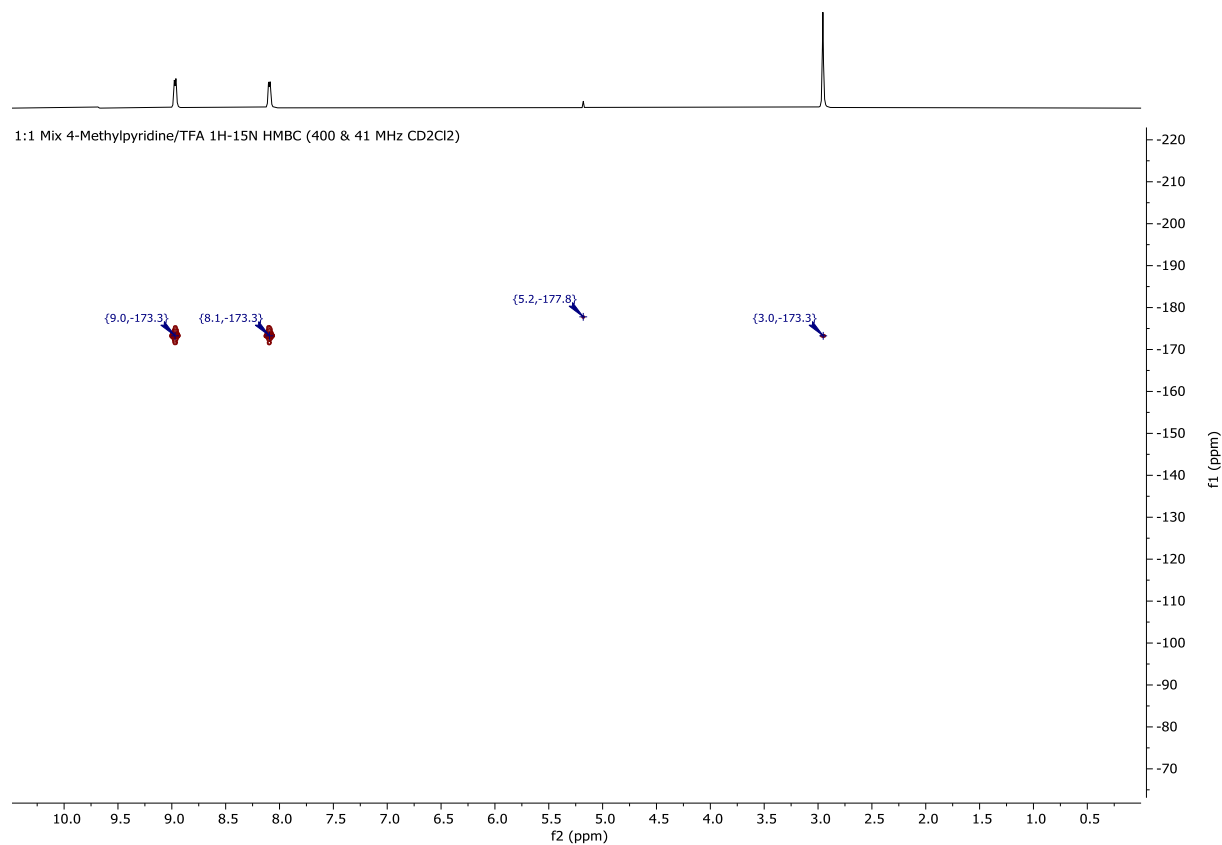


**Figure S55.** <sup>1</sup>H-<sup>15</sup>N HMBC NMR spectrum of 4-methylpyridine with added trifluoroacetic acid (120 mol%), with capillary of 1-methylpyridinium iodide in CD<sub>3</sub>CN (400 & 41 MHz, CD<sub>2</sub>Cl<sub>2</sub>, 25°C).

(2) + H<sub>2</sub>O (5 mol%) 1H (for 1H-15N HMBC) (400 MHz CD<sub>2</sub>Cl<sub>2</sub>)

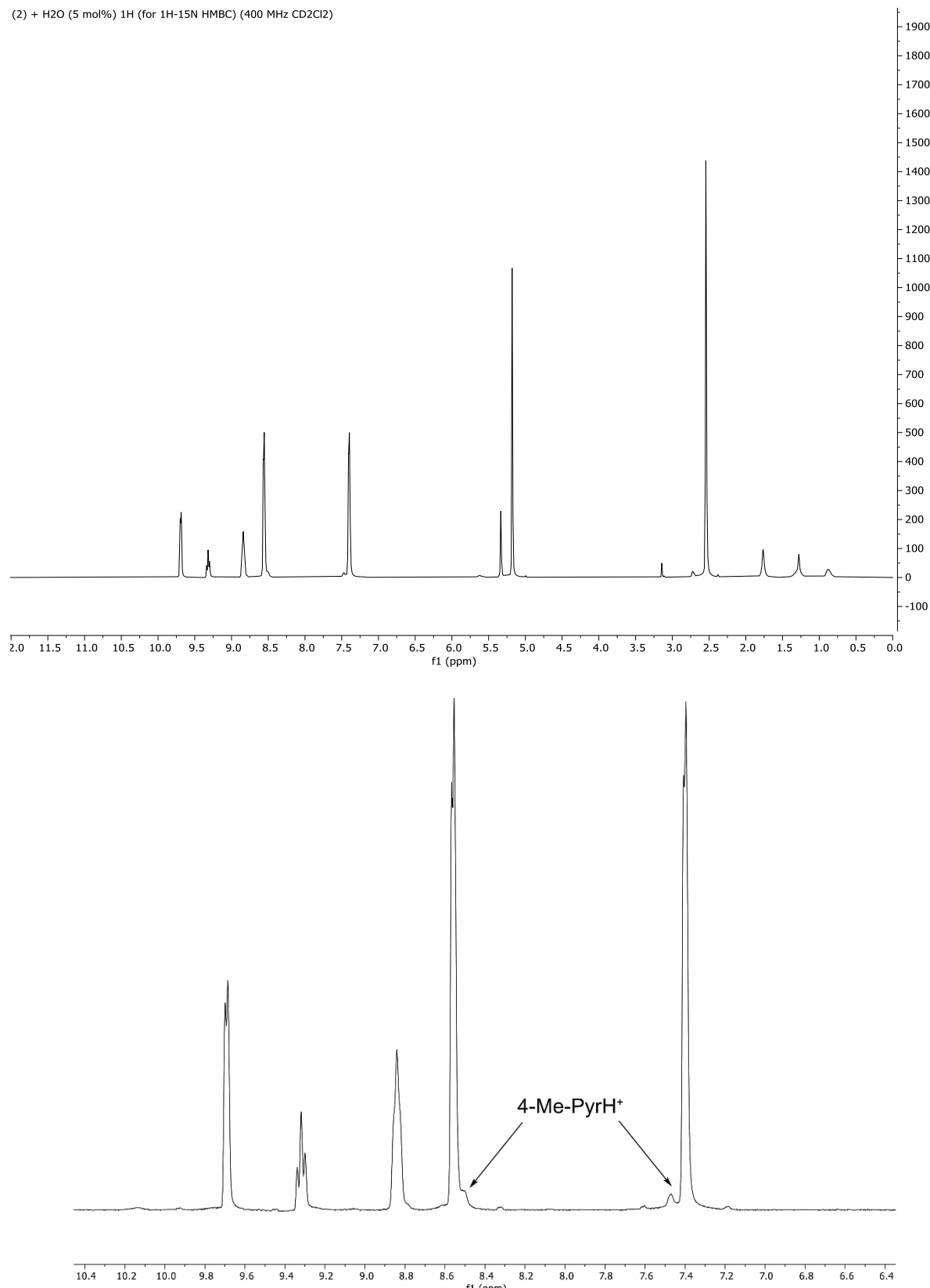


**Figure S56.** <sup>1</sup>H NMR spectrum of [bis(4-methylpyridine)iodine(I)]hexafluorophosphate (**2**) with added H<sub>2</sub>O (5 mol%), with capillary of 1-methylpyridinium iodide in CD<sub>3</sub>CN (400 MHz, CD<sub>2</sub>Cl<sub>2</sub>, 25°C). The expansion below highlights the signals of protonated 4-methylpyridinium ions that are formed upon decomposition of the iodine(I) complex.

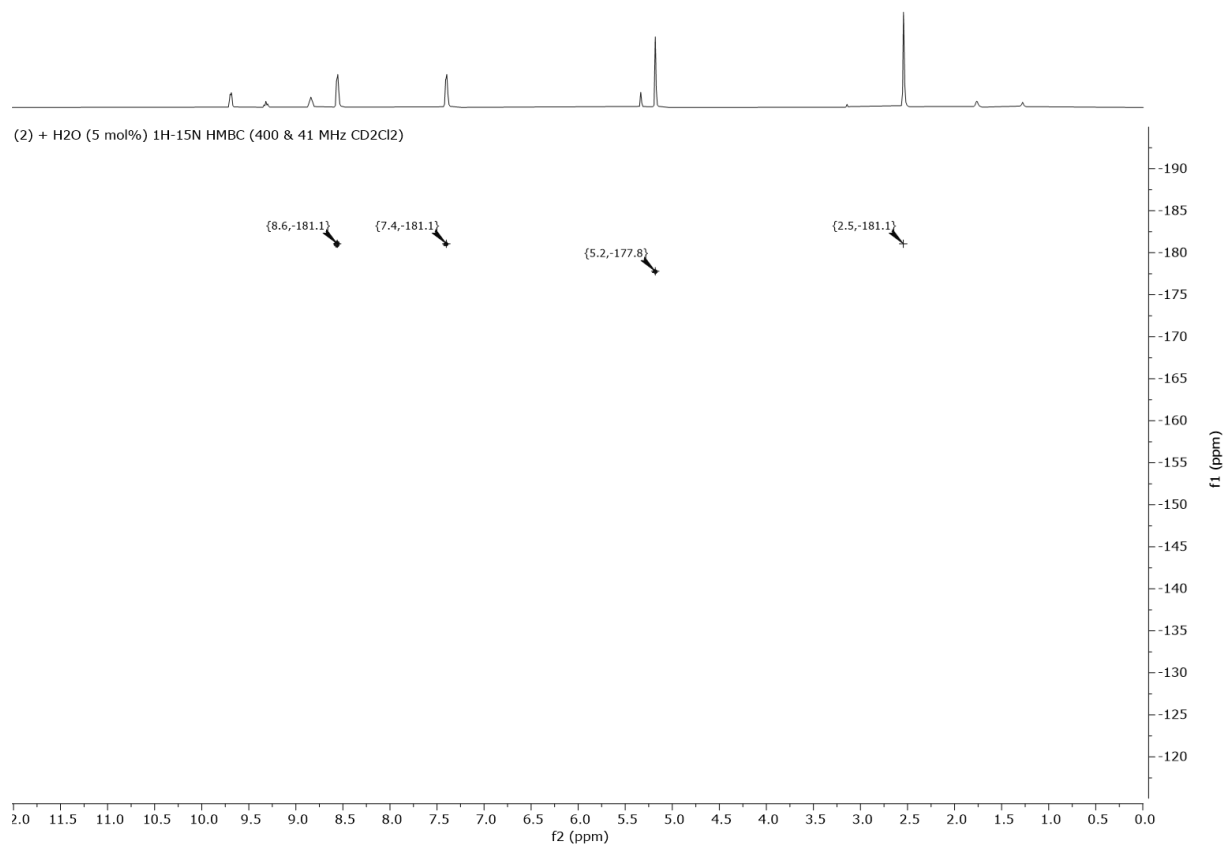


**Figure S57.**  $^1\text{H}$ - $^{15}\text{N}$  HMBC NMR spectrum of [bis(4-methylpyridine)iodine(I)]hexafluorophosphate (**2**) with added H<sub>2</sub>O (5 mol%), with capillary of 1-Methylpyridinium iodide in CD<sub>3</sub>CN (400 & 41 MHz, CD<sub>2</sub>Cl<sub>2</sub>, 25°C).

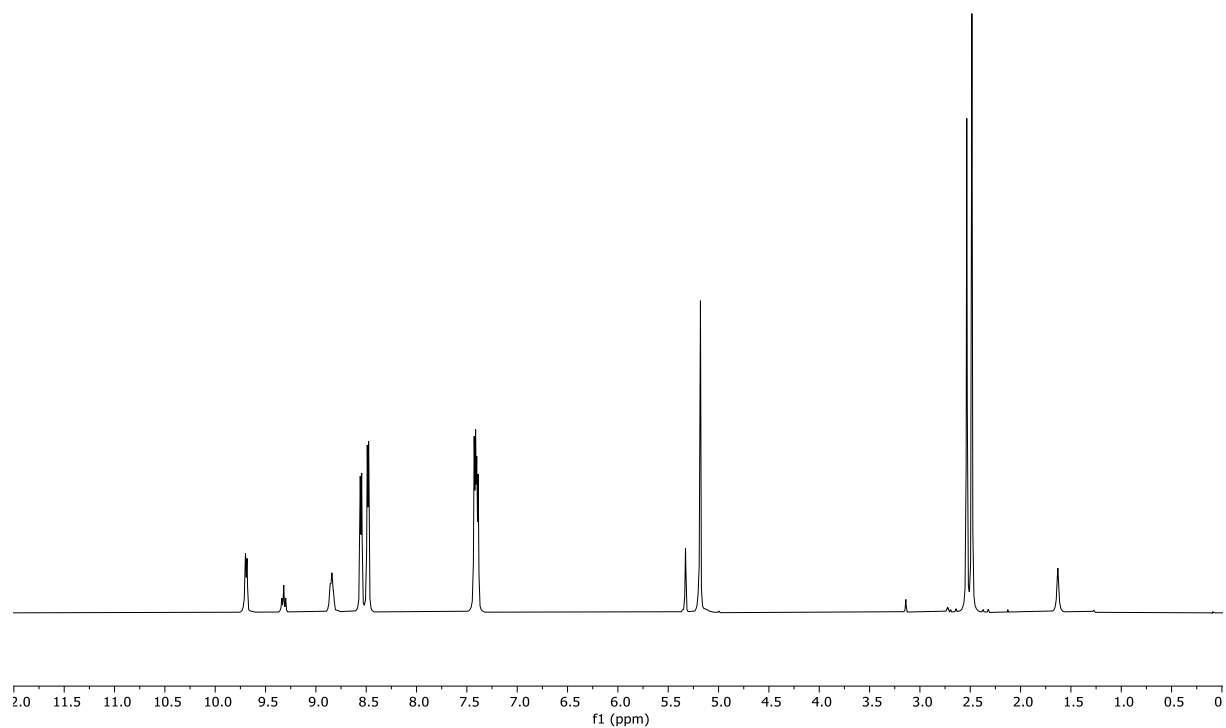


**Figure S58.** <sup>1</sup>H NMR spectrum of a 2:2 mixture of [bis(4-methylpyridine)silver(I)]hexafluorophosphate (**1**) and [bis(4-methylpyridine)iodine(I)]hexafluorophosphate (**2**), with added H<sub>2</sub>O (50 mol%) and with a capillary of 1-methylpyridinium iodide in CD<sub>3</sub>CN (400 MHz, CD<sub>2</sub>Cl<sub>2</sub>, 25°C).

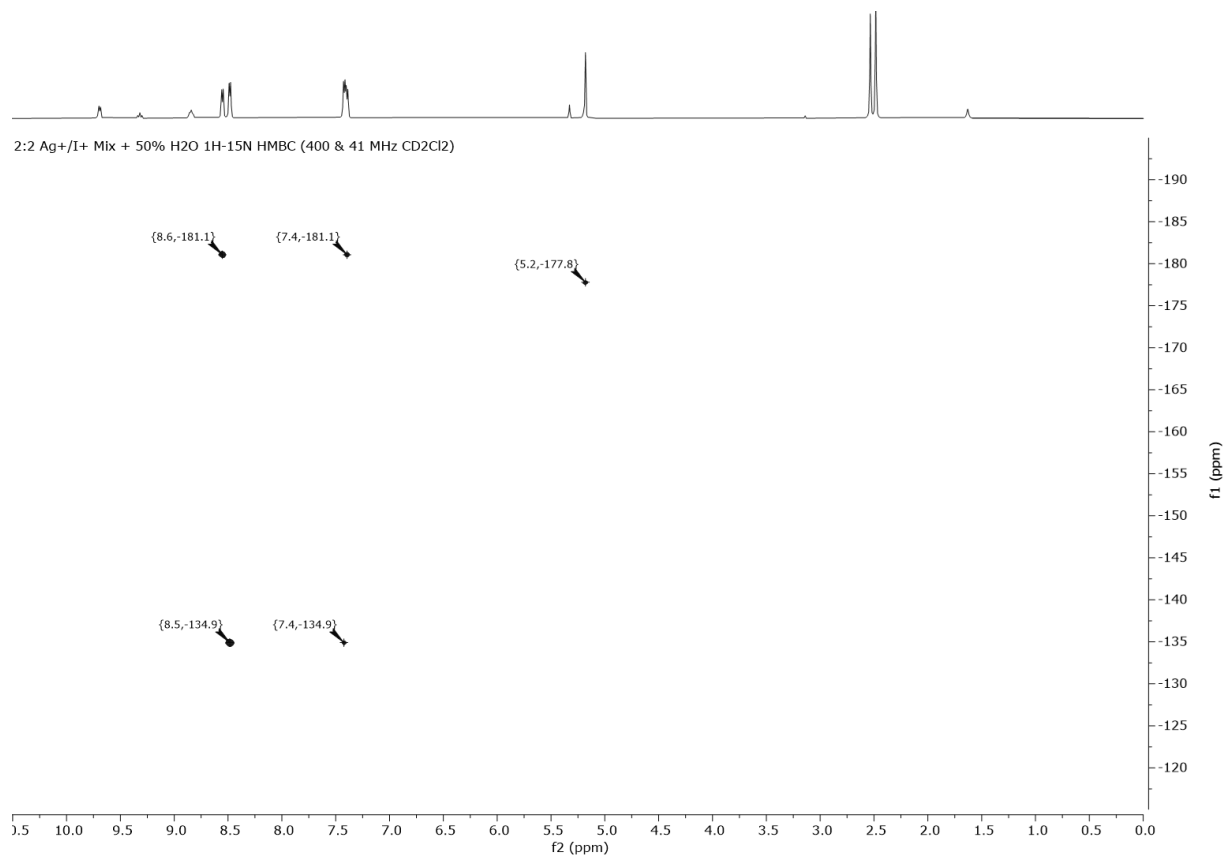


**Figure S59.**  $^1\text{H}$ - $^{15}\text{N}$  spectrum of a 2:2 mixture of [bis(4-methylpyridine)silver(I)]hexafluorophosphate (**1**) and [bis(4-methylpyridine)iodine(I)]hexafluorophosphate (**2**), with added H<sub>2</sub>O (50 mol%) and with a capillary of 1-methylpyridinium iodide in CD<sub>3</sub>CN (400 & 41 MHz, CD<sub>2</sub>Cl<sub>2</sub>, 25°C).

2:2 Ag+/I+ Mix + 5% 4-MePy 1H (for 1H-15N HMBC) (400 MHz CD<sub>2</sub>Cl<sub>2</sub>)

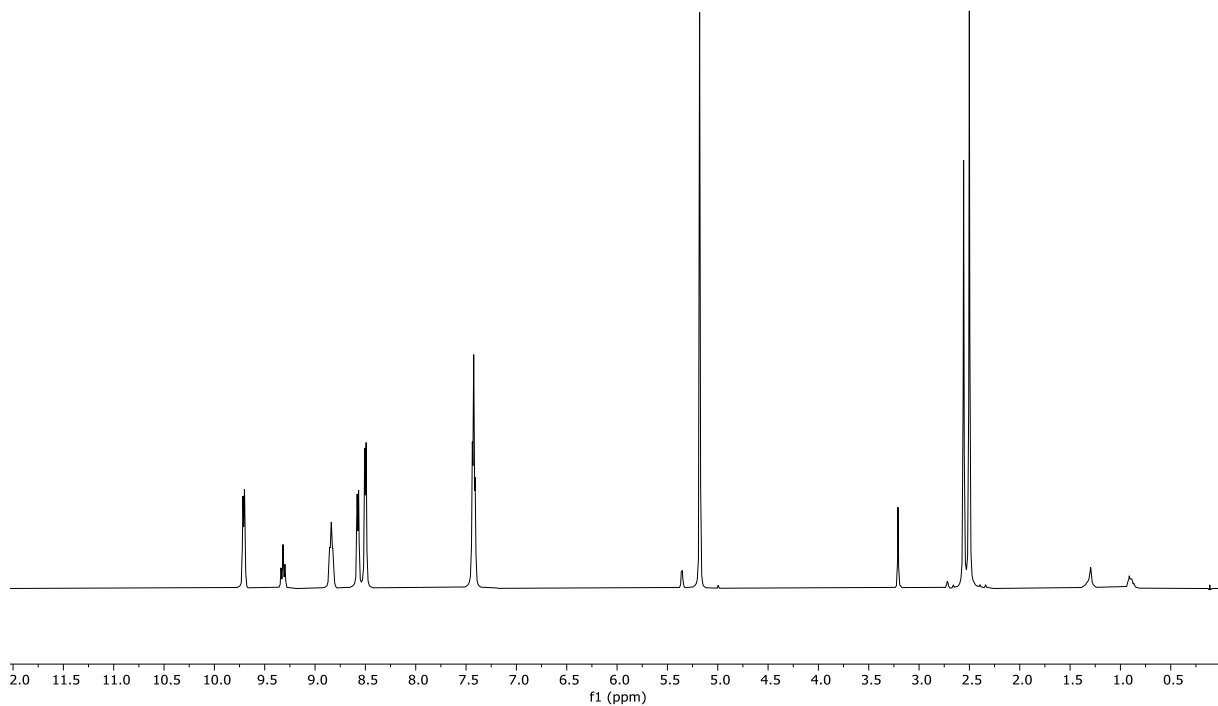


**Figure S60.** <sup>1</sup>H NMR spectrum of a 2:2 mixture of [bis(4-methylpyridine)silver(I)]hexafluorophosphate (**1**) and [bis(4-methylpyridine)iodine(I)]hexafluorophosphate (**2**), with added 4-methylpyridine (5 mol%) and with a capillary of 1-methylpyridinium iodide in CD<sub>3</sub>CN (400 MHz, CD<sub>2</sub>Cl<sub>2</sub>, 25°C).

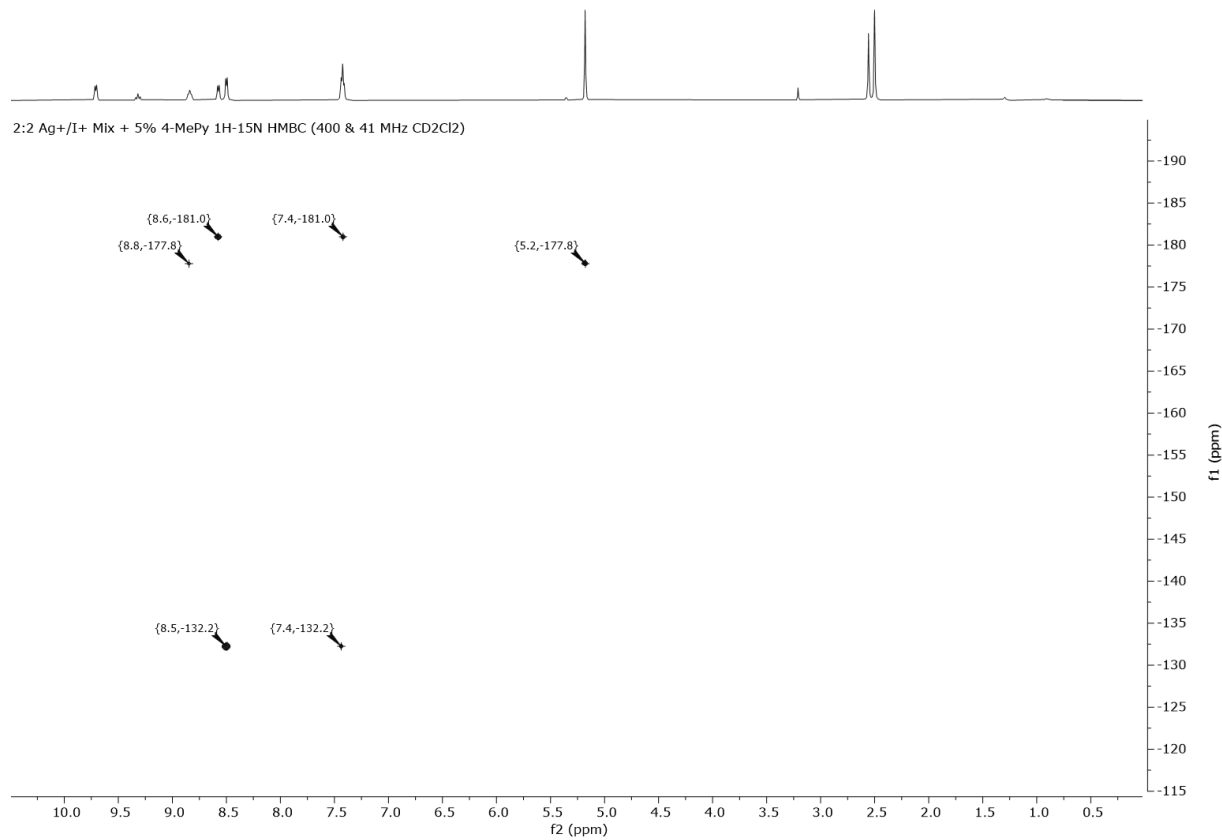


**Figure S61.**  $^1\text{H}$ - $^{15}\text{N}$  spectrum of a 2:2 mixture of [bis(4-methylpyridine)silver(I)]hexafluorophosphate (**1**) and [bis(4-methylpyridine)iodine(I)]hexafluorophosphate (**2**), with added 4-methylpyridine (5 mol%) and with a capillary of 1-methylpyridinium iodide in  $\text{CD}_3\text{CN}$  (400 & 41 MHz,  $\text{CD}_2\text{Cl}_2$ , 25°C).

1:1 Mix of (4)/(5)  $^1\text{H}$  NMR (400 MHz  $\text{CD}_2\text{Cl}_2$ )

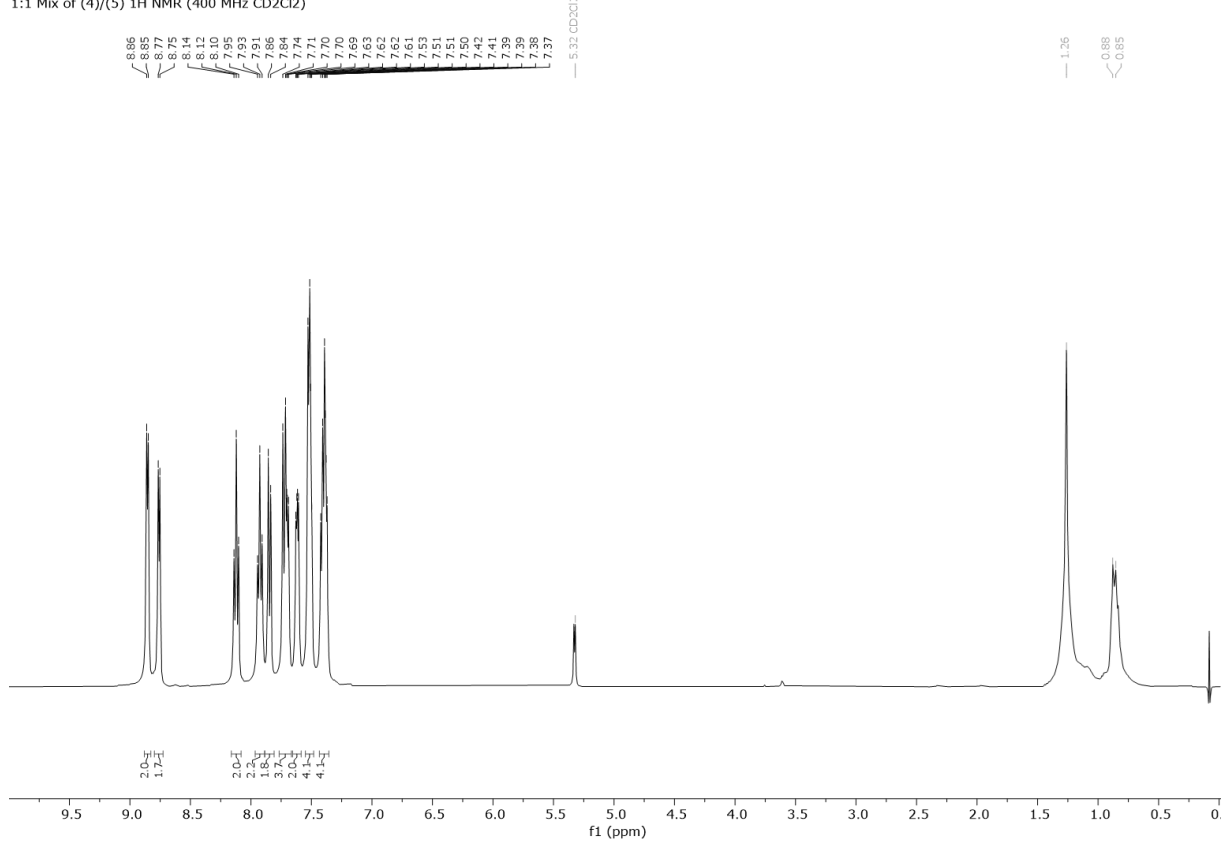


**Figure S62.**  $^1\text{H}$  NMR spectrum of a 1:1 mix of [(1,2-bis(pyridin-2-ylethynyl)benzene)silver(I)]tetrafluoroborate (**4**) and [(1,2-bis(pyridin-2-ylethynyl)benzene)iodine(I)]tetrafluoroborate (**5**) (400 MHz,  $\text{CD}_2\text{Cl}_2$ , 25°C).

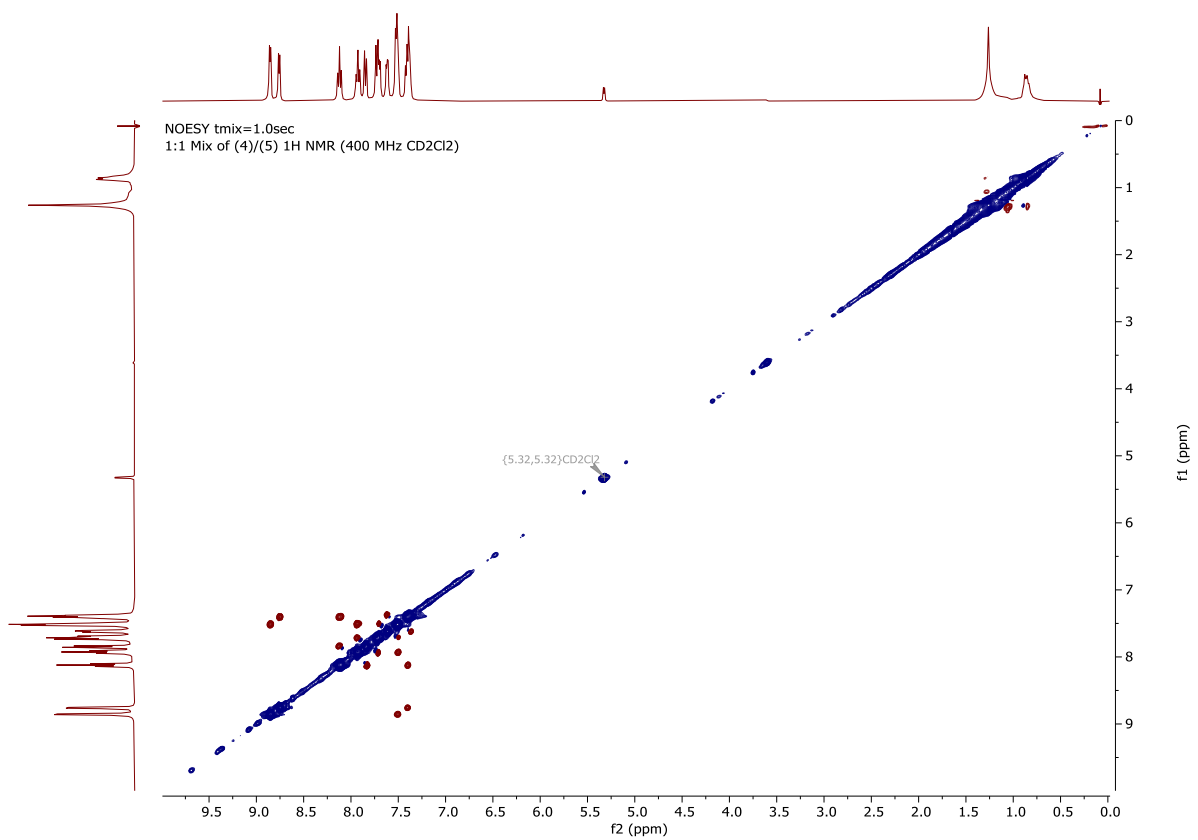


**Figure S63.** <sup>1</sup>H-<sup>1</sup>H NOESY spectrum of a 1:1 mix of [(1,2-bis(pyridin-2-ylethynyl)benzene)silver(I)]tetrafluoroborate (**4**) and [(1,2-bis(pyridin-2-ylethynyl)benzene)iodine(I)]tetrafluoroborate (**5**),  $t_{mix} = 1$  s (400 MHz, CD<sub>2</sub>Cl<sub>2</sub>, 25°C).

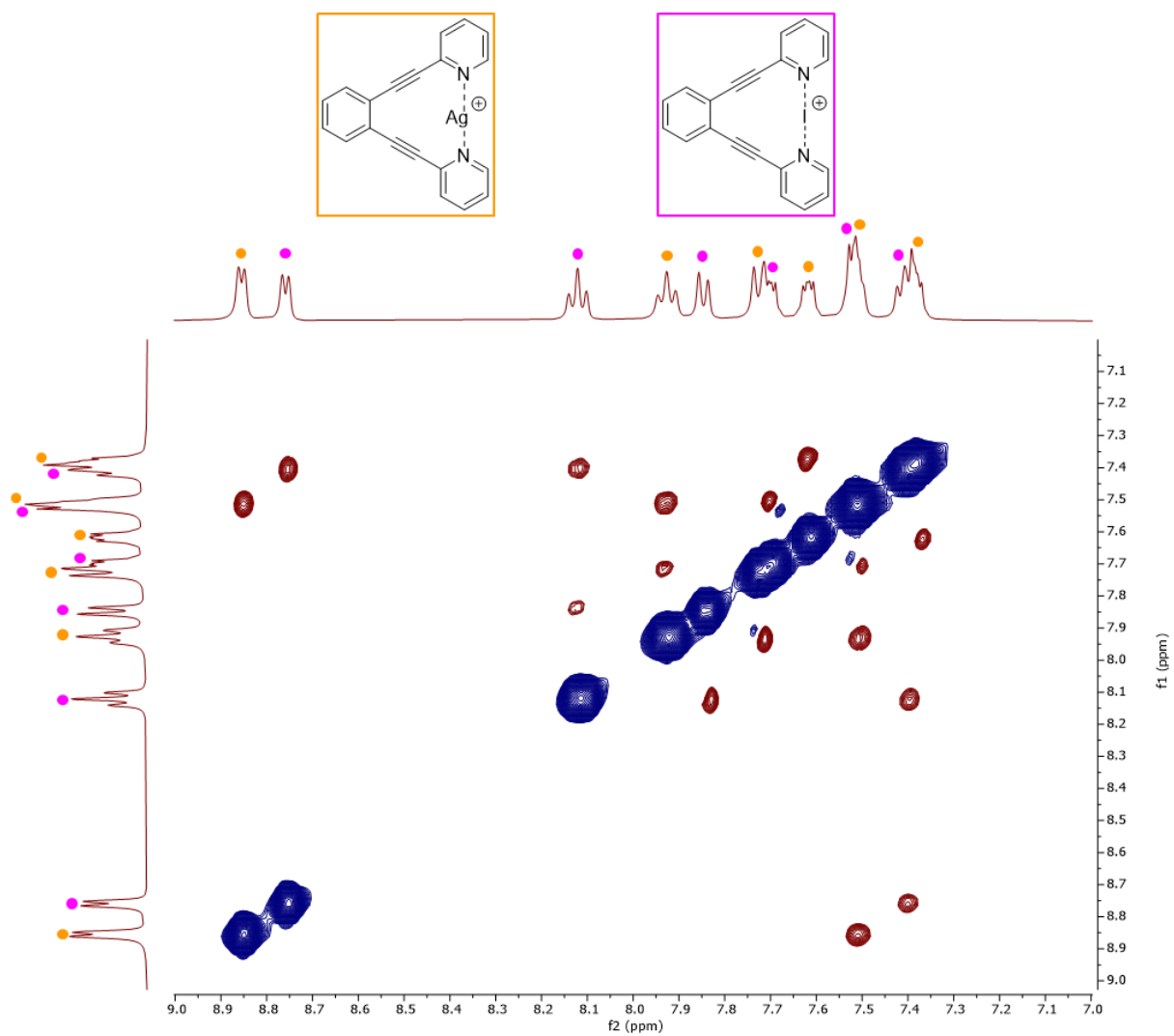


**Figure S64.** Expansion of Fig. S63 showing a lack of EXSY crosspeaks between the two species in solution.

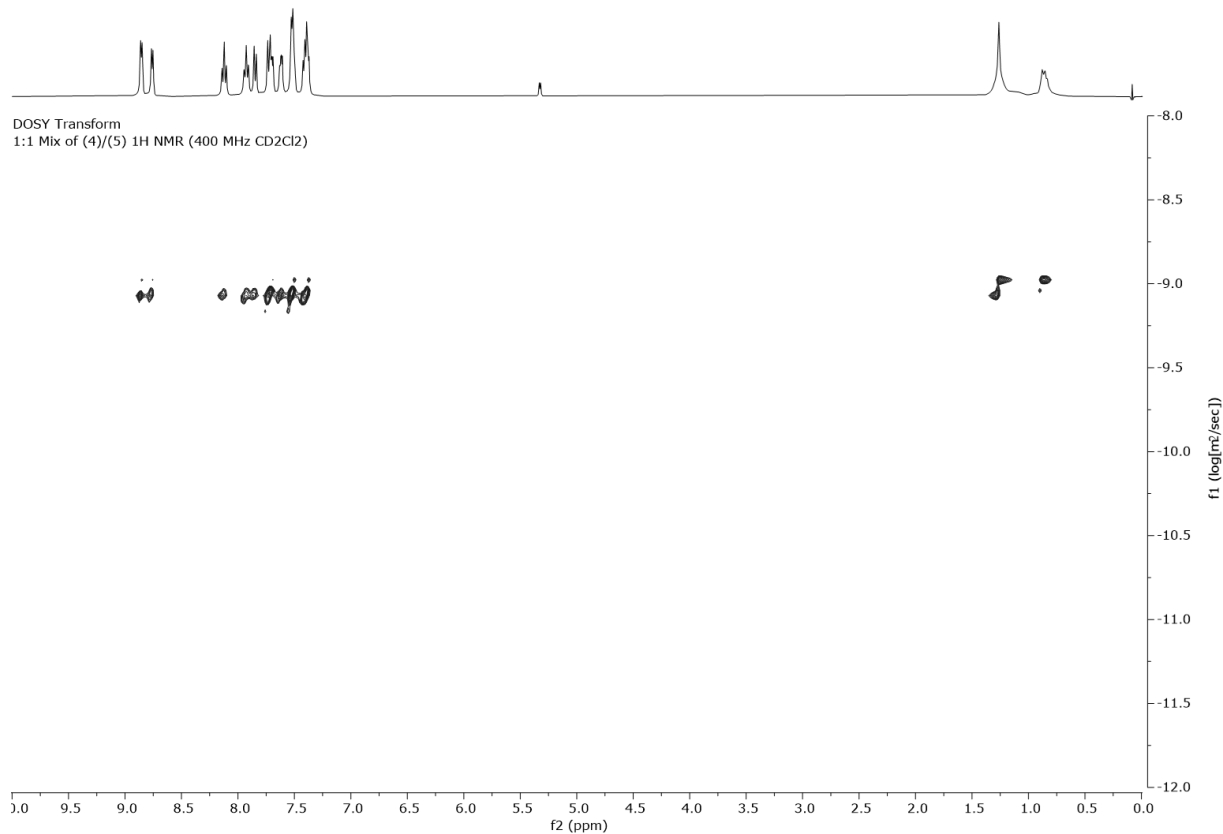


**Figure S65.** <sup>1</sup>H DOSY Transform NMR spectrum of a 1:1 mix of [(1,2-bis(pyridin-2-ylethynyl)benzene)silver(I)] tetrafluoroborate (**4**) and [(1,2-bis(pyridin-2-ylethynyl)benzene)iodine(I)] tetrafluoroborate (**5**) (400 MHz, CD<sub>2</sub>Cl<sub>2</sub>, 25°C).

**Table S2.** <sup>15</sup>N NMR chemical shifts and <sup>1</sup>H NMR translational diffusion coefficients of [(1,2-bis(pyridin-2-ylethynyl)benzene)silver(I)] tetrafluoroborate (**4**) and [(1,2-bis(pyridin-2-ylethynyl)benzene)iodine(I)] tetrafluoroborate (**5**) complexes at different molar ratios yet at a constant overall concentration (40.0 mM, below given as 2 eq).

Molar Equivalents		$\delta^{15}\text{N}$ (ppm)		$D \times 10^{-10} \text{ m/s}^2$	
Ag <sup>+</sup> Complex ( <b>4</b> )	I <sup>-</sup> Complex ( <b>5</b> )	( <b>4</b> )	( <b>5</b> )	( <b>4</b> )	( <b>5</b> )
2	0	-119.9		9.21	
1	1	-119.9	-163.5	9.18	9.51
0	2		-163.6		9.56

### 3. Computations

#### 3.1 Computational Methods

Starting from the previously reported X-ray structure,<sup>7</sup> the equilibrium geometries of 2-coordinate iodine(I) and silver(I) complexes in solution were obtained using the M06-2X<sup>8</sup>, ωB97X-D<sup>9</sup> and B3LYP<sup>10,11</sup> functionals augmented with Grimme's D3 dispersion correction<sup>12</sup> and Ahlrichs' Def2-TZVP basis set.<sup>13</sup> These three functionals are known to accurately describe systems exhibiting weak interactions.<sup>14</sup> The polarizable continuum model (PCM) was used to account for dichloromethane solvation effects.<sup>15</sup> Vibrational frequency calculations were conducted at the same level of theory to ensure the equilibrium geometry corresponding to a minimum on the potential energy surface by the absence of imaginary frequency.

All geometry optimization calculations were performed using the Gaussian 16 Rev. C.01,<sup>16</sup> while the interaction energy calculations were conducted using the ORCA 5.0.1.<sup>17</sup> The counterpoise correction of Boys and Bernadi procedure<sup>18</sup> was used to deal with the basis set superposition error (BSSE) as implemented in ORCA. The free energy calculations were corrected using the Grimme's quasi rigid rotor approximation,<sup>19</sup> as implemented in ORCA and in the Goodvibes program.<sup>20</sup> The electron density and energy density at the Ag<sup>+</sup>...I<sup>-</sup> and π···π bond critical points were calculated using the AIMALL version 19.10.12 software.<sup>21</sup> Reduced density gradient (RDG),<sup>22</sup> independent gradient model (IGM),<sup>23</sup> density overlap regions indicator (DORI),<sup>24</sup> interaction region indicator (IRI),<sup>25</sup> and van der Waals surface analyses were carried out using the Multiwfn 3.7 program.<sup>26</sup> The RDG plot were constructed using the 0.4 a.u. isosurface cutoff and color scale of -0.035 – 0.035 a.u. Local mode force constants were calculated using the LModeA 2.02 program.<sup>26</sup> All analyses were computed using the M06-2X/def2-TZVP level of theory.

### 3.2 Computational Results

**Table S3.** Bond distances, electron density ( $\rho_c$ ), energy density ( $H_c$ ), bond energy ( $H_c/\rho_c$ ), and local force constant of the  $\text{Ag}^+ \cdots \text{I}^-$  interactions.

Level of theory	R (Å)	$\rho_c$ (e/Å <sup>3</sup> )	$H_c$ (h/Å <sup>3</sup> )	$H_c/\rho_c$ (h/e)	$k^a$ (mdyn/Å)
M06-2X/def2-TZVP	3.376	0.106	-0.001	-0.005	0.173
B3LYP-D3/def2-TZVP	3.739	0.060	0.003	0.055	0.157

**Table S4.** Bond distances, electron density ( $\rho_c$ ), energy density ( $H_c$ ), bond energy ( $H_c/\rho_c$ ), and local force constant of the  $\pi \cdots \pi$  interactions.

Level of theory	R (Å)	$\rho_c$ (e/Å <sup>3</sup> )	$H_c$ (h/Å <sup>3</sup> )	$H_c/\rho_c$ (h/e)	$k^a$ (mdyn/Å)
M06-2X/def2-TZVP	3.552	0.027	0.006	0.234	0.083
B3LYP-D3/def2-TZVP	3.736	0.030	0.006	0.194	0.150

**Table S5.** Calculated Gibbs free energy ( $\Delta G$ ) of 2-coordinate iodine(I) and silver(I) complexes.

Level of theory	$\Delta E$ (kcal/mol)	$\Delta H$ (kcal/mol)	$-\Delta S$ (kcal/mol)	$\Delta G$ (kcal/mol)
$\omega$ B97X-D/def2-TZVP	+26.93	+28.48	+16.04	+44.51
M06-2X/def2-TZVP	-6.16	-4.80	+16.11	+11.31
B3LYP-D3/def2-TZVP	-9.53	-7.59	+17.38	+9.79
DLPNO-CCSD(T)/def2-TZVP//M06-2X/def2-TZVP	-6.50	-5.14	+16.11	+9.54

The energies shown in Table S4, in contrast to those in Table 2 in the main text, do not include correction for basis set superposition error (BSSE). The Gibbs free energies shown were calculated at the optimized structure and at the given level of theory, whereas for the energies given in Table 2, the geometries were computed on the M06-2X/Def2-TZVP level of theory. The electronic, enthalpic and entropic contributions were estimated at 1 atm, 298 K at various levels of theory, with the overall conclusion from the different computations showing identical trend apart from that performed with  $\omega$ B97X-D/def2-TZVP. In our hands, computations performed at the  $\omega$ B97X-D/def2-TZVP level of theory are not suitable for the estimation of the interaction energy of the studied iodine(I) and silver(I) complexes. All other functionals provide comparable electronic energies, enthalpies, entropies and Gibbs free energies, thereby mutually confirming each other.

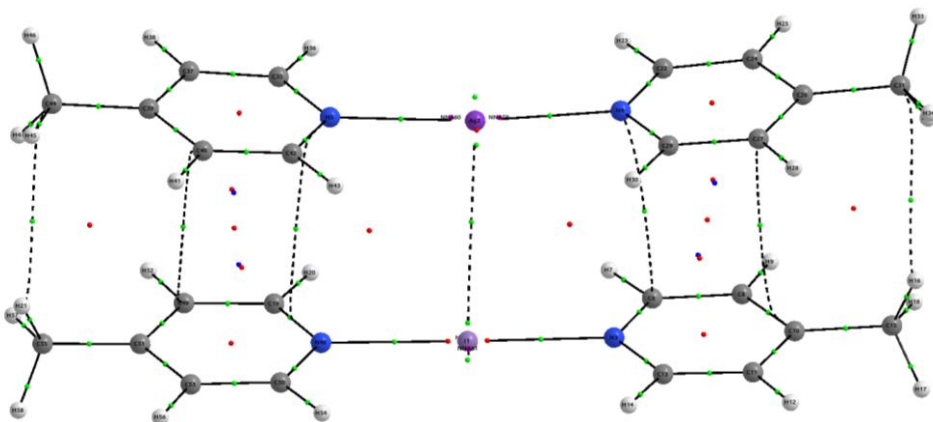


**Figure S66.** Distribution of bond critical points (green dots), ring critical points (red dots), and bond paths (dashed lines) of 2-coordinate iodine(I) and silver(I) complexes calculated at the M06-2X/def2-TZVP level of theory. The bond path and bond critical point are found for the  $\text{Ag}^+ \cdots \text{I}^+$ .

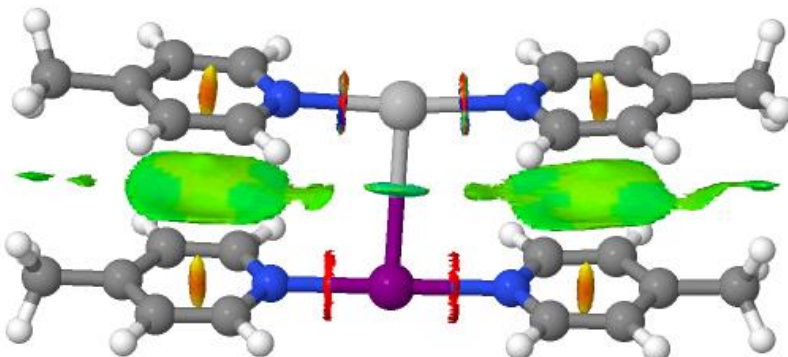


**Figure S67.** Reduced density gradient (RDG) plot. The red, green, and blue surfaces correspond to repulsive, weak and strong attractive interactions, respectively. RDG plot show the weak interactions between  $\text{Ag}^+ \cdots \text{I}^-$ .

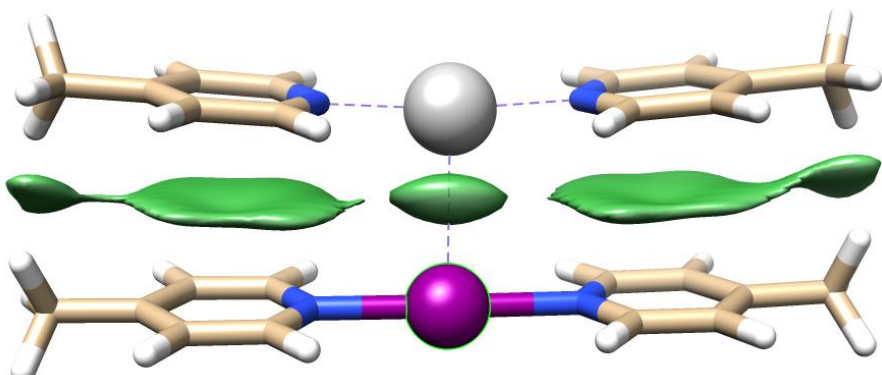


**Figure S68.** Independent gradient model (IGM) plot, where the green surfaces show the weak attractive interactions between  $\text{Ag}^+ \cdots \text{I}^-$ .

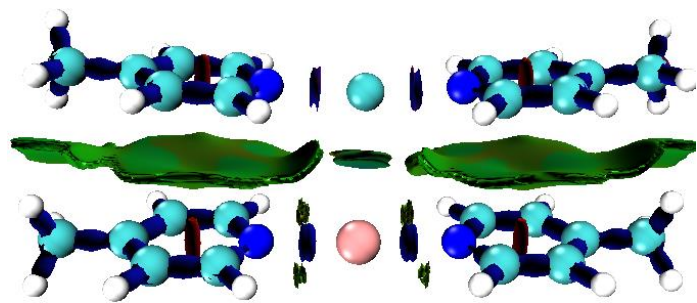


**Figure S69.** Density overlaps regions indicator (DORI) plot. The green surfaces show the weak attractive interactions between  $\text{Ag}^+ \cdots \text{I}^-$ .

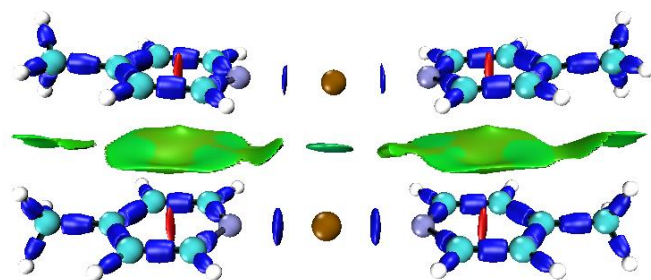


**Figure S70.** Interaction region indicator (IRI) plot. The green surfaces show the weak attractive interactions between  $\text{Ag}^+ \cdots \text{I}^-$ . The red, green, and blue surfaces correspond to repulsive, weak and strong attractive interactions, respectively. IRI plot show the weak interactions between  $\text{Ag}^+ \cdots \text{I}^-$ .

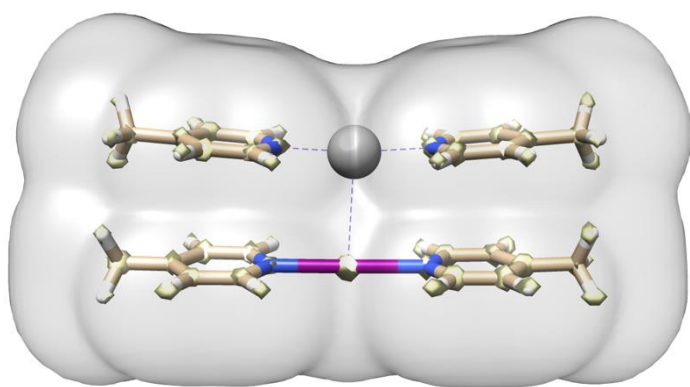


**Figure S71.** Van der Waals surface of 2-coordinate iodine(I) and silver(I) complexes.

### 3.3 Cartesian coordinates (Å) of optimized structures

**(4-Me-Pyr)<sub>2</sub>Ag<sup>+</sup>** optimized at the B3LYP-D3/Def2-TZVP/PCM(Dichloromethane)

Zero-point correction= 0.235736

Thermal correction to Energy= 0.251590

Thermal correction to Enthalpy= 0.252534

Thermal correction to Gibbs Free Energy= 0.186796

Sum of electronic and zero-point Energies= -722.172269

Sum of electronic and thermal Energies= -722.156414

Sum of electronic and thermal Enthalpies= -722.155470

Sum of electronic and thermal Free Energies= -722.221208

Ag -0.00000100 0.00550800 0.00010100

N 2.14107600 0.00181200 -0.00024300

N -2.14107400 0.00189400 0.00033600

C 2.83217500 -1.06160500 -0.44361900

H 2.25292800 -1.90288200 -0.79794900

C 4.21426300 -1.10187600 -0.45326700

H 4.71328000 -1.98889200 -0.81979300

C 4.94784500 -0.00946000 0.00846900

C 4.21964400 1.08861200 0.46819100

H 4.72405100 1.96822300 0.84549500

C 2.83822900 1.06005300 0.44874400

H 2.26301300 1.90386000 0.80362100

C 6.44632300 -0.00122800 -0.01035100

H 6.85125600 -1.01254200 -0.00445200

H 6.80249900 0.49493300 -0.91732900

H 6.84857300 0.54766400 0.84122300

C -2.83218400 -1.06154000 0.44364900

H -2.25295000 -1.90279900 0.79804500

C -4.21427200 -1.10185700 0.45315000

H -4.71328900 -1.98889500 0.81962000

C -4.94784500 -0.00946900 -0.00866700

C -4.21963100 1.08863300 -0.46830700

H -4.72402400 1.96823200 -0.84565900

C -2.83821900 1.06011600 -0.44871600

H -2.26299300 1.90394100 -0.80353200

C -6.44632300 -0.00129200 0.01001900

H -6.84854100 0.54788200 -0.84138400

H -6.85122700 -1.01261600 0.00377000

H -6.80257200 0.49453800 0.91715700

**(4-Me-Pyr)<sub>2</sub>Ag<sup>+</sup>** optimized at the ωB97X-D/Def2-TZVP/PCM(Dichloromethane)

Zero-point correction= 0.237885  
Thermal correction to Energy= 0.253694  
Thermal correction to Enthalpy= 0.254639  
Thermal correction to Gibbs Free Energy= 0.188718  
Sum of electronic and zero-point Energies= -721.935896  
Sum of electronic and thermal Energies= -721.920087  
Sum of electronic and thermal Enthalpies= -721.919143  
Sum of electronic and thermal Free Energies= -721.985063

Ag	0.00000000	0.00464200	-0.00006600
N	2.13630100	0.00133600	0.00097200
N	-2.13630100	0.00127400	-0.00097800
C	2.82439400	-1.06130400	-0.43254300
H	2.24399500	-1.90533100	-0.77992300
C	4.20256400	-1.10231100	-0.44310400
H	4.70181700	-1.99203000	-0.80266600
C	4.93264400	-0.00839700	0.00823100
C	4.20725100	1.09036500	0.45854300
H	4.71134900	1.97330200	0.82836600
C	2.82980900	1.05951800	0.43960100
H	2.25294600	1.90564400	0.78774200
C	6.42881900	0.00005700	-0.01099300
H	6.83160200	-1.01156300	-0.00054600
H	6.78213500	0.49241100	-0.92001200
H	6.82898400	0.55196100	0.83889100
C	-2.82440100	-1.06135600	0.43254600
H	-2.24400800	-1.90539300	0.77991300
C	-4.20257300	-1.10233700	0.44315600
H	-4.70183300	-1.99204700	0.80273200
C	-4.93264500	-0.00840000	-0.00812700
C	-4.20724600	1.09033600	-0.45849200
H	-4.71134100	1.97327800	-0.82830400
C	-2.82980600	1.05946600	-0.43959700
H	-2.25293800	1.90558300	-0.78775300
C	-6.42881500	0.00012900	0.01118600
H	-6.82898900	0.55165000	-0.83894700
H	-6.83165600	-1.01147200	0.00124600
H	-6.78205500	0.49296000	0.91997400

**(4-Me-Pyr)<sub>2</sub>Ag<sup>+</sup>** optimized at the M06-2X/Def2-TZVP/PCM(Dichloromethane)

Zero-point correction= 0.237346  
Thermal correction to Energy= 0.253228  
Thermal correction to Enthalpy= 0.254172  
Thermal correction to Gibbs Free Energy= 0.189134  
Sum of electronic and zero-point Energies= -721.762574  
Sum of electronic and thermal Energies= -721.746693  
Sum of electronic and thermal Enthalpies= -721.745748  
Sum of electronic and thermal Free Energies= -721.810787

Ag	-0.00006700	0.00057200	0.08946600
N	-2.20729300	0.00295800	0.02069600
N	2.20734700	0.00079800	0.02368800
C	-2.91154400	-1.07919300	0.37711000
H	-2.34200200	-1.94103700	0.69900000
C	-4.29030200	-1.11516300	0.34234600
H	-4.80761100	-2.01736500	0.64127600
C	-5.00171700	0.00755700	-0.07665400
C	-4.26138300	1.12495600	-0.44505300
H	-4.75192300	2.02867100	-0.78057800
C	-2.88039400	1.08429700	-0.38313800
H	-2.28912900	1.94543800	-0.66573800
C	-6.49862500	-0.00086900	-0.12000900
H	-6.85512400	-0.82119000	-0.74392100
H	-6.90229100	-0.15517300	0.88169400
H	-6.88990400	0.93496600	-0.51265600
C	2.88298100	-1.08319800	-0.37732200
H	2.29172500	-1.94452300	-0.65904100
C	4.26153500	-1.12387100	-0.43331400
H	4.75417600	-2.02927900	-0.76214700
C	5.00224800	-0.00369500	-0.06368300
C	4.29086900	1.11654300	0.35315000
H	4.80568200	2.01763300	0.65836600
C	2.90929400	1.08048400	0.38231000
H	2.33987100	1.94239500	0.70454700
C	6.49810300	-0.00575400	-0.13509700
H	6.92373500	0.79687700	0.46352200
H	6.90123300	-0.95863200	0.20570900
H	6.81794000	0.13546400	-1.16948800

**(4-Me-Pyr)<sub>2</sub>I<sup>+</sup>** optimized at the B3LYP-D3/Def2-TZVP/PCM(Dichloromethane)

Zero-point correction= 0.235879  
Thermal correction to Energy= 0.251569  
Thermal correction to Enthalpy= 0.252513  
Thermal correction to Gibbs Free Energy= 0.186923  
Sum of electronic and zero-point Energies= -872.865063  
Sum of electronic and thermal Energies= -872.849373  
Sum of electronic and thermal Enthalpies= -872.848429  
Sum of electronic and thermal Free Energies= -872.914019

I	-0.00000200	0.00199200	-0.00502700
N	2.28787600	0.00165500	-0.00363300
C	2.96196500	1.15970600	0.00233700
H	2.37230400	2.06587500	0.00498400
C	4.34279300	1.19161900	0.00256500
H	4.84621300	2.14866300	0.00451500
C	5.06973300	0.00023800	-0.00220600
C	4.34079300	-1.19134500	-0.01090800
H	4.84387000	-2.14870700	-0.01975700
C	2.96121400	-1.15816100	-0.01073000
H	2.37012900	-2.06331800	-0.01830300
C	6.56692400	-0.00641300	0.02624000
H	6.91459200	-0.15535200	1.05219400
H	6.96800000	-0.82219400	-0.57523400
H	6.97800700	0.93617200	-0.33207300
C	-2.96197400	1.15978300	-0.01084200
H	-2.37234700	2.06594900	-0.01841700
H	-6.91461300	-0.15554700	1.05238300
N	-2.28787700	0.00178600	-0.00388500
C	-4.34285300	1.19167300	-0.01077200
C	-2.96120400	-1.15809200	0.00202200
C	-5.06972600	0.00032100	-0.00209100
H	-4.84630400	2.14867000	-0.01944400
C	-4.34073100	-1.19129800	0.00234100
H	-2.37007900	-2.06325000	0.00457100
C	-6.56691400	-0.00651500	0.02647300
H	-4.84383400	-2.14868900	0.00418400
H	-6.97831800	0.93569800	-0.33234300
H	-6.96761400	-0.82272400	-0.57475400

**(4-Me-Pyr)<sub>2</sub>I<sup>+</sup>** optimized at the ωB97X-D/Def2-TZVP/PCM(Dichloromethane)

Zero-point correction= 0.238134 (Hartree/Particle)

Thermal correction to Energy= 0.253726

Thermal correction to Enthalpy= 0.254670

Thermal correction to Gibbs Free Energy= 0.189251

Sum of electronic and zero-point Energies= -872.614048

Sum of electronic and thermal Energies= -872.598456

Sum of electronic and thermal Enthalpies= -872.597512

Sum of electronic and thermal Free Energies= -872.662930

I 0.00001100 0.00130700 -0.00478200

N 2.25971800 0.00139300 -0.00381100

C 2.93167300 1.15504600 -0.01709400

H 2.34163000 2.06178500 -0.02936200

C 4.30825500 1.18903300 -0.01735700

H 4.81166300 2.14594800 -0.03144900

C 5.03223900 0.00072000 -0.00223200

C 4.30672100 -1.18834700 0.00891700

H 4.81034700 -2.14536900 0.01617900

C 2.93151400 -1.15382500 0.00844100

H 2.34046800 -2.05989800 0.01618900

C 6.52709000 -0.00535100 0.02514400

H 6.87303100 -0.15151100 1.05104000

H 6.92539200 -0.82249000 -0.57531900

H 6.93530700 0.93651200 -0.33684500

C -2.93096900 1.15539800 0.00922500

H -2.34069000 2.06204400 0.01707200

H -6.87693800 -0.27501600 1.02229400

N -2.25968300 0.00176900 -0.00354900

C -4.30787200 1.18997100 0.01060400

C -2.93216300 -1.15345700 -0.01648200

C -5.03225000 0.00232900 -0.00061300

H -4.81080900 2.14712800 0.01882400

C -4.30705600 -1.18738200 -0.01605600

H -2.34137400 -2.05963800 -0.02861500

C -6.52722400 -0.00593100 0.02315000

H -4.81104700 -2.14422400 -0.02901500

H -6.93556600 0.97106500 -0.22814500

H -6.92199100 -0.74695900 -0.67173200

**(4-Me-Pyr)<sub>2</sub>I<sup>+</sup>** optimized at the M06-2X/Def2-TZVP/PCM(Dichloromethane)

Zero-point correction= 0.238008  
Thermal correction to Energy= 0.253506  
Thermal correction to Enthalpy= 0.254450  
Thermal correction to Gibbs Free Energy= 0.190676  
Sum of electronic and zero-point Energies= -872.401832  
Sum of electronic and thermal Energies= -872.386334  
Sum of electronic and thermal Enthalpies= -872.385390  
Sum of electronic and thermal Free Energies= -872.449165

I 0.00001500 0.00192900 -0.00343600  
N 2.24971800 0.00168800 -0.00295600  
C 2.91939400 1.15696600 -0.01520700  
H 2.32511500 2.06108800 -0.02603600  
C 4.29837200 1.19076300 -0.01648800  
H 4.80397500 2.14648300 -0.03002900  
C 5.02058400 0.00042900 -0.00353800  
C 4.29621300 -1.19049800 0.00668300  
H 4.80168200 -2.14659700 0.01209600  
C 2.91886100 -1.15565900 0.00734400  
H 2.32315100 -2.05879600 0.01414000  
C 6.51640000 -0.00685000 0.02182800  
H 6.86280500 -0.16838500 1.04479300  
H 6.91069800 -0.81622000 -0.59077100  
H 6.92227700 0.93991000 -0.32766400  
C -2.91879100 1.15754600 0.00848000  
H -2.32439400 2.06164600 0.01548000  
H -6.86722600 -0.29936000 1.01111300  
N -2.24968900 0.00242600 -0.00234600  
C -4.29816500 1.19182400 0.00878500  
C -2.91942000 -1.15507200 -0.01420200  
C -5.02059500 0.00214000 -0.00167500  
H -4.80339100 2.14773000 0.01537400  
C -4.29638400 -1.18940800 -0.01488500  
H -2.32385000 -2.05824700 -0.02468500  
C -6.51653500 -0.00783900 0.01916200  
H -4.80218200 -2.14536400 -0.02713600  
H -6.92281100 0.97393900 -0.21281100  
H -6.90643300 -0.73488200 -0.69236100

**(4-Me-Pyr)<sub>2</sub>Ag<sup>+</sup>···(4-Me-Pyr)<sub>2</sub>I<sup>+</sup>** optimized at the B3LYP-D3/Def2-TZVP/PCM(Dichloromethane)  
 Zero-point correction= 0.475210  
 Thermal correction to Energy= 0.507189  
 Thermal correction to Enthalpy= 0.508133  
 Thermal correction to Gibbs Free Energy= 0.407053  
 Sum of electronic and zero-point Energies= -1595.048918  
 Sum of electronic and thermal Energies= -1595.016939  
 Sum of electronic and thermal Enthalpies= -1595.015995  
 Sum of electronic and thermal Free Energies= -1595.117075

I	-0.06657500	-1.84812700	-0.11080300
Ag	0.06684500	1.88611300	0.02195400
N	2.21845000	-1.85518600	-0.09767600
N	2.21437900	1.89483900	0.07588100
N	-2.07958700	1.90080300	0.13562800
C	2.88894900	-1.31721300	-1.12513300
H	2.29806800	-0.88055300	-1.91785800
C	4.26938200	-1.32083700	-1.16750800
H	4.76939400	-0.87170000	-2.01415900
C	4.99910100	-1.89332200	-0.12605900
C	4.27387500	-2.44347400	0.93413000
H	4.78036000	-2.90183900	1.77264100
C	2.89524300	-2.40963800	0.91988800
H	2.30687700	-2.82843900	1.72411600
C	6.49611300	-1.90674300	-0.12325100
H	6.87513400	-1.26588800	0.67640400
H	6.87060400	-2.91355700	0.06769600
H	6.90395500	-1.55329700	-1.06826600
C	-2.97500300	-1.20555100	-1.19839700
H	-2.34737800	-0.75940800	-1.95692700
H	-7.00891800	-1.14983300	0.54363600
C	2.95264400	2.44290300	-0.90551900
H	2.41099300	2.87809100	-1.73362200
C	4.33315700	2.45978000	-0.87690400
H	4.87368600	2.91416300	-1.69659000
C	5.01675400	1.89542200	0.20152900
C	4.24149100	1.33128700	1.21260900
H	4.70469900	0.86988500	2.07415700
C	2.86190800	1.34733100	1.11675200
H	2.24990100	0.90574700	1.89085300
C	6.51412900	1.88816800	0.24837100
H	6.91477100	1.30417700	-0.58333700
H	6.90627500	2.90165400	0.14623800
H	6.88602000	1.46356600	1.17915100
C	-2.84224700	2.52756000	-0.77734500
H	-2.32218100	3.00564900	-1.59550800
C	-4.22000700	2.56902900	-0.69304000
H	-4.78157300	3.08676400	-1.45934100
C	-4.87394000	1.94722600	0.37210200
C	-4.07342800	1.30118500	1.31186000
H	-4.51349800	0.79271700	2.15864700
C	-2.69863300	1.29671900	1.16218700
H	-2.06622500	0.79159300	1.87911300

C	-6.36795500	1.97107900	0.48089700
H	-6.71542600	1.45432600	1.37369100
H	-6.73202200	2.99983900	0.51136800
H	-6.81982600	1.49763900	-0.39321300
N	-2.35226800	-1.80124900	-0.17280200
C	-4.35319000	-1.15980400	-1.27848900
C	-3.07573500	-2.36980000	0.80428600
C	-5.13047900	-1.74333200	-0.27844500
H	-4.81382100	-0.66202800	-2.12043200
C	-4.45431100	-2.35734200	0.77925800
H	-2.52535100	-2.83615600	1.60920900
C	-6.62652300	-1.70631000	-0.31483600
H	-5.00009100	-2.82638500	1.58666900
H	-6.99682700	-1.23735100	-1.22432600
H	-7.03537700	-2.71632000	-0.25019300

**(4-Me-Pyr)<sub>2</sub>Ag<sup>+</sup>···(4-Me-Pyr)<sub>2</sub>I<sup>+</sup>** optimized at the ωB97X-D/Def2-TZVP/PCM(Dichloromethane)  
 Zero-point correction= 0.478205  
 Thermal correction to Energy= 0.510836  
 Thermal correction to Enthalpy= 0.511780  
 Thermal correction to Gibbs Free Energy= 0.406302  
 Sum of electronic and zero-point Energies= -1594.504846  
 Sum of electronic and thermal Energies= -1594.472215  
 Sum of electronic and thermal Enthalpies= -1594.471270  
 Sum of electronic and thermal Free Energies= -1594.576749

I	-0.04388500	-1.80314500	-0.11433200
Ag	0.04342500	1.79098400	0.06999100
N	2.21372800	-1.80553800	-0.08752500
N	2.17428600	1.82283800	0.06786000
N	-2.08626400	1.84134400	0.14246400
C	2.89101000	-1.31911100	-1.13175100
H	2.30446600	-0.93053400	-1.95378800
C	4.26591900	-1.31727800	-1.16295100
H	4.77298200	-0.91547000	-2.02957600
C	4.98714100	-1.83390600	-0.08950800
C	4.25735000	-2.33613400	0.98512600
H	4.75710100	-2.75559200	1.84783500
C	2.88179200	-2.30917400	0.95488400
H	2.28833600	-2.69781400	1.77224500
C	6.48083900	-1.87018800	-0.10144800
H	6.88950500	-1.77915500	0.90411000
H	6.82028400	-2.82609200	-0.50740500
H	6.89355900	-1.08192300	-0.72929000
C	-2.93336600	-1.19484300	-1.19279900
H	-2.31191600	-0.75669900	-1.96245200
H	-7.00753800	-1.73009200	0.67149800
C	2.87346500	2.34082200	-0.95100700
H	2.30480900	2.72386800	-1.78754200
C	4.24983100	2.39978800	-0.95416500
H	4.75698100	2.83350000	-1.80573300
C	4.96919600	1.91545400	0.13384000
C	4.23283300	1.38083400	1.18638600
H	4.72679400	0.99059500	2.06613800
C	2.85798300	1.35261000	1.11975300
H	2.27629900	0.94415500	1.93545500
C	6.46153300	1.99118600	0.18116200
H	6.89705000	1.89052300	-0.81240500
H	6.76732200	2.96358000	0.57412500
H	6.87978400	1.22706500	0.83488400
C	-2.81583700	2.43541100	-0.81112200
H	-2.27389800	2.87009900	-1.64029200
C	-4.19092500	2.50591800	-0.75911200
H	-4.72398900	3.00198500	-1.55919600
C	-4.87550200	1.95243500	0.31799700
C	-4.10752800	1.33783800	1.30242900
H	-4.57359600	0.88985800	2.16976200
C	-2.73676000	1.30278700	1.18286800
H	-2.13039900	0.82921600	1.94373000

C	-6.36401000	2.03703400	0.42731800
H	-6.76929900	1.20669800	1.00420300
H	-6.64187800	2.95995000	0.94167700
H	-6.83593500	2.05591400	-0.55422500
N	-2.30097900	-1.77228200	-0.16699900
C	-4.30608500	-1.16088300	-1.26835700
C	-3.01339400	-2.33745700	0.81252200
C	-5.07309800	-1.73985900	-0.26038200
H	-4.77561900	-0.68502700	-2.11844000
C	-4.38953400	-2.33594600	0.79653200
H	-2.45583800	-2.79936800	1.61694900
C	-6.56599800	-1.74443200	-0.32405800
H	-4.92613400	-2.80722000	1.60883500
H	-6.94307000	-0.89785500	-0.89596000
H	-6.90774200	-2.65571900	-0.82065900

**(4-Me-Pyr)<sub>2</sub>Ag<sup>+</sup>···(4-Me-Pyr)<sub>2</sub>I<sup>+</sup>** optimized at the M06-2X/Def2-TZVP/PCM(Dichloromethane)

Zero-point correction= 0.477531  
Thermal correction to Energy= 0.509835  
Thermal correction to Enthalpy= 0.510779  
Thermal correction to Gibbs Free Energy= 0.408139  
Sum of electronic and zero-point Energies= -1594.172042  
Sum of electronic and thermal Energies= -1594.139738  
Sum of electronic and thermal Enthalpies= -1594.138794  
Sum of electronic and thermal Free Energies= -1594.241435

I	-0.11095700	-1.74349700	-0.13814500
Ag	0.11361600	1.62195000	0.01276700
N	2.13385400	-1.76963000	-0.15293900
N	2.34242200	1.69543800	0.10446300
N	-2.11490400	1.76001300	0.11039000
C	2.79544900	-1.22282600	-1.17610900
H	2.19568800	-0.79181000	-1.96781400
C	4.17429700	-1.20906400	-1.21745000
H	4.67414100	-0.75453400	-2.06212000
C	4.90251100	-1.77339100	-0.17392100
C	4.18633100	-2.34646600	0.87679000
H	4.69868400	-2.80455500	1.71193800
C	2.80958200	-2.32619200	0.85890100
H	2.21946200	-2.75608900	1.65756600
C	6.39722900	-1.74164300	-0.15295500
H	6.73579200	-1.04533200	0.61803000
H	6.80009600	-2.72285600	0.09696900
H	6.80304800	-1.42092800	-1.10967000
C	-2.99718100	-1.09316400	-1.16613900
H	-2.38167000	-0.66072900	-1.94497500
H	-6.96145900	-0.93517700	0.65973900
C	3.06260400	2.29137000	-0.85473300
H	2.50789500	2.70791400	-1.68536900
C	4.43856700	2.38389700	-0.80439000
H	4.96964800	2.87989300	-1.60624600
C	5.12953400	1.84589500	0.27980700
C	4.37322800	1.22511700	1.26831500
H	4.84758500	0.78355900	2.13547000
C	2.99632500	1.16982000	1.14466300
H	2.39135800	0.68881600	1.90407000
C	6.62235600	1.93662800	0.35861100
H	7.07647300	1.39452700	-0.47283600
H	6.94257400	2.97599700	0.27943600
H	6.99933400	1.52511100	1.29265700
C	-2.82689400	2.37681400	-0.84132300
H	-2.26848500	2.77335600	-1.67929700
C	-4.19865800	2.51369000	-0.77540700
H	-4.72316100	3.02402600	-1.57261400
C	-4.89339800	1.99694900	0.31631000
C	-4.14599600	1.35482700	1.29798600
H	-4.62488600	0.92962000	2.17036600
C	-2.77321400	1.25840100	1.16015400
H	-2.17522900	0.76256600	1.91576500

C	-6.38188600	2.12869800	0.41163700
H	-6.76417300	1.68371100	1.32786700
H	-6.66999500	3.18039600	0.38704500
H	-6.85884700	1.64340400	-0.44175200
N	-2.35655800	-1.68666700	-0.15569600
C	-4.37512300	-1.03587100	-1.21065500
C	-3.05299900	-2.24186500	0.84293100
C	-5.12465100	-1.60445800	-0.18456300
H	-4.85777400	-0.54359900	-2.04422100
C	-4.42969700	-2.21891600	0.85705200
H	-2.47983900	-2.70784400	1.63366500
C	-6.61922900	-1.54813200	-0.17666700
H	-4.95904300	-2.67900600	1.68050500
H	-7.00784100	-1.12573500	-1.10026300
H	-7.03681500	-2.54579300	-0.03888600

#### 4. References

1. A. Mix, J. H. Lamm, J. Schwabedissen, E. Gebel, H. G. Stammler and N. W. Mitzel, *Chem. Commun.*, 2022, **58**, 3645.
2. P. S. Pregosin, *Prog. Nucl. Magn. Spectr.*, 2006, **49**, 261.
3. M. Bedin, A. Karim, M. Reitti, A. C. Carlsson, F. Topic, M. Cetina, F. Pan, V. Havel, F. Al-Ameri, V. Sindelar, K. Rissanen, J. Grafenstein and M. Erdelyi, *Chem Sci*, 2015, **6**, 3746.
4. A.-C. C. Carlsson, J. Grafenstein, J. L. Laurila, J. Bergquist and M. Erdelyi, *Chem. Commun.*, 2012, **48**, 1458.
5. A.-C. C. Carlsson, J. Grafenstein, A. Budnjo, J. L. Laurila, J. Bergquist, A. Karim, R. Kleinmaier, U. Brath and M. Erdelyi, *J. Am. Chem. Soc.*, 2012, **134**, 5706.
6. A.-C. C. Carlsson, K. Mehmeti, M. Uhrbom, A. Karim, M. Bedin, R. Puttreddy, R. Kleinmaier, A. A. Neverov, B. Nekoueishahraki, J. Grafenstein, K. Rissanen and M. Erdelyi, *J. Am. Chem. Soc.*, 2016, **138**, 9853.
7. J. S. Ward, A. Frontera and K. Rissanen, *Chem. Commun.*, 2021, **57**, 5094.
8. Y. Zhao and D. G. Truhlar, *Theor. Chem. Acc.*, 2008, **120**, 215.
9. J. D. Chai and M. Head-Gordon, *Phys. Chem. Chem. Phys.*, 2008, **10**, 6615.
10. A. D. Becke, *Phys. Rev. A*, 1988, **38**, 3098.
11. C. Lee, W. Yang and R. G. Parr, *Phys. Rev. B*, 1988, **37**, 785.
12. S. Grimme, J. Antony, S. Ehrlich and H. Krieg, *J. Chem. Phys.*, 2010, **132**, 154104.
13. F. Weigend and R. Ahlrichs, *Phys. Chem. Chem. Phys.*, 2005, **7**, 3297.
14. D. Sethio, G. Raggi, R. Lindh and M. Erdélyi, *J. Chem. Theory Comput.*, 2020, **16**, 7690.
15. J. Tomasi, B. Mennucci and R. Cammi, *Chem. rev.*, 2005, **105**, 2999.
16. M. J. Frisch, G. W. Trucks, H. B. Schlegel, G. E. Scuseria, M. A. Robb, J. R. Cheeseman, G. Scalmani, V. Barone, G. A. Petersson, H. Nakatsuji, X. Li, M. Caricato, A. V. Marenich, J. Bloino, B. G. Janesko, R. Gomperts, B. Mennucci, H. P. Hratchian, J. V. Ortiz, A. F. Izmaylov, J. L. Sonnenberg, Williams, F. Ding, F. Lipparini, F. Egidi, J. Goings, B. Peng, A. Petrone, T. Henderson, D. Ranasinghe, V. G. Zakrzewski, J. Gao, N. Rega, G. Zheng, W. Liang, M. Hada, M. Ehara, K. Toyota, R. Fukuda, J. Hasegawa, M. Ishida, T. Nakajima, Y. Honda, O. Kitao, H. Nakai, T. Vreven, K. Throssell, J. A. Montgomery Jr., J. E. Peralta, F. Ogliaro, M. J. Bearpark, J. J. Heyd, E. N. Brothers, K. N. Kudin, V. N. Staroverov, T. A. Keith, R. Kobayashi, J. Normand, K. Raghavachari, A. P. Rendell, J. C. Burant, S. S. Iyengar, J. Tomasi, M. Cossi, J. M. Millam, M. Klene, C. Adamo, R. Cammi, J. W. Ochterski, R. L. Martin, K. Morokuma, O. Farkas, J. B. Foresman and D. J. Fox, CT, **2016**.
17. F. Neese, F. Wennmohs, U. Becker and C. Ripplinger, *J. Chem. Phys.*, 2020, **152**, 224108.
18. S. F. Boys and F. Bernardi, *Mol. Phys.*, 1970, **19**, 553.
19. S. Grimme, *Chem. Eur. J.*, 2012, **18**, 9955.
20. G. Luchini, J. Alegre-Requena, I. Funes-Ardoiz, J. Rodríguez-Guerra, J. T. Chen and R. Paton, GoodVibes v3.0.0, 2019; Zenodo DOI:10.5281/zenodo.3346166.
21. T. A. Keith, TK Gristmill Software, Overland Park, KS, **2019**.
22. J. Contreras-García, E. R. Johnson, S. Keinan, R. Chaudret, J.-P. Piquemal, D. N. Beratan and W. Yang, *J. Chem. Theory Comput.*, 2011, **7**, 625.
23. C. Lefebvre, G. Rubez, H. Khatabil, J.-C. Boisson, J. Contreras-García and E. Hénon, *Phys. Chem. Chem. Phys.*, 2017, **19**, 17928.
24. P. de Silva and C. Corminboeuf, *J. Chem. Theory Comput.*, 2014, **10**, 3745.
25. T. Lu and Q. Chen, *Chem. Methods*, 2021, **1**, 231.
26. T. Lu and F. Chen, *J. Comput. Chem.*, 2012, **33**, 580.